

## Appendix 3JJ Soil Structure Interaction Soil Profiles and Input Motions

### 3JJ.0 Introduction

**Subsection 3.7.1.1.1** summarizes the development of the Foundation Input Response Spectra (FIRS), the safe shutdown earthquake (SSE) motion, the strain-compatible soil profiles, and the development of acceleration time histories for use as input motions in soil-structure interaction (SSI) analysis. **Appendix 3JJ** discusses these steps in detail.

In **Subsection 3JJ.1**, the site response analysis leading to the development of amplification factors at the FIRS horizon is discussed. **Subsection 3JJ.2** presents the developed FIRS while **Subsection 3JJ.3** presents the calculation of the SSE motion and **Subsection 3JJ.4** provides the calculated strain-compatible soil profiles. The matching of acceleration time histories to the 5 percent damping SSE acceleration response spectra (ARS) is discussed in **Subsection 3JJ.5** and the final acceleration time histories suitable for use in SSI analysis are presented in **Subsection 3JJ.6**. **Subsection 3JJ.7** provides a description of the sensitivity assessment of the updated geotechnical properties on the SSI input motions and properties.

### 3JJ.1 Development of Amplification Factors at FIRS Horizon

The Uniform Hazard Response Spectra (UHRS), described in **Subsection 2.5.2.4**, are defined on hard rock characterized with a shear wave velocity of  $V_s = 9200$  feet/second (2.8 kilometers/second), which is located at about 10,000 feet (3000 meters) below the ground surface. **Subsection 2.5.2.5** describes the development of the site amplification factors at the GMRS horizon that results from the transmission of the seismic waves through the thick soil column. The effect is modeled by randomized soil columns, extending from the finished ground surface (including structural fill) to randomized hard rock depths varying between 7400 feet (2256 meters) and 11,400 feet (3476 meters), and an adjustment to the soil damping within the soil column to represent the anelastic attenuation of ground motion by the entire soil column (the “kappa” value). The same procedures are followed in this section to develop amplification factors at the FIRS horizon at the bottom of the nuclear island foundation.

The full soil columns used for computation of soil amplification factors represent two site conditions. The site condition far from the nuclear island consists of in situ soil layers except for the upper 30.5 feet (9.3 meters) of structural fill. This is the fill required for the general site to raise the site grade elevation from the existing grade to the final grade, and is designated as “FAR” in this section. In addition, a second soil column represents the site conditions near the nuclear island where, in addition to the general fill, lean concrete and structural fill replace the in situ soils down to a depth of 60.5 feet (18.4 meters). This second column is designated “NI” in the following discussion.

The site response analysis is conducted on a set of 60 randomized profiles, for each of the two base soil profiles, to account for the variability in the dynamic soil properties. The randomization procedure is described in detail in **Subsection 2.5.2.5.2**. **Figures 3JJ-201** and **3JJ-202** present the low-strain randomized shear-wave velocity profiles for NI and FAR site conditions respectively. The “input median” used as input for randomization and the median of the 60 randomized profiles (“Randomized Median”) are compared in these figures. The apparent mismatch at depths greater than 7400 feet (2256 meters) is due to the termination of certain randomized profiles at that depth. Therefore the “Randomized Median” is calculated for the remaining profiles only and shows lower values than the “Input Median”, as expected.

Using the randomized profiles, the soil column analysis is performed with the de-aggregated low frequency (LF) and high frequency (HF) spectra of hard rock motion at  $10^{-4}$  and  $10^{-5}$  annual-frequency-of-exceedance, presented in **Subsection 2.5.2.4**, following the same methodology described in **Subsection 2.5.2.5**. The 5 percent damping ARS are calculated as “outcrop” motion at

the selected horizons at 301 frequencies between 0.1 and 100 Hz. Amplification factors are calculated as the ratio of the calculated ARS at the selected horizon to the input UHRS at the bottom of the soil column.

Log-mean (median) amplification factors are developed for both FAR and NI site conditions at the ground surface at elevation +25.5 feet (7.8 meters) as well as at the FIRS horizon, located at the bottom of the NI foundation at elevation –16 feet (–4.9 meters) corresponding to a depth of 41.5 feet (12.7 meters) below the finished ground surface.

Figures 3JJ-203 and 3JJ-204 present the amplification factors at the FIRS horizon from analyses of the 60 randomized profiles, for NI and FAR site conditions respectively, for different rock input motions. Figures 3JJ-205 and 3JJ-206 present the amplification factors at the ground surface. Note that LF amplification factors for the low frequency range are larger than the corresponding HF ones, and that amplification greater than 1.0 of the ARS is observed in the low frequency range, while at higher frequencies, de-amplification occurs. The amplification due to the  $10^{-5}$  level of input motion is smaller than for the  $10^{-4}$  level of input motion, at frequencies larger than 0.8 Hz, due to the higher strain levels and nonlinearity in the soil column.

The median of maximum strains versus depth from analyses of the 60 randomized profiles for LF and HF,  $10^{-4}$  and  $10^{-5}$  input motions, are presented in Figures 3JJ-207 and 3JJ-208 for NI and FAR site conditions, respectively. Note that strains are generally low and do not exceed 0.045 percent for both NI and FAR site conditions. Comparison of the profiles of median maximum strains clearly confirms that the strains due to LF motions are larger than under HF motions.

### 3JJ.2 Development of FIRS

The recommended horizontal and vertical FIRS are calculated for elevation –16 feet horizon. This horizon corresponds to the bottom of the nuclear island foundation horizon, refer to Subsection 3JJ.1. The same Regulatory Guide (RG) 1.208 methodology used for the development of the GMRS design response spectra in Subsection 2.5.2.6 is used for the recommended FIRS design response spectra. For the development of the FIRS, however, the methodology is performed twice: once to develop a design response spectrum (DRS) for the FAR soil column, and once to develop a DRS for the NI soil column. The horizontal FIRS is defined as the envelope of the FAR and NI DRS. The vertical FIRS is obtained by scaling the horizontal FIRS by the same V:H ratios as presented in Subsection 2.5.2.6. Similar to the GMRS, the recommended FIRS design response spectra are for 5 percent spectral damping.

With the site-specific amplification calculations described in the previous subsection, the site horizontal design response spectrum (DRS) for both FAR and NI soil columns were determined as follows. Figures 3JJ-209 and 3JJ-210 show the  $10^{-4}$  and  $10^{-5}$  horizontal HF and LF ARS resulting from the site response analysis, plotted on a linear spectral acceleration scale for the FAR and NI soil columns, respectively. The “LF SA(g)” and “HF SA(g)” columns in Tables 3JJ-201 and 3JJ-202 list these ARS at a 38-frequency subset of the 301 frequencies analyzed for the annual frequencies of exceedance of  $10^{-4}$  and  $10^{-5}$ , respectively. For each soil column the HF and LF  $10^{-4}$  and  $10^{-5}$  horizontal site spectra are enveloped to give a “raw” soil UHRS and smoothed to remove small frequency-to-frequency variations, using a smoothing function that averages over spectral accelerations at adjacent frequencies. Figures 3JJ-211 and 3JJ-212 show the smoothed, UHRS calculated in this way, plotted on a linear spectral acceleration scale for the FAR and NI soil columns, respectively. Tables 3JJ-201 and 3JJ-202 tabulate the “raw” and smoothed UHRS for both FAR and NI soil columns for the annual frequencies of exceedance of  $10^{-4}$  and  $10^{-5}$ , respectively.

The horizontal DRS for both soil columns are calculated at each frequency using the following equations:

$$A_R = SA(10^{-5})/SA(10^{-4}) \quad \text{Equation 3JJ-1}$$

$$DF = 0.6 \times A_R^{0.8} \quad \text{Equation 3JJ-2}$$

$$DRS = \max[SA(10^{-4}) \times \max(1.0, DF), 0.45 \times SA(10^{-5})] \quad \text{Equation 3JJ-3}$$

where  $SA(10^{-4})$  is the smoothed UHRS as spectral acceleration for the  $10^{-4}$  hazard level at each spectral frequency (and similarly for  $10^{-5}$ ), and DRS is the design response spectrum at that spectral frequency. These equations follow the procedure in RG 1.208 to determine the DRS from the  $10^{-4}$  and  $10^{-5}$  response spectra.

Figures 3JJ-211 and 3JJ-212 show the FAR and NI horizontal DRS, respectively, calculated with the above equations at each spectral frequency from the smoothed  $10^{-4}$  and  $10^{-5}$  horizontal spectra. Tables 3JJ-203 and 3JJ-204 document the smoothed  $10^{-4}$  and  $10^{-5}$  horizontal spectral amplitudes, the calculation of  $A_R$  and DF from Equations 3JJ-1 and 3JJ-2, and the horizontal DRS calculated according to Equation 3JJ-3 for the FAR and NI soil columns, respectively. At low spectral frequencies (about 2 Hz and below), the hazard curves are steep, so  $A_R$  in Equation 3JJ-2 above is low, and the DRS from Equation 3JJ-3 is nearly equal to the  $10^{-4}$  UHRS.

To calculate vertical spectra, V:H ratios from RG 1.60 are adopted, as in Subsection 2.5.2.6 in development of the GMRS. The V:H ratios are applied to the smoothed  $10^{-4}$  and  $10^{-5}$  horizontal spectra to calculate  $10^{-4}$  and  $10^{-5}$  vertical UHRS, and Equations 3JJ-1 through 3JJ-3 are applied to the  $10^{-4}$  and  $10^{-5}$  vertical spectral accelerations to calculate a vertical DRS for both FAR and NI soil columns. The resulting vertical  $10^{-4}$  and  $10^{-5}$  spectra and vertical DRS are plotted in Figures 3JJ-213 and 3JJ-214 for the FAR and NI soil columns, respectively. Tables 3JJ-205 and 3JJ-206 document the V:H ratios, the  $10^{-4}$  and  $10^{-5}$  vertical spectral amplitudes, the calculation of  $A_R$  and DF from Equations 3JJ-1 and 3JJ-2, and the vertical DRS calculated according to Equation 3JJ-3 for the FAR and NI soil columns, respectively.

Finally, the FIRS is defined as the envelope of the DRS for FAR and NI soil columns. Figure 3JJ-215 plots the horizontal and vertical FIRS, and Table 3JJ-207 provides a tabulation of the horizontal and vertical FIRS spectra.

In addition to the FIRS, from the same set of soil amplification analysis, DRS at the ground surface for both NI and FAR soil profiles are developed and enveloped. The surface DRS are calculated using the ground surface amplification factors presented in Subsection 3JJ.1 following the same procedure for development of FIRS. Surface DRS are used to check the adequacy of the SSI input motion as described in Subsection 3JJ.6.

### 3JJ.3 Safe Shutdown Earthquake Motion

To satisfy the requirements of Appendix S to 10 CFR Part 50, namely that the SSE motion, for the purpose of soil-structure interaction analysis, must be an adequate ARS with a minimum PGA of 0.1 g (also referred to as the minimum required response spectra), the site-specific FIRS and the minimum required response spectra are enveloped.

Subsection 3JJ.2 provides the site-specific DRS at foundation level or FIRS. The 5 percent damping horizontal and vertical ARS defined in RG 1.60 scaled to a PGA of 0.1 g is considered as the minimum required response spectra satisfying the requirements of Appendix S to 10 CFR Part 50. The 5 percent damped ARS for the minimum required response spectra and the horizontal and

vertical FIRS are plotted in [Figure 3JJ-238](#). The envelope of the FIRS and RG motions, horizontal and vertical, constitute the SSE for the Turkey Point site.

### 3JJ.4 Strain-Compatible Soil Property Profiles

Two sets of strain-compatible profiles are developed for the NI and FAR site conditions, respectively. Each set consists of best estimate (BE), lower bound (LB) and upper bound (UB) strain-compatible shear-wave velocity, P-wave velocity and damping profiles. The soil properties are developed consistent with the developed 5 percent damping SSE ARS as described below. The upper bound and the lower bound shear wave velocity profiles maintain the minimum coefficient of variation of 0.50 in terms of the best estimate soil shear modulus.

A set of LB, BE, and UB profiles is developed for each of the NI and FAR soil columns that are strain-compatible with the SSE motion, described in [Subsection 3JJ.3](#). The approach used is iterative and consists of propagating modified rock motions (input at bedrock) convolved through each set of 60 simulated profiles (NI and FAR) and computing the response at the foundation elevation horizon. The analysis is repeated, modifying the input rock motion each time, until the 5 percent damping mean ARS at the foundation horizon closely matches the 5 percent damping SSE ARS.

[Figure 3JJ-239](#) presents a comparison of the horizontal SSE motion and the mean ARS of the propagated motion through the NI soil column profiles. [Figure 3JJ-240](#) presents a similar comparison in the case of the FAR soil column. Note that a close match is achieved, especially at the lower frequency range of the ARS, which holds the most effect on the level of strain in the soil column and, therefore, its iterated properties.

P-wave velocities are calculated using Equation 3JJ-4 where  $\nu$  is the Poisson's ratio corresponding to each soil layer. In addition, below the ground water level at elevation +1 feet (0.3 meters), a minimum P-wave velocity of 5000 feet/sec (1524 meter/sec) is maintained, on the condition that  $\nu$  does not exceed 0.48 to avoid numerical problems in SSI analysis.

$$V_p = V_s \sqrt{\frac{2 - 2\nu}{1 - 2\nu}}$$

Equation 3JJ-4

The resulting profiles are plotted in [Figures 3JJ-216, 3JJ-217, and 3JJ-218](#) for NI site conditions and in [Figures 3JJ-219, 3JJ-220, and 3JJ-221](#) for FAR site conditions. Note that the lower bound SSI soil profile is composed of the lower bound shear-wave velocity profile, the lower bound P-wave velocity profile and the upper bound (larger) damping profile. Similarly, the soil property profiles are combined for the upper bound SSI soil profiles. The presented profiles are recommended for use in the SSI analysis of the nuclear island.

As described in [Subsection 2.5.4.6.2](#), grouting is planned to provide a barrier against water intrusion as part of the dewatering construction activities. Seismic site response sensitivity analyses were conducted to examine the effect of the change in properties of the grouted layers underneath the NI on the strain-compatible properties and acceleration response spectra at the ground level and NI foundation level. The analyses show that the effect of the grouted rock on the strain-compatible properties is minimal. Similarly, the sensitivity analyses show that the effect of the grouted rock on the ground surface and NI foundation level acceleration response spectra results in slightly lower response spectra. Thus, the response spectra computed without grouted properties is slightly conservative. Based on these analyses it was concluded that the FIRS at the NI foundation elevation and at the ground surface developed without considering the grout effect are valid for use in seismic design and evaluation.

### 3JJ.5 Spectral Matching of Acceleration Time Histories

Spectrum-compatible acceleration time histories are presented in this section. The first step in the development of spectrum-compatible time histories was the selection of appropriate seed acceleration time histories. These selected input seed time histories were taken from the database of candidate time histories given in NUREG/CR-6728 based on the low frequency de-aggregation results (i.e., magnitudes  $> 7$  and distances  $> 500$  km). For the analysis, the three component (i.e., two horizontal and one vertical component) strong ground motion recordings from the 1999 Chi-Chi earthquake (magnitude=7.6) recorded at the TAP024 station (closest distance=100.2 km) were selected and matched to the 5 percent damping SSE ARS developed earlier (see [Subsection 3JJ.3](#)).

The spectral matching procedure is a time domain procedure and emphasis was placed on maintaining the phase characteristics of the initial time history in the final modified spectrum-compatible time history. In addition, emphasis was placed on maintaining the characteristic of the normalized Arias intensities (the integral of the square of the acceleration-time history, a ground motion parameter that captures the potential destructiveness of an earthquake) of the initial and final modified spectrum-compatible time histories. These time histories were modified to be spectrum-compatible to the SSE ARS following the spectral matching criteria given in NUREG-0800 Rev. 3 (3.7.1). In most cases, an additional constant scale factor was applied after the spectral matching procedure to comply with the spectral matching criteria given in NUREG-0800 Rev. 3 (3.7.1). Scale factors of 1.01, 1.015, and 1.015 were applied for the two horizontal directions (H1, H2), and vertical direction (UP) components, respectively.

The modified spectrum-compatible acceleration, velocity, and displacement time histories prior to the application of the noted constant scale factors are plotted in [Figure 3JJ-222a](#) for the H1 component. [Figure 3JJ-222c](#) shows target horizontal SSE spectrum, 1.3\*SSE target spectrum, 0.9\*SSE target spectrum and the modified time history response spectrum including the 1.01 constant scale factor. The normalized Arias intensities for the first horizontal (H1) component initial and modified spectrum-compatible time histories are plotted in [Figure 3JJ-222b](#). The results for the second horizontal (H2) component and the UP component are shown in [Figures 3JJ-223a, 3JJ-223b, and 3JJ-223c](#) and [Figures 3JJ-224a, 3JJ-224b, and 3JJ-224c](#), respectively. The zero-lag cross correlation values were computed for the combinations between the three spectrum-compatible acceleration time histories and are listed in [Table 3JJ-208](#). These values are all less than the required value of 0.16.

### 3JJ.6 SSI Acceleration Time Histories

Acceleration time histories, suitable for use in SSI analysis of the nuclear island, are presented in this section. [Subsection 3JJ.5](#) provides a set of two horizontal motions and one vertical motion, spectrally matched to 5 percent damping SSE ARS. The acceleration time histories are propagated through the developed strain-compatible profiles, presented in [Subsection 3JJ.4](#), where they are used as input “outcrop” motions in the soil column at the FIRS horizon and the “within” acceleration time histories at the same horizon are computed. No further iterations on soil properties are performed.

These analyses result in a set of 3 “within” motions for each soil profile in the H1 and H2 directions and the UP direction, respectively. Note that while for horizontal motions, strain-compatible shear-wave velocity profiles are used to describe the shear modulus of the soil column, in the case of vertical motions, P-wave velocity profiles are used instead. Six (6) sets of 3 orthogonal motions are developed corresponding to the LB, BE and UB profiles for NI and FAR site conditions.

From the same set of soil amplification analyses, the 5 percent damping ARS at the ground surface level are calculated. Checks are made with respect to the corresponding surface design response spectra (DRS), discussed in [Subsection 3JJ.2](#), per applicable requirements ([References 201 and 202](#)) to ensure that the envelope of LB, BE and UB surface ARS, in each direction and site condition,



envelops the corresponding surface DRS. Figures 3JJ-225, 3JJ-226, and 3JJ-227 present this comparison for NI site condition in the 3 orthogonal directions. Figures 3JJ-228, 3JJ-229, and 3JJ-230 present the same plots for FAR site condition. In these figures, the surface-DRS-to-envelope-ARS ratios (DRS/ENV) are also plotted.

Note that for horizontal motions, the DRS/ENV exceed unity on the order of 1 percent for the NI case, and on the order of 7 percent in the FAR case. Therefore, the horizontal motions are increased by an adjustment factor to ensure the surface ARS plots envelop the surface DRS in the horizontal directions for both NI and FAR site conditions. In the case of vertical motions and for both site conditions, an increase of approximately 12 percent is needed. The adjustment factors applied to each of the within motions are presented in Table 3JJ-209.

The resulting adjusted acceleration time histories are presented in Figures 3JJ-232, 3JJ-233, and 3JJ-234 for NI site condition and in Figures 3JJ-235, 3JJ-236, and 3JJ-237 for FAR site condition. The “within” acceleration time histories are recommended for use in the SSI analysis of the nuclear island SSI model that includes embedment. The time histories are to be applied at the FIRS horizon as “within” motion and shall be used in combination with the respective SSI soil profiles discussed in Subsection 3JJ.4.

### **3JJ.7 SSI Input Motions and Properties Sensitivity Assessment**

The subsurface investigation for the Turkey Points Units 6 & 7 site took part in two stages. An initial investigation was conducted in 2008, and supplemental site information was collected in 2013. The supplemental data was used to update the site profile (S-wave velocity, layer thickness, and unit weight), as well as the nonlinear curves ( $G/G_{\max}$  and damping). A sensitivity assessment was performed to determine the effect of the updated site properties on the GMRS, FIRS, and SSI properties on both the NI and FAR profiles. The site response sensitivity analyses were performed for the LB, BE, and UB S-wave velocity profiles, using the HF4, LF4, HF5, and LF5 input motions. This subsection describes the results of these sensitivity assessments.

#### **3JJ.7.1 Description of Sensitivity Analysis Input**

Input to the sensitivity analyses included the input motion, site profiles, and results from the existing analyses described in Appendix 3JJ. For clarity, the targeted ground motion elevations are summarized in Table 3JJ-210.

In the sensitivity analysis, two site column locations were considered: 1) NI, and 2) FAR site conditions. These site columns were defined in the following fashion: the S-wave velocity for each profile was characterized by BE value and a logarithmic standard deviation ( $\sigma_{\ln V_s}$ ); then, the LB and UB profiles were developed by  $\pm 1\sigma_{\ln V_s}$  variation.

The first profile set used in the initial SSI evaluations, is referred to as the “initial” analyses, and serves as the reference condition to which the changes are compared.

The second profile set considered is referred to as “updated” and includes the unit thickness, unit weight, S-wave velocity, and nonlinear curves based on data collected by the initial and supplemental site investigations. The logarithmic standard deviation of the S-wave velocity ( $\sigma_{\ln V_s}$ ) is limited to vary between 0.15 and 0.35. Comparison of the results between the “initial” and “updated” profile evaluated the sensitivity of the updated properties and different methods for computing the S-wave velocity, mean and standard deviation.

The two different characterizations of the FAR and NI site columns are presented in Tables 3JJ-211 through 3JJ-214. Comparisons of the upper 600 feet of S-wave velocity profiles for the FAR and NI

columns are shown in Figures 3JJ-241 and 3JJ-242, respectively. The  $\sigma_{InVs}$  profiles for the FAR and NI columns are shown in Figures 3JJ-243 and 3JJ-244, respectively.

The nonlinear curves used in the analyses are plotted in Figures 3JJ-245 through 3JJ-249. The curves for the Structural Fill and Miami Limestone (Figures 3JJ-245 and 3JJ-246) are unchanged from the initial analyses. For the sensitivity assessment, the Key Largo Formation was subdivided into the Key Largo and Fort Thompson with differing  $G/G_{max}$  curves and the same damping (D) curves, shown in Figure 3JJ-247. The  $G/G_{max}$  curves for the Natural Soils (above and below El. -151 ft) were modified, and assigned one updated damping curve for both Natural Soils, shown in Figures 3JJ-248 and 3JJ-249.

### 3JJ.7.2 Methodology for Sensitivity Assessment

As described in Subsection 2.5.2.5.3, the program P-SHAKE was used for the Turkey Point Units 6 & 7 site response analysis. The analysis was performed using both an iterative process, and a truncated column methodology.

The 5 percent ARS was computed at elevations of interest at 301 frequencies log-spaced from 0.1 to 100 Hz.

The site response results were then used to develop DRS, FIRS, and the GMRS. In total, four different response spectra were developed, as presented in Table 3JJ-215. These spectra were calculated site responses, modeled using either full column with iterations, or truncated column without iteration.

For the sensitivity assessment, only the LB, BE, and UB S-wave velocity profiles were calculated. Thus, the mean ARS was computed by the average from these three profiles (instead of the 60 used in the initial analyses). Instead of the SSE, the RG 1.60 spectrum, with a PGA of 0.1g, was used for the input motion; the difference is a slight decrease (less than 1.5 percent between 0.51 Hz and 0.56 Hz) for the RG 1.60 motion. The iterative process was repeated for 10 iterations.

As described in Subsection 3JJ.1, development of site amplification factors for the initial analysis was based on 60 simulated profiles to compute the logarithmic mean site amplification at the site. For this sensitivity analysis, the site amplification was estimated using the following process:

1. For a specific input motion (e.g., HF4), the arithmetic mean site amplification was computed for the LB, BE, and UB S-wave velocity profiles from the “initial” and “updated” profiles. The ratio of the site amplification from the “initial” and “updated” profiles is representative of the change in site amplification due to the change in the site properties.
2. This ratio is smoothed by a running mean with a width of 21 points, which corresponds to 1/5 of a decade in frequency. At the tails of the frequency range, the width is reduced to accommodate the smaller possible range (i.e., first and last point are not averaged). Smoothing the ratio removes irregularities in the ratio caused by slight differences in the dynamic response of the site. The corrective ratio is conservatively limited to be above unity.
3. The site amplification was then approximated by applying this ratio to the site amplification computed by the original rigorous analyses. The approach used include the uncertainty of the site properties and an update to the site properties.

The strain compatible soil profiles for SSI analyses, developed based on initial site investigations, used 60 simulated profiles, which allowed for defining BE, LB, and UB values for the  $V_s$ ,  $V_p$ , and damping. The best-estimate strain-compatible properties were then computed using the logarithmic mean (i.e., geometric mean) of the 60 simulated profiles. The lower- and upper-bound profiles were

then developed based on the variation from the simulations, as well as the minimum variation specified by ASCE 4-98.

In the sensitivity assessment, the best-estimate profile computed in the initial analyses with 60 simulated site profiles was compared with the best-estimate profile computed using the logarithmic mean of three profiles.

For the RG 1.60 input motion, the best-estimate profile is computed solely based on the logarithmic mean of the three profiles.

For the site-specific input motions, the strain-compatible properties that correspond to DRS motions are calculated using  $A_R$  and  $DF$  factors at the finished grade (El. +25.5 ft). Observing that  $A_R$  (Equation 3JJ-1) is the ratio of  $ARS_{1E-5}$  to  $ARS_{1E-4}$  and similarly  $DF$  (Equation 3JJ-2) is the ratio of DRS to  $ARS_{1E-4}$ , a weighing factor ( $W(f)$ ) is computed by:

$$W(f) = \frac{\ln\left(\frac{DRS(f)}{ARS_{1E-4}(f)}\right)}{\ln\left(\frac{ARS_{1E-5}(f)}{ARS_{1E-4}(f)}\right)} = \frac{\ln(DF(f))}{\ln(A_R(f))} \quad \text{Equation 3JJ-5}$$

where  $W(f)$  and  $1-W(f)$  are the weights of  $ARS_{1E-4}$  and  $ARS_{1E-5}$ , respectively, in calculating DRS at ground surface as a function of frequency. Average  $W(f)$  values are calculated over all frequencies and assigned a constant value of average weight factor,  $\omega$ .

The following procedure is used to compute the best-estimate S-wave velocity and damping for use in the SSI analysis. At the  $10^{-4}$  hazard level, the logarithmic mean for the LF4 and HF4 analyses ( $\mu_{ln,1E-4}$ ) is computed. Similarly, the logarithmic mean at the  $10^{-5}$  hazard level ( $\mu_{ln,1E-5}$ ) is computed using the HF5 and LF5 motions. The average parameter consistent with the DRS is then computed using  $\omega$ :

$$\mu_{DRS} = (\mu_{ln,1E-4})^{\omega} \cdot (\mu_{ln,1E-5})^{1-\omega} \quad \text{Equation 3JJ-6}$$

Strain-compatible P-wave velocity profiles were developed through consideration of the strain-compatible S-wave velocity, the groundwater table, and a maximum Poisson's ratio. For numerical purposes, the Poisson's ratio is limited to be less than 0.48. If the soil layer is above the groundwater table, the P-wave velocity ( $V_p$ ) is computed by:

$$V_p(V_s, \nu) = V_s \sqrt{\frac{2 - 2\nu}{1 - 2\nu}} \quad \text{Equation 3JJ-7}$$

where  $\nu$  is the Poisson's ratio of the soil. For soil layers below the groundwater table, the calculation of the P-wave is as follows: if the P-wave velocity of the material is higher than that of water (4800 ft/s) the P-wave will travel at the P-wave velocity of the material; if the P-wave velocity of the material is less than water, the P-wave will travel at the P-wave velocity of water unless it results in too high (>0.48) of a Poisson's ratio. For soft soils under the groundwater table, the combination of low  $V_s$  of soil and high  $V_p$  of water can introduce numerical stability issues as the Poisson's ratio approaches



0.50. Thus, a maximum of 0.48 is applied to  $\nu$  (i.e.,  $\nu_{\max}=0.48$ ). To summarize, the following equation is used to compute  $V_p$  of the soil ( $V_p^{\text{soil}}$ ) below the groundwater table:

$$V_p^{\text{soil}} = \max\{V_p(V_s^{\text{soil}}, \nu_{\text{soil}}), \min[V_p^{\text{water}}, V_p(V_s^{\text{soil}}, \nu_{\max})]\}$$
Equation 3JJ-8

where:

- $V_s^{\text{soil}}$  is the S-wave velocity of the soil,
- $\nu_{\text{soil}}$  is the Poisson's ratio of the soil,
- $V_p^{\text{water}}$  is the P-wave velocity of the water (4800 ft/s), and
- $\nu_{\max}$  is the maximum allowable Poisson's ratio (0.48).

In this sensitivity assessment, the best-estimate profile computed in the initial analyses using 60 simulated profiles was compared with the best-estimate profile computed using the logarithmic mean of three profiles.

### 3JJ.7.3 Site Response Analyses

The site response analyses performed in the sensitivity assessment were used to develop estimated site amplification and ARS and strain-compatible properties. An example of the sensitivity assessment is illustrated using the FAR site column and the HF4 and LF5 input motions that produce the smallest and largest corrective ratios due to the induced strain level. The mean ARS at the surface is computed as the arithmetic mean, Equation 3JJ-2, of the ARS computed by the LB, BE, and UB “updated” profiles, shown in [Figure 3JJ-250](#). The associated site amplification is shown in [Figure 3JJ-251](#). This process is repeated for the “initial” profile and the HF4 input motion, shown in [Figure 3JJ-252](#). The results indicate that these two profiles provide quite similar site amplifications.

While the dominant characteristics of the Turkey Point Units 6 & 7 site are captured by the limited number of soil column analysis, there are some differences between the sensitivity results and the site amplification computed in the original analyses. These differences are attributed to the greater number of profiles (i.e., 3 compared to 60) considered in the initial analyses. The computed corrected ratio for the HF4 input motion is shown in [Figure 3JJ-253](#).

A similar comparison for the LF5 motion is shown in [Figure 3JJ-254](#). In this case, the “updated” profile provides different results than the “initial” profile. This indicates that the differences are not due to the method used to develop the velocity profile. Instead, these differences are attributed to differing nonlinear curves; thus dependent on the induced strain level. Using the ratio between the “initial” and “updated” results, a corrective ratio is developed as shown in [Figure 3JJ-255](#). This ratio was applied to both the site amplification and ARS computed in the original analysis to estimate the rigorous results using the updated site properties. The sensitivity surface site amplification and ARS are shown in [Figures 3JJ-256 and 3JJ-257](#). This process of computing the results using the “initial” and “updated” site properties is repeated for all of the input motions, locations (NI and FAR), and elevations of interest.

The sensitivity assessment results of the site amplification and ARS are shown in [Figures 3JJ-258 through 3JJ-272](#).

In the RG 1.60 analyses, strain-compatible profiles were developed using full-column iterative site response to achieve a RG 1.60 spectrum at the foundation elevation. The approach used here is

iterative and consists of running the site response analysis using P-SHAKE, with modified rock motions (input at bedrock) convolved through each of the 3 profiles (LB, BE and UB) and computing the response at the foundation elevation horizon. The analysis is repeated, modifying the input rock motion each time, until the 5 percent damped mean ARS at the foundation horizon closely matches the SSE. As an example of this process, the first and tenth iterative of the FAR profile with “updated” site profiles are shown in [Figures 3JJ-273 and 3JJ-274](#), respectively. As shown in [Figure 3JJ-274](#), the computed spectra closely match the RG 1.60 spectrum, particularly at low- to mid-range frequencies which are important for strain-compatible soil properties. The iterative process is applied to both the “initial” and “updated” NI and FAR site columns. The best-estimate SSI profiles were computed using the logarithmic mean of the LB, BE, and UB S-wave velocity profiles.

Soil properties for input into the SSI analyses were developed based on the RG 1.60 motion at the foundation level, and for the Seismic Category II structures using the site-specific ground motion.

The associated strain compatible S-wave, P-wave and damping profiles for the RG 1.60 and site-specific input motions are shown in [Figures 3JJ-275 through 3JJ-286](#). The “estimated BE” in these figures is computed as the logarithmic mean of the three profiles (LB, BE and UB).

### 3JJ.7.4 Sensitivity Conclusions

A sensitivity assessment was performed using updated site properties obtained from supplemental site investigations to assess the impact on the GMRS, FIRS, and SSI properties for both the nuclear NI and FAR profiles. The following conclusions were made:

1. The RG 1.60 spectrum with a PGA of 0.1g motion envelopes the sensitivity NI FIRS (see [Figure 3JJ-262](#)) computed with three soil profiles as described in [Subsections 3JJ.7.2 and 3JJ.7.3](#). Thus, the previously established SSE is still valid, which was partially based on the RG 1.60 spectrum with a PGA of 0.1g motion.
2. The sensitivity horizontal GMRS (developed using the updated site characteristics) was also determined using three soil profiles and found to be slightly higher than the initial GMRS shown in [Figure 2.5.2-253](#). At a frequency of 100 Hz, the sensitivity horizontal GMRS increased from 0.058g to 0.062g at 100 Hz (a ratio of 1.07); with a maximum ground-motion change from 0.0635g to 0.0698g (a ratio of 1.10) at 45 Hz. Although the ratio of these differences may indicate a significant change due to the updated site properties, the difference of 0.004g at a frequency of 100 Hz and 0.006g at a frequency of 45 Hz is well within the confidence bounds of PSHA and seismic site response. Therefore, the GMRS developed based on either the initial or updated site properties both characterize the Turkey Point Units 6 & 7 site as a site with low seismic hazard.

The sensitivity assessment provided estimated motions and SSI properties as input for further sensitivity evaluations of the NI and Seismic Category II structures as described in [Appendix 3KK](#).

### 3JJ.8 References

201. U.S. Nuclear Regulatory Agency Letter, Nilesh C Chokshi, Deputy Division Director, Office of New Reactors, NRC to Adrian P. Hymer, Senior Director, NEI, dated January 9, 2009, Subject NEI Draft White Paper *Consistent Site-Response/Soil-Structure Interaction Analysis and Evaluation*, NRC ADAMS Accession No. ML083580072.
202. Nuclear Energy Institute letter, Adrian P Hymer, Senior Director of NEI to Nilesh C Chokshi, Deputy division director, Office of New Reactors, NRC, dated October 10, 2008, *Subject White paper in support of New Plant Applications*, NRC ADAMS Accession No. ML083020171.

**Table 3JJ-201 (Sheet 1 of 2)**  
**HF and LF Horizontal 10<sup>-4</sup> Site Spectra, and Raw and Smoothed Envelope**  
**UHRs Spectra for the FAR and NI Soil Columns at FIRS Horizon**

Horizontal 10 <sup>-4</sup> Site Spectra UHRs (g)								
Freq. Hz	FAR Soil Column FIRS Horizon UHRs		Raw Envelope	Smooth Envelope	NI Soil Column FIRS Horizon UHRs		Raw Envelope	Smooth Envelope
	LF SA(g)	HF SA(g)	SA(g)	SA(g)	LF SA(g)	HF SA(g)	SA(g)	SA(g)
100	4.84E-02	3.04E-02	4.84E-02	4.84E-02	4.73E-02	2.90E-02	4.73E-02	4.73E-02
90	4.85E-02	3.06E-02	4.85E-02	4.85E-02	4.74E-02	2.92E-02	4.74E-02	4.74E-02
80	4.88E-02	3.09E-02	4.88E-02	4.88E-02	4.76E-02	2.95E-02	4.76E-02	4.76E-02
70	4.93E-02	3.17E-02	4.93E-02	4.93E-02	4.81E-02	3.01E-02	4.81E-02	4.81E-02
60	5.03E-02	3.32E-02	5.03E-02	5.03E-02	4.91E-02	3.15E-02	4.91E-02	4.91E-02
50	5.23E-02	3.64E-02	5.23E-02	5.23E-02	5.06E-02	3.39E-02	5.06E-02	5.06E-02
45	5.36E-02	3.85E-02	5.36E-02	5.35E-02	5.14E-02	3.52E-02	5.14E-02	5.15E-02
40	5.48E-02	4.05E-02	5.48E-02	5.48E-02	5.28E-02	3.73E-02	5.28E-02	5.28E-02
35	5.64E-02	4.32E-02	5.64E-02	5.65E-02	5.50E-02	4.10E-02	5.50E-02	5.51E-02
30	6.01E-02	4.91E-02	6.01E-02	6.03E-02	5.90E-02	4.73E-02	5.90E-02	5.90E-02
25	6.67E-02	5.86E-02	6.67E-02	6.66E-02	6.35E-02	5.40E-02	6.35E-02	6.35E-02
20	6.90E-02	6.19E-02	6.90E-02	6.86E-02	6.47E-02	5.59E-02	6.47E-02	6.44E-02
15	6.47E-02	5.61E-02	6.47E-02	6.45E-02	6.24E-02	5.27E-02	6.24E-02	6.24E-02
12.5	6.35E-02	5.45E-02	6.35E-02	6.34E-02	6.15E-02	5.20E-02	6.15E-02	6.17E-02
10	6.57E-02	5.62E-02	6.57E-02	6.55E-02	6.32E-02	5.35E-02	6.32E-02	6.32E-02
9	6.73E-02	5.84E-02	6.73E-02	6.71E-02	6.41E-02	5.43E-02	6.41E-02	6.41E-02
8	6.83E-02	5.94E-02	6.83E-02	6.82E-02	6.44E-02	5.49E-02	6.44E-02	6.48E-02
7	6.77E-02	5.85E-02	6.77E-02	6.76E-02	6.64E-02	5.70E-02	6.64E-02	6.58E-02
6	6.63E-02	5.63E-02	6.63E-02	6.68E-02	6.72E-02	5.79E-02	6.72E-02	6.77E-02
5	6.97E-02	6.03E-02	6.97E-02	6.94E-02	7.21E-02	6.23E-02	7.21E-02	7.15E-02
4	6.57E-02	5.09E-02	6.57E-02	6.63E-02	6.55E-02	5.05E-02	6.55E-02	6.64E-02
3	8.08E-02	6.12E-02	8.08E-02	8.06E-02	7.97E-02	5.94E-02	7.97E-02	7.92E-02
2.5	8.98E-02	6.00E-02	8.98E-02	8.82E-02	8.34E-02	5.49E-02	8.34E-02	8.23E-02
2	7.41E-02	4.11E-02	7.41E-02	7.34E-02	6.92E-02	3.78E-02	6.92E-02	6.89E-02
1.5	6.72E-02	2.87E-02	6.72E-02	6.72E-02	6.42E-02	2.69E-02	6.42E-02	6.43E-02
1.25	7.35E-02	2.71E-02	7.35E-02	7.35E-02	7.15E-02	2.62E-02	7.15E-02	7.18E-02
1	8.45E-02	2.48E-02	8.45E-02	8.59E-02	8.34E-02	2.43E-02	8.34E-02	8.49E-02
0.9	1.00E-01	2.60E-02	1.00E-01	9.94E-02	9.86E-02	2.54E-02	9.86E-02	9.79E-02
0.8	1.10E-01	2.47E-02	1.10E-01	1.07E-01	1.09E-01	2.43E-02	1.09E-01	1.06E-01
0.7	9.93E-02	1.89E-02	9.93E-02	9.99E-02	9.97E-02	1.88E-02	9.97E-02	1.00E-01
0.6	9.19E-02	1.49E-02	9.19E-02	9.18E-02	9.31E-02	1.50E-02	9.31E-02	9.28E-02
0.5	7.97E-02	1.09E-02	7.97E-02	7.76E-02	8.02E-02	1.09E-02	8.02E-02	7.82E-02
0.4	4.72E-02	6.38E-03	4.72E-02	4.80E-02	4.80E-02	6.45E-03	4.80E-02	4.88E-02
0.3	3.09E-02	4.19E-03	3.09E-02	3.10E-02	3.12E-02	4.21E-03	3.12E-02	3.14E-02
0.2	2.05E-02	2.80E-03	2.05E-02	2.05E-02	2.03E-02	2.76E-03	2.03E-02	2.02E-02
0.15	1.30E-02	1.81E-03	1.30E-02	1.31E-02	1.28E-02	1.78E-03	1.28E-02	1.29E-02

**Table 3JJ-201 (Sheet 2 of 2)**  
**HF and LF Horizontal  $10^{-4}$  Site Spectra, and Raw and Smoothed Envelope**  
**UHRs Spectra for the FAR and NI Soil Columns at FIRS Horizon**

Horizontal $10^{-4}$ Site Spectra UHRs (g)								
Freq. Hz	FAR Soil Column FIRS Horizon UHRs		Raw Envelope	Smooth Envelope	NI Soil Column FIRS Horizon UHRs		Raw Envelope	Smooth Envelope
	LF SA(g)	HF SA(g)	SA(g)	SA(g)	LF SA(g)	HF SA(g)	SA(g)	SA(g)
0.125	9.55E-03	1.36E-03	9.55E-03	9.48E-03	9.45E-03	1.34E-03	9.45E-03	9.38E-03
0.1	5.71E-03	8.02E-04	5.71E-03	5.71E-03	5.67E-03	7.95E-04	5.67E-03	5.67E-03

**Notes:**

FIRS = Foundation input response spectrum  
 UHRs = Uniform hazard response spectra  
 LF = Low frequencies  
 HF = High frequencies  
 SA = Spectral acceleration  
 Amp = Amplitude

**Table 3JJ-202 (Sheet 1 of 2)**  
**HF and LF Horizontal 10<sup>-5</sup> Site Spectra, and Raw and Smoothed Envelope**  
**UHRs Spectra for the FAR and NI Soil Columns at FIRS Horizon**

Horizontal 10 <sup>-5</sup> Site Spectra UHRs (g)								
Freq. Hz	FAR Soil Column FIRS Horizon UHRs		Raw Envelope	Smooth Envelope	NI Soil Column FIRS Horizon UHRs		Raw Envelope	Smooth Envelope
	LF SA(g)	HF SA(g)	SA(g)	SA(g)	LF SA(g)	HF SA(g)	SA(g)	SA(g)
100	1.05E-01	8.62E-02	1.05E-01	1.05E-01	1.02E-01	8.24E-02	1.02E-01	1.02E-01
90	1.05E-01	8.68E-02	1.05E-01	1.05E-01	1.02E-01	8.30E-02	1.02E-01	1.02E-01
80	1.05E-01	8.79E-02	1.05E-01	1.05E-01	1.03E-01	8.40E-02	1.03E-01	1.03E-01
70	1.06E-01	9.02E-02	1.06E-01	1.06E-01	1.04E-01	8.62E-02	1.04E-01	1.04E-01
60	1.09E-01	9.51E-02	1.09E-01	1.09E-01	1.06E-01	9.06E-02	1.06E-01	1.06E-01
50	1.13E-01	1.06E-01	1.13E-01	1.13E-01	1.10E-01	9.88E-02	1.10E-01	1.10E-01
45	1.17E-01	1.14E-01	1.17E-01	1.17E-01	1.12E-01	1.04E-01	1.12E-01	1.12E-01
40	1.21E-01	1.21E-01	1.21E-01	1.22E-01	1.17E-01	1.12E-01	1.17E-01	1.17E-01
35	1.28E-01	1.33E-01	1.33E-01	1.34E-01	1.25E-01	1.26E-01	1.26E-01	1.28E-01
30	1.42E-01	1.56E-01	1.56E-01	1.57E-01	1.40E-01	1.52E-01	1.52E-01	1.52E-01
25	1.68E-01	1.95E-01	1.95E-01	1.94E-01	1.58E-01	1.80E-01	1.80E-01	1.79E-01
20	1.78E-01	2.06E-01	2.06E-01	2.04E-01	1.65E-01	1.87E-01	1.87E-01	1.85E-01
15	1.62E-01	1.76E-01	1.76E-01	1.75E-01	1.56E-01	1.67E-01	1.67E-01	1.67E-01
12.5	1.54E-01	1.63E-01	1.63E-01	1.62E-01	1.50E-01	1.58E-01	1.58E-01	1.58E-01
10	1.60E-01	1.65E-01	1.65E-01	1.64E-01	1.55E-01	1.59E-01	1.59E-01	1.59E-01
9	1.63E-01	1.66E-01	1.66E-01	1.67E-01	1.58E-01	1.60E-01	1.60E-01	1.59E-01
8	1.68E-01	1.70E-01	1.70E-01	1.69E-01	1.58E-01	1.59E-01	1.59E-01	1.59E-01
7	1.67E-01	1.65E-01	1.67E-01	1.67E-01	1.61E-01	1.59E-01	1.61E-01	1.60E-01
6	1.58E-01	1.50E-01	1.58E-01	1.59E-01	1.57E-01	1.50E-01	1.57E-01	1.59E-01
5	1.63E-01	1.58E-01	1.63E-01	1.62E-01	1.75E-01	1.72E-01	1.75E-01	1.73E-01
4	1.54E-01	1.33E-01	1.54E-01	1.55E-01	1.56E-01	1.34E-01	1.56E-01	1.58E-01
3	1.70E-01	1.46E-01	1.70E-01	1.70E-01	1.70E-01	1.44E-01	1.70E-01	1.68E-01
2.5	1.84E-01	1.46E-01	1.84E-01	1.82E-01	1.73E-01	1.34E-01	1.73E-01	1.72E-01
2	1.55E-01	9.90E-02	1.55E-01	1.53E-01	1.43E-01	9.06E-02	1.43E-01	1.43E-01
1.5	1.32E-01	6.54E-02	1.32E-01	1.32E-01	1.25E-01	6.12E-02	1.25E-01	1.26E-01
1.25	1.41E-01	6.07E-02	1.41E-01	1.41E-01	1.37E-01	5.85E-02	1.37E-01	1.37E-01
1	1.53E-01	5.41E-02	1.53E-01	1.56E-01	1.51E-01	5.32E-02	1.51E-01	1.54E-01
0.9	1.81E-01	5.65E-02	1.81E-01	1.80E-01	1.78E-01	5.52E-02	1.78E-01	1.77E-01
0.8	2.05E-01	5.40E-02	2.05E-01	1.99E-01	2.03E-01	5.31E-02	2.03E-01	1.98E-01
0.7	1.91E-01	4.13E-02	1.91E-01	1.91E-01	1.92E-01	4.11E-02	1.92E-01	1.92E-01
0.6	1.78E-01	3.19E-02	1.78E-01	1.78E-01	1.80E-01	3.21E-02	1.80E-01	1.80E-01
0.5	1.56E-01	2.29E-02	1.56E-01	1.52E-01	1.57E-01	2.29E-02	1.57E-01	1.53E-01
0.4	9.26E-02	1.33E-02	9.26E-02	9.42E-02	9.43E-02	1.34E-02	9.43E-02	9.57E-02
0.3	6.01E-02	8.64E-03	6.01E-02	6.04E-02	6.08E-02	8.70E-03	6.08E-02	6.11E-02
0.2	3.98E-02	5.78E-03	3.98E-02	3.98E-02	3.93E-02	5.69E-03	3.93E-02	3.93E-02
0.15	2.53E-02	3.82E-03	2.53E-02	2.54E-02	2.50E-02	3.76E-03	2.50E-02	2.51E-02



**Table 3JJ-202 (Sheet 2 of 2)**  
**HF and LF Horizontal  $10^{-5}$  Site Spectra, and Raw and Smoothed Envelope**  
**UHRs Spectra for the FAR and NI Soil Columns at FIRS Horizon**

Horizontal $10^{-5}$ Site Spectra UHRs (g)								
Freq. Hz	FAR Soil Column FIRS Horizon UHRs		Raw Envelope	Smooth Envelope	NI Soil Column FIRS Horizon UHRs		Raw Envelope	Smooth Envelope
	LF SA(g)	HF SA(g)	SA(g)	SA(g)	LF SA(g)	HF SA(g)	SA(g)	SA(g)
0.125	1.86E-02	2.86E-03	1.86E-02	1.85E-02	1.84E-02	2.82E-03	1.84E-02	1.83E-02
0.1	1.11E-02	1.69E-03	1.11E-02	1.11E-02	1.10E-02	1.67E-03	1.10E-02	1.10E-02

**Notes:**

FIRS = Foundation input response spectrum  
 UHRs = Uniform hazard response spectra  
 LF = Low frequencies  
 HF = High frequencies  
 SA = Spectral acceleration  
 Amp = Amplitude

**Table 3JJ-203 (Sheet 1 of 2)**  
**Horizontal  $10^{-4}$  and  $10^{-5}$  Smoothed Site Spectra, Values of  $A_R$  and  $DF$ , and**  
**DRS for the FAR Soil Column at FIRS Horizon**

Freq. Hz	Horizontal $10^{-4}$	Horizontal $10^{-5}$	$A_R$	$DF$	Horizontal DRS
100	4.84E-02	1.05E-01	2.16	1.11	5.38E-02
90	4.85E-02	1.05E-01	2.16	1.11	5.39E-02
80	4.88E-02	1.05E-01	2.16	1.11	5.42E-02
70	4.93E-02	1.06E-01	2.16	1.11	5.47E-02
60	5.03E-02	1.09E-01	2.16	1.11	5.59E-02
50	5.23E-02	1.13E-01	2.17	1.11	5.82E-02
45	5.35E-02	1.17E-01	2.19	1.12	6.01E-02
40	5.48E-02	1.22E-01	2.23	1.14	6.25E-02
35	5.65E-02	1.34E-01	2.37	1.20	6.76E-02
30	6.03E-02	1.57E-01	2.61	1.29	7.78E-02
25	6.66E-02	1.94E-01	2.91	1.41	9.41E-02
20	6.86E-02	2.04E-01	2.97	1.43	9.83E-02
15	6.45E-02	1.75E-01	2.71	1.33	8.59E-02
12.5	6.34E-02	1.62E-01	2.56	1.27	8.07E-02
10	6.55E-02	1.64E-01	2.50	1.25	8.17E-02
9	6.71E-02	1.67E-01	2.48	1.24	8.34E-02
8	6.82E-02	1.69E-01	2.48	1.24	8.47E-02
7	6.76E-02	1.67E-01	2.46	1.23	8.34E-02
6	6.68E-02	1.59E-01	2.38	1.20	8.03E-02
5	6.94E-02	1.62E-01	2.34	1.18	8.22E-02
4	6.63E-02	1.55E-01	2.33	1.18	7.84E-02
3	8.06E-02	1.70E-01	2.10	1.09	8.77E-02
2.5	8.82E-02	1.82E-01	2.06	1.07	9.45E-02
2	7.34E-02	1.53E-01	2.09	1.08	7.94E-02
1.5	6.72E-02	1.32E-01	1.96	1.03	6.92E-02
1.25	7.35E-02	1.41E-01	1.92	1.01	7.43E-02
1	8.59E-02	1.56E-01	1.82	1.00	8.59E-02
0.9	9.94E-02	1.80E-01	1.82	1.00	9.94E-02
0.8	1.07E-01	1.99E-01	1.86	1.00	1.07E-01
0.7	9.99E-02	1.91E-01	1.92	1.01	1.01E-01
0.6	9.18E-02	1.78E-01	1.94	1.02	9.36E-02
0.5	7.76E-02	1.52E-01	1.96	1.03	7.98E-02
0.4	4.80E-02	9.42E-02	1.96	1.03	4.94E-02
0.3	3.10E-02	6.04E-02	1.95	1.02	3.17E-02
0.2	2.05E-02	3.98E-02	1.94	1.02	2.09E-02
0.15	1.31E-02	2.54E-02	1.95	1.02	1.34E-02

**Table 3JJ-203 (Sheet 2 of 2)**  
**Horizontal  $10^{-4}$  and  $10^{-5}$  Smoothed Site Spectra, Values of  $A_R$  and  $DF$ , and**  
**DRS for the FAR Soil Column at FIRS Horizon**

<b>Freq. Hz</b>	<b>Horizontal <math>10^{-4}</math></b>	<b>Horizontal <math>10^{-5}</math></b>	<b><math>A_R</math></b>	<b><math>DF</math></b>	<b>Horizontal DRS</b>
0.125	9.48E-03	1.85E-02	1.95	1.02	9.69E-03
0.1	5.71E-03	1.11E-02	1.94	1.02	5.83E-03

**Notes:**

FIRS = Foundation input response spectrum

$A_R$  and  $DF$  are defined in Equations 3JJ-1 and 3JJ-2, respectively.

DRS = Design response spectrum, defined in Equation 3JJ-3

**Table 3JJ-204 (Sheet 1 of 2)**  
**Horizontal  $10^{-4}$  and  $10^{-5}$  Smoothed Site Spectra, Values of  $A_R$  and  $DF$ , and**  
**DRS for the NI Soil Column at FIRS Horizon**

Freq. Hz	Horizontal $10^{-4}$	Horizontal $10^{-5}$	$A_R$	$DF$	Horizontal DRS
100	4.73E-02	1.02E-01	2.16	1.11	5.25E-02
90	4.74E-02	1.02E-01	2.16	1.11	5.27E-02
80	4.76E-02	1.03E-01	2.16	1.11	5.29E-02
70	4.81E-02	1.04E-01	2.16	1.11	5.34E-02
60	4.91E-02	1.06E-01	2.16	1.11	5.45E-02
50	5.06E-02	1.10E-01	2.17	1.11	5.64E-02
45	5.15E-02	1.12E-01	2.18	1.12	5.77E-02
40	5.28E-02	1.17E-01	2.22	1.13	5.99E-02
35	5.51E-02	1.28E-01	2.32	1.18	6.49E-02
30	5.90E-02	1.52E-01	2.58	1.28	7.54E-02
25	6.35E-02	1.79E-01	2.82	1.37	8.73E-02
20	6.44E-02	1.85E-01	2.87	1.40	8.99E-02
15	6.24E-02	1.67E-01	2.67	1.32	8.22E-02
12.5	6.17E-02	1.58E-01	2.57	1.28	7.87E-02
10	6.32E-02	1.59E-01	2.51	1.25	7.92E-02
9	6.41E-02	1.59E-01	2.49	1.24	7.97E-02
8	6.48E-02	1.59E-01	2.46	1.23	7.99E-02
7	6.58E-02	1.60E-01	2.43	1.22	8.03E-02
6	6.77E-02	1.59E-01	2.35	1.19	8.04E-02
5	7.15E-02	1.73E-01	2.42	1.22	8.71E-02
4	6.64E-02	1.58E-01	2.38	1.20	7.97E-02
3	7.92E-02	1.68E-01	2.13	1.10	8.69E-02
2.5	8.23E-02	1.72E-01	2.08	1.08	8.89E-02
2	6.89E-02	1.43E-01	2.07	1.08	7.41E-02
1.5	6.43E-02	1.26E-01	1.95	1.03	6.59E-02
1.25	7.18E-02	1.37E-01	1.91	1.01	7.22E-02
1	8.49E-02	1.54E-01	1.82	1.00	8.49E-02
0.9	9.79E-02	1.77E-01	1.81	1.00	9.79E-02
0.8	1.06E-01	1.98E-01	1.86	1.00	1.06E-01
0.7	1.00E-01	1.92E-01	1.92	1.01	1.01E-01
0.6	9.28E-02	1.80E-01	1.94	1.02	9.46E-02
0.5	7.82E-02	1.53E-01	1.96	1.03	8.04E-02
0.4	4.88E-02	9.57E-02	1.96	1.03	5.02E-02
0.3	3.14E-02	6.11E-02	1.95	1.02	3.21E-02
0.2	2.02E-02	3.93E-02	1.94	1.02	2.06E-02
0.15	1.29E-02	2.51E-02	1.95	1.02	1.32E-02

**Table 3JJ-204 (Sheet 2 of 2)**  
**Horizontal  $10^{-4}$  and  $10^{-5}$  Smoothed Site Spectra, Values of  $A_R$  and  $DF$ , and**  
**DRS for the NI Soil Column at FIRS Horizon**

<b>Freq. Hz</b>	<b>Horizontal <math>10^{-4}</math></b>	<b>Horizontal <math>10^{-5}</math></b>	<b><math>A_R</math></b>	<b><math>DF</math></b>	<b>Horizontal DRS</b>
0.125	9.38E-03	1.83E-02	1.95	1.02	9.59E-03
0.1	5.67E-03	1.10E-02	1.94	1.02	5.79E-03

**Notes:**

FIRS = Foundation input response spectrum

$A_R$  and  $DF$  are defined in Equations 3JJ-1 and 3JJ-2, respectively.

DRS = Design response spectrum, defined in Equation 3JJ-3



**Table 3JJ-205 (Sheet 1 of 2)**  
**V/H Ratios, Vertical  $10^{-4}$  and  $10^{-5}$  Smoothed Site Spectra, Values of  $A_R$  and DF, and DRS for the FAR Soil Column at FIRS Horizon**

Freq. Hz	V/H	Vertical $10^{-4}$	Vertical $10^{-5}$	$A_R$	DF	Vertical DRS
100	1.000	4.84E-02	1.05E-01	2.16	1.11	5.38E-02
90	1.000	4.85E-02	1.05E-01	2.16	1.11	5.39E-02
80	1.000	4.88E-02	1.05E-01	2.16	1.11	5.42E-02
70	1.000	4.93E-02	1.06E-01	2.16	1.11	5.47E-02
60	1.000	5.03E-02	1.09E-01	2.16	1.11	5.59E-02
50	1.000	5.23E-02	1.13E-01	2.17	1.11	5.82E-02
45	1.000	5.35E-02	1.17E-01	2.19	1.12	6.01E-02
40	1.000	5.48E-02	1.22E-01	2.23	1.14	6.25E-02
35	1.000	5.65E-02	1.34E-01	2.37	1.20	6.76E-02
30	1.000	6.03E-02	1.57E-01	2.61	1.29	7.78E-02
25	1.000	6.66E-02	1.94E-01	2.91	1.41	9.41E-02
20	1.000	6.86E-02	2.04E-01	2.97	1.43	9.83E-02
15	1.000	6.45E-02	1.75E-01	2.71	1.33	8.59E-02
12.5	1.000	6.34E-02	1.62E-01	2.56	1.27	8.07E-02
10	1.000	6.55E-02	1.64E-01	2.50	1.25	8.17E-02
9	1.000	6.71E-02	1.67E-01	2.48	1.24	8.34E-02
8	1.000	6.82E-02	1.69E-01	2.48	1.24	8.47E-02
7	1.000	6.76E-02	1.66E-01	2.46	1.23	8.34E-02
6	0.999	6.68E-02	1.59E-01	2.38	1.20	8.03E-02
5	0.999	6.93E-02	1.62E-01	2.34	1.18	8.21E-02
4	0.999	6.63E-02	1.55E-01	2.33	1.18	7.83E-02
3	0.857	6.90E-02	1.45E-01	2.10	1.09	7.51E-02
2.5	0.715	6.31E-02	1.30E-01	2.06	1.07	6.76E-02
2	0.710	5.21E-02	1.09E-01	2.09	1.08	5.64E-02
1.5	0.704	4.73E-02	9.29E-02	1.96	1.03	4.87E-02
1.25	0.701	5.15E-02	9.88E-02	1.92	1.01	5.20E-02
1	0.696	5.98E-02	1.09E-01	1.82	1.00	5.98E-02
0.9	0.694	6.89E-02	1.25E-01	1.82	1.00	6.89E-02
0.8	0.691	7.42E-02	1.38E-01	1.86	1.00	7.42E-02
0.7	0.689	6.88E-02	1.32E-01	1.92	1.01	6.95E-02
0.6	0.686	6.30E-02	1.22E-01	1.94	1.02	6.42E-02
0.5	0.682	5.29E-02	1.04E-01	1.96	1.03	5.44E-02
0.4	0.678	3.25E-02	6.38E-02	1.96	1.03	3.35E-02
0.3	0.672	2.08E-02	4.06E-02	1.95	1.02	2.13E-02
0.2	0.668	1.37E-02	2.66E-02	1.94	1.02	1.40E-02
0.15	0.668	8.73E-03	1.70E-02	1.95	1.02	8.93E-03

**Table 3JJ-205 (Sheet 2 of 2)**  
**V/H Ratios, Vertical  $10^{-4}$  and  $10^{-5}$  Smoothed Site Spectra, Values of  $A_R$  and DF, and DRS for the FAR Soil Column at FIRS Horizon**

<b>Freq. Hz</b>	<b>V/H</b>	<b>Vertical <math>10^{-4}</math></b>	<b>Vertical <math>10^{-5}</math></b>	<b><math>A_R</math></b>	<b>DF</b>	<b>Vertical DRS</b>
0.125	0.668	6.34E-03	1.23E-02	1.95	1.02	6.48E-03
0.1	0.668	3.82E-03	7.42E-03	1.94	1.02	3.90E-03

**Notes:**

FIRS = Foundation input response spectrum

$A_R$  and DF are defined in Equations 3JJ-1 and 3JJ-2, respectively.

DRS = Design response spectrum, defined in Equation 3JJ-3

**Table 3JJ-206 (Sheet 1 of 2)**  
**V/H Ratios, Vertical  $10^{-4}$  and  $10^{-5}$  Smoothed Site Spectra, Values of  $A_R$  and DF, and DRS for the NI Soil Column at FIRS Horizon**

Freq. Hz	V/H	Vertical $10^{-4}$	Vertical $10^{-5}$	$A_R$	DF	Vertical DRS
100	1.000	4.73E-02	1.02E-01	2.16	1.11	5.25E-02
90	1.000	4.74E-02	1.02E-01	2.16	1.11	5.27E-02
80	1.000	4.76E-02	1.03E-01	2.16	1.11	5.29E-02
70	1.000	4.81E-02	1.04E-01	2.16	1.11	5.34E-02
60	1.000	4.91E-02	1.06E-01	2.16	1.11	5.45E-02
50	1.000	5.06E-02	1.10E-01	2.17	1.11	5.64E-02
45	1.000	5.15E-02	1.12E-01	2.18	1.12	5.77E-02
40	1.000	5.28E-02	1.17E-01	2.22	1.13	5.99E-02
35	1.000	5.51E-02	1.28E-01	2.32	1.18	6.49E-02
30	1.000	5.90E-02	1.52E-01	2.58	1.28	7.54E-02
25	1.000	6.35E-02	1.79E-01	2.82	1.37	8.73E-02
20	1.000	6.44E-02	1.85E-01	2.87	1.40	8.99E-02
15	1.000	6.24E-02	1.67E-01	2.67	1.32	8.22E-02
12.5	1.000	6.17E-02	1.58E-01	2.57	1.28	7.87E-02
10	1.000	6.32E-02	1.59E-01	2.51	1.25	7.92E-02
9	1.000	6.41E-02	1.59E-01	2.49	1.24	7.97E-02
8	1.000	6.48E-02	1.59E-01	2.46	1.23	7.99E-02
7	1.000	6.58E-02	1.60E-01	2.43	1.22	8.03E-02
6	0.999	6.76E-02	1.59E-01	2.35	1.19	8.04E-02
5	0.999	7.14E-02	1.73E-01	2.42	1.22	8.70E-02
4	0.999	6.63E-02	1.58E-01	2.38	1.20	7.96E-02
3	0.857	6.78E-02	1.44E-01	2.13	1.10	7.45E-02
2.5	0.715	5.89E-02	1.23E-01	2.08	1.08	6.36E-02
2	0.710	4.89E-02	1.01E-01	2.07	1.08	5.26E-02
1.5	0.704	4.53E-02	8.85E-02	1.95	1.03	4.64E-02
1.25	0.701	5.03E-02	9.59E-02	1.91	1.01	5.06E-02
1	0.696	5.91E-02	1.07E-01	1.82	1.00	5.91E-02
0.9	0.694	6.79E-02	1.23E-01	1.81	1.00	6.79E-02
0.8	0.691	7.36E-02	1.37E-01	1.86	1.00	7.36E-02
0.7	0.689	6.90E-02	1.32E-01	1.92	1.01	6.97E-02
0.6	0.686	6.37E-02	1.23E-01	1.94	1.02	6.49E-02
0.5	0.682	5.33E-02	1.05E-01	1.96	1.03	5.48E-02
0.4	0.678	3.31E-02	6.49E-02	1.96	1.03	3.40E-02
0.3	0.672	2.11E-02	4.11E-02	1.95	1.02	2.16E-02
0.2	0.668	1.35E-02	2.63E-02	1.94	1.02	1.38E-02
0.15	0.668	8.61E-03	1.68E-02	1.95	1.02	8.81E-03

**Table 3JJ-206 (Sheet 2 of 2)**  
**V/H Ratios, Vertical  $10^{-4}$  and  $10^{-5}$  Smoothed Site Spectra, Values of  $A_R$  and DF, and DRS for the NI Soil Column at FIRS Horizon**

<b>Freq. Hz</b>	<b>V/H</b>	<b>Vertical <math>10^{-4}</math></b>	<b>Vertical <math>10^{-5}</math></b>	<b><math>A_R</math></b>	<b>DF</b>	<b>Vertical DRS</b>
0.125	0.668	6.27E-03	1.22E-02	1.95	1.02	6.41E-03
0.1	0.668	3.79E-03	7.37E-03	1.94	1.02	3.87E-03

**Notes:**

FIRS = Foundation input response spectrum

$A_R$  and DF are defined in Equations 3JJ-1 and 3JJ-2, respectively.

DRS = Design response spectrum, defined in Equation 3JJ-3

**Table 3JJ-207**  
**Recommended Horizontal and Vertical FIRS**

<b>FIRS Frequency (Hz)</b>	<b>Horizontal Sa(g)</b>	<b>Vertical Sa(g)</b>
100	5.38E-02	5.38E-02
90	5.39E-02	5.39E-02
80	5.42E-02	5.42E-02
70	5.47E-02	5.47E-02
60	5.59E-02	5.59E-02
50	5.82E-02	5.82E-02
45	6.01E-02	6.01E-02
40	6.25E-02	6.25E-02
35	6.76E-02	6.76E-02
30.0	7.78E-02	7.78E-02
25	9.41E-02	9.41E-02
20	9.83E-02	9.83E-02
15	8.59E-02	8.59E-02
12.5	8.07E-02	8.07E-02
10	8.17E-02	8.17E-02
9	8.34E-02	8.34E-02
8	8.47E-02	8.47E-02
7	8.34E-02	8.34E-02
6	8.04E-02	8.04E-02
5	8.71E-02	8.70E-02
4	7.97E-02	7.96E-02
3	8.77E-02	7.51E-02
2.5	9.45E-02	6.76E-02
2	7.94E-02	5.64E-02
1.5	6.92E-02	4.87E-02
1.25	7.43E-02	5.20E-02
1	8.59E-02	5.98E-02
0.9	9.94E-02	6.89E-02
0.8	1.07E-01	7.42E-02
0.7	1.01E-01	6.97E-02
0.6	9.46E-02	6.49E-02
0.5	8.04E-02	5.48E-02
0.4	5.02E-02	3.40E-02
0.3	3.21E-02	2.16E-02
0.2	2.09E-02	1.40E-02
0.15	1.34E-02	8.93E-03
0.125	9.69E-03	6.48E-03
0.1	5.83E-03	3.90E-03



**Table 3JJ-208**  
**Absolute Value of the Zero-Lag Cross Correlations Between Components for**  
**the Spectrum Compatible Time Histories Developed for the SSI Analysis**

Components	Cross Correlation
H1 - H2	0.078
H1 - UP	0.036
H2 - UP	0.051

**Table 3JJ-209**  
**SSI Motion Adjustment Factors**

Site Condition	Run Label	Adjustment Factor
Near Nuclear Island (NI)	NI-H1-LB	1.00
	NI-H2-LB	1.01
	NI-UP-LB	1.00
	NI-H1-BE	1.00
	NI-H2-BE	1.00
	NI-UP-BE	1.00
	NI-H1-UB	1.00
	NI-H2-UB	1.00
	NI-UP-UB	1.12
Far From Nuclear Island (FAR)	FAR-H1-LB	1.00
	FAR-H2-LB	1.00
	FAR-UP-LB	1.00
	FAR-H1-BE	1.00
	FAR-H2-BE	1.00
	FAR-UP-BE	1.00
	FAR-H1-UB	1.07
	FAR-H2-UB	1.04
	FAR-UP-UB	1.12

**Table 3JJ-210**  
**Key Elevations for Calculation of the Ground Motion**

<b>Description</b>	<b>Elevation [ft]</b>	<b>Depth Below Grade [ft]</b>	<b>NI Profile</b>	<b>FAR Profile</b>
Finished Grade	+25.5	0.0	X	X
Top of MSE Wall	+20.5	5.0		X
Turbine Building Peripheral East and West Sections	+18.5	7.0	X	X
Bottom of Turbine Building Foundation	+1.3	24.2	X	X
Bottom of MSE Wall	+0.5	25.0		X
NI Foundation	-16.0	41.5	X	X
GMRS Elevation	-35.0	60.5		X

Note: The groundwater table level is defined at El. +0.5 ft, at a depth of 25 ft below finished grade.

**Table 3JJ-211**  
**Site Profiles for the “Initial” Models**

Far Field (FAR)			Nuclear Island (NI)		
Layer	Elevation Top [ft]	Thickness [ft]	Layer	Elevation Top [ft]	Thickness [ft]
Fill	25.5	30.5	Fill	25.5	41.5*
Miami Limestone	-5.0	26.0	Concrete	-16.0*	19.0*
Key Largo Limestone	-31.0	90.0	Key Largo Limestone	-35.0*	86.0*
Tamiami/Hawthorn	-121.0	330.0	Tamiami/Hawthorn	-121.0	330.0
Hawthorn Lower	-451.0	160.0	Hawthorn Lower	-451.0	160.0
Sonic-log data (linear)	-611.0	11364.0	Sonic-log data (linear)	-611.0	11364.0
Half-space	-11975.0	—	Half-space	-11975.0	—

\* Indicates different values between the FAR and NI profiles.

**Table 3JJ-212**  
**Site Profiles for the Sensitivity Model**

Far Field (FAR)			Nuclear Island (NI)		
Layer	Elevation Top [ft]	Thickness [ft]	Layer	Elevation Top [ft]	Thickness [ft]
Fill	25.5	30.2*	Fill	25.5	41.5*
Miami Limestone	-4.7*	22.2*	Concrete	-16.0*	19.0*
Key Largo Limestone	-26.9*	22.5*	Key Largo Limestone	-35.0*	14.4*
Fort Thompson Limestone	-49.4	66.0	Fort Thompson Limestone	-49.4	66.0
Upper Tamiami Formation	-115.4	52.2	Upper Tamiami Formation	-115.4	52.2
Lower Tamiami Formation	-167.6	50.2	Lower Tamiami Formation	-167.6	50.2
Peace River Formation	-217.8	237.0	Peace River Formation	-217.8	237.0
Arcadia	-454.8	156.2	Arcadia	-454.8	156.2
Sonic-log data (linear)	-611.0	11364.0	Sonic-log data (linear)	-611.0	11364.0
Half-space	-11975.0	—	Half-space	-11975.0	—

\* Indicates different values between the FAR and NI profiles.

**Table 3JJ-213**  
**G/G<sub>max</sub> and Damping Model and Units Weights used for the Units in the “Initial” Profile**

Layer	Unit Wt. [pcf]	G/G <sub>max</sub> Model	Damping Model
Fill	130.0	Structural Fill	Structural Fill
Concrete	150.0	Linear	Linear (D=1.00%)
Miami Limestone	125.0	Miami Limestone	Miami Limestone
Key Largo Limestone	136.0	Linear	Linear (D=1.00%)
Tamiami/Hawthorn	120.0	Natural Soil (El.>-151 ft) (Original) Natural Soil (El.<-151 ft) (Original)	Natural Soil (Original)
Hawthorn Lower	130.0	Natural Soil (El.<-151 ft) (Original)	Natural Soil (Original)
Sonic-log data (linear)	130.0	Linear	Linear (D=0.32%)
Half-space	170.0	Linear	Linear (D=1.00%)

**Table 3JJ-214**  
**G/G<sub>max</sub> and Damping Models and Units Weights used for the Units in the Sensitivity Model**

Layer	Unit Wt. [pcf]	G/G <sub>max</sub> Model	Damping Model
Fill	130.0*	Structural Fill*	Structural Fill*
Concrete	150.0*	Linear*	Linear (D=1.00%)*
Miami Limestone	125.0*	Miami Limestone*	Miami Limestone*
Key Largo Limestone	137.1	Key Largo	Key Largo & Fort Thompson
Fort Thompson Limestone	137.0	Fort Thompson	
Upper Tamiami Formation	119.3	Natural Soil (El.>-151 ft) (Updated) Natural Soil (El.<-151 ft) (Updated)	Natural Soil (Updated)
Lower Tamiami Formation	116.7	Natural Soil (El.<-151 ft) (Updated)	
Peace River Formation	120.6		
Arcadia	129.0		
Sonic-log data (linear)	130.0*	Linear*	Linear (D=0.32%)*
Half-space	170.0*		Linear (D=1.00%)*

\*Indicates that updated values were not provided and values from the “initial” model were selected for use

**Table 3JJ-215**  
**Summary of Computed FIRS, DRS, and GMRS**

DRS Description	Horizons Considered	Elevation [ft]	Depth Below Grade [ft]	Profile Type	Profile	
					NI	FAR
NI FIRS	Bottom of NI Foundation	-16.0	41.5	Full Column	X	X
Surface DRS for Annex Building (AB)	Finished Grade	+25.5	0.0	Full Column	X	X
	Top of MSE Wall	+20.5	5.0	Full Column		X
	Bottom of MSE Wall	+0.5	25.0	Full Column		X
Turbine Building (TB) FIRS	Finished Grade	+25.5	0.0	Full Column	X	X
	Peripheral East and West Sections	+18.5	7.0	Truncated Column	X	X
	Bottom of TB Foundation	+1.3	24.2	Truncated Column	X	X
GMRS	GMRS Elevation	-35.0	60.5	Truncated Column		X



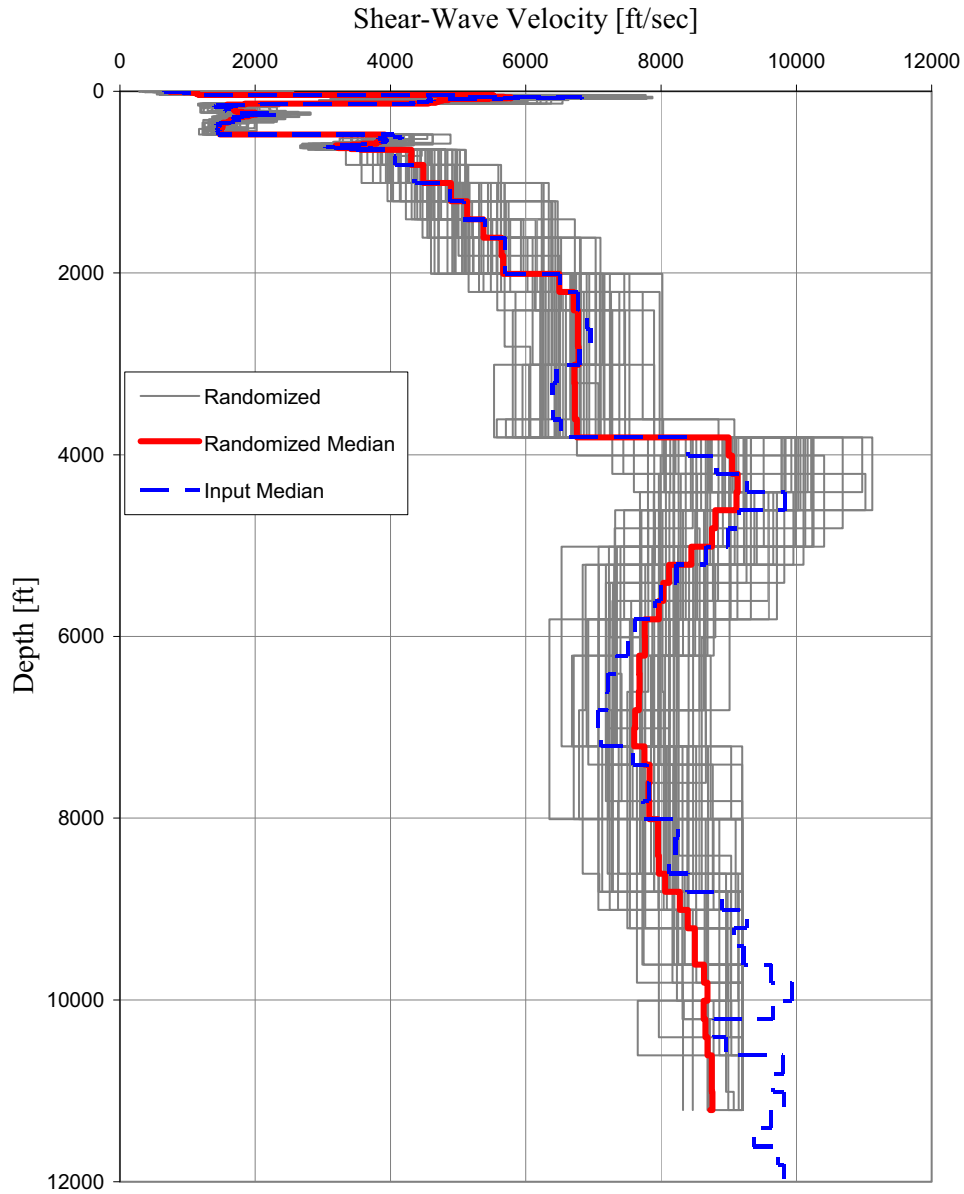


**Figure 3JJ-201 Randomized Shear Wave Velocity Profiles,  
Median Shear Wave Velocity Profile and the Input Median Profile  
Used for Randomization — NI Site Conditions**

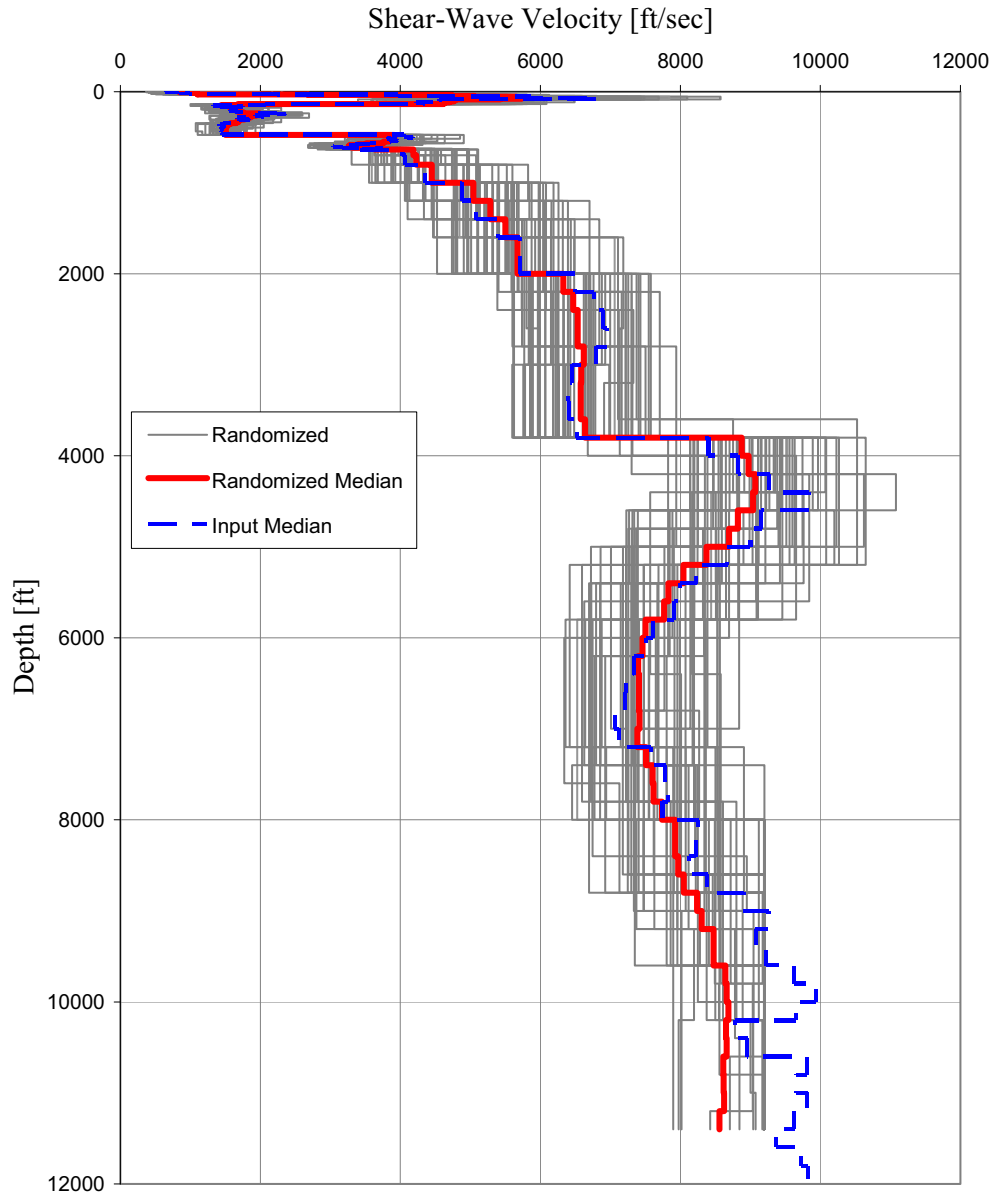


**Figure 3JJ-202 Randomized Shear Wave Velocity Profiles, Median Shear Wave Velocity Profile and the Input Median Profile Used for Randomization — FAR Site Conditions**

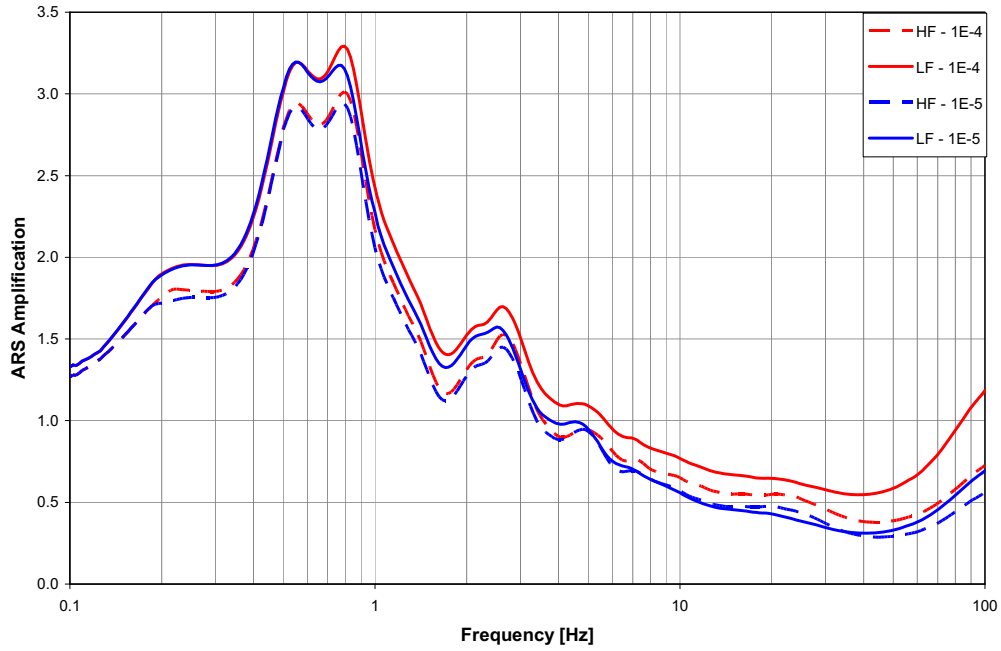


**Figure 3JJ-203 ARS Amplification Factors at FIRS Horizon — NI Site Conditions**

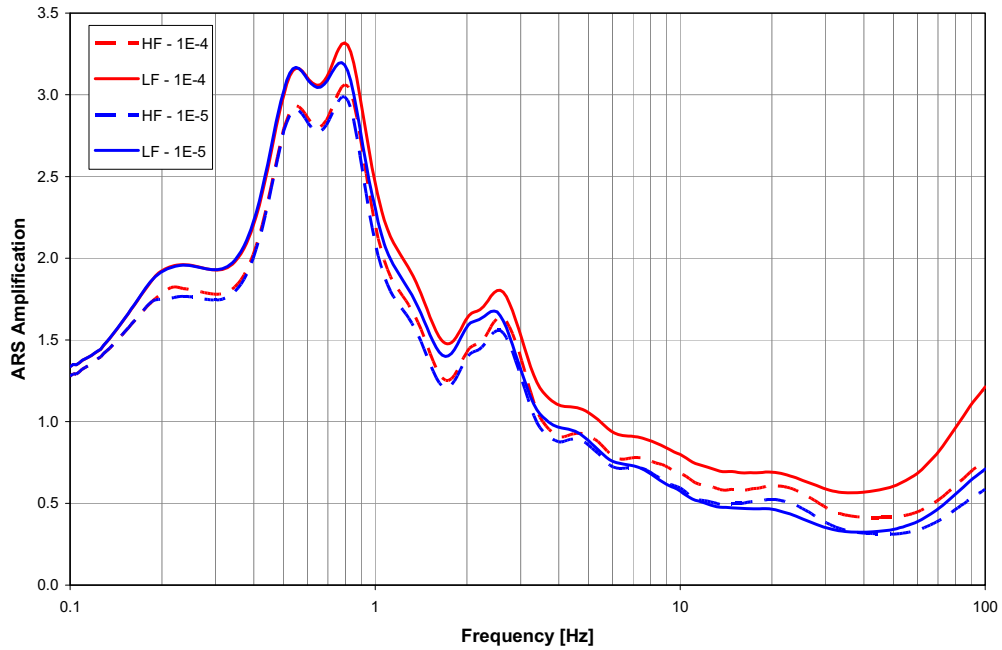


**Figure 3JJ-204 ARS Amplification Factors at FIRS Horizon — FAR Site Conditions**

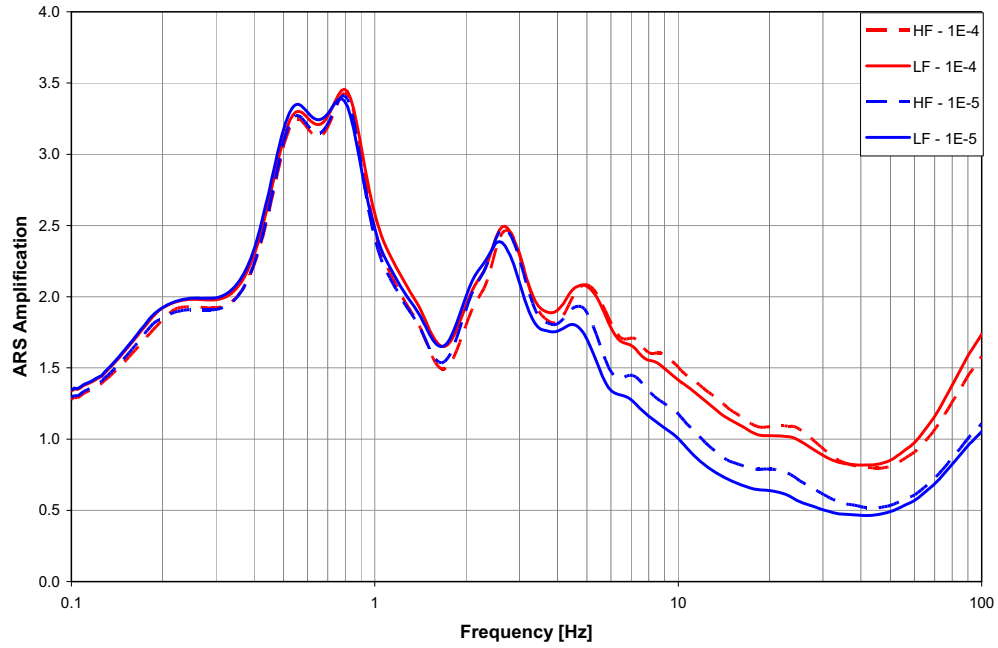


**Figure 3JJ-205 ARS Amplification Factors at Ground Surface — NI Site Conditions**

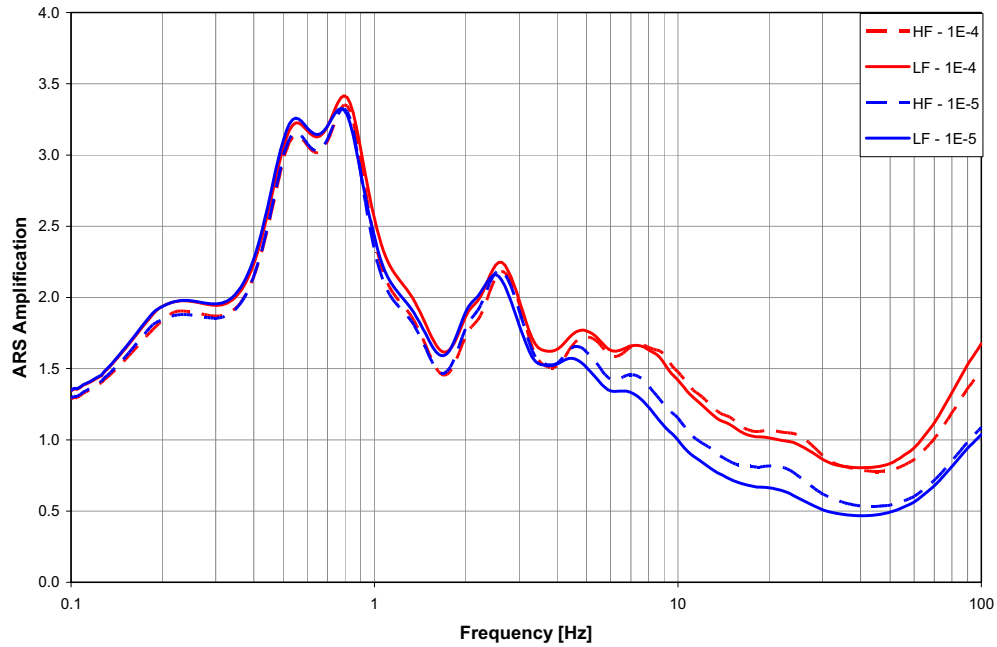


**Figure 3JJ-206 ARS Amplification Factors at Ground Surface — FAR Site Conditions**

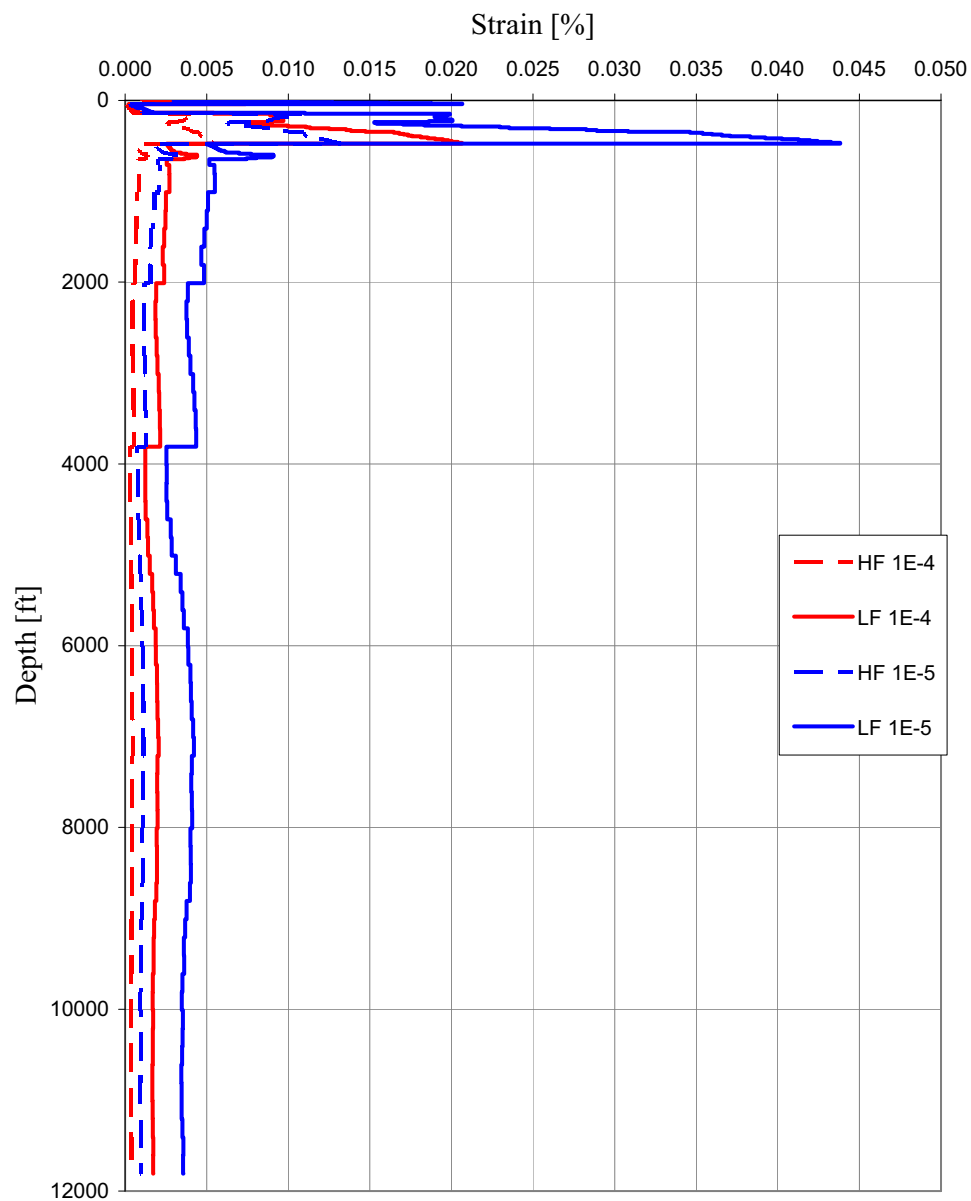


**Figure 3JJ-207 Strain Profiles — NI Site Conditions**

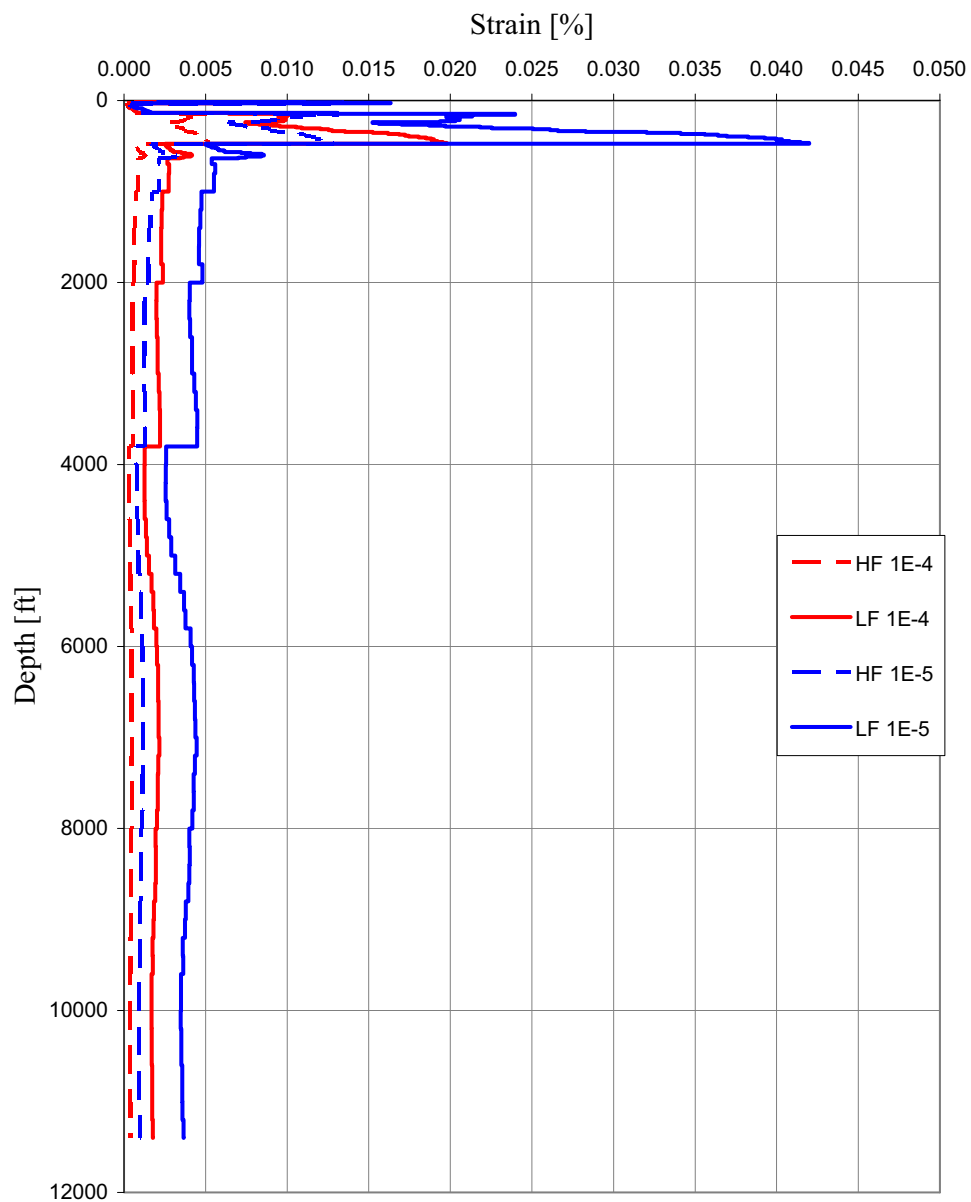


**Figure 3JJ-208 Strain Profiles — FAR Site Conditions**

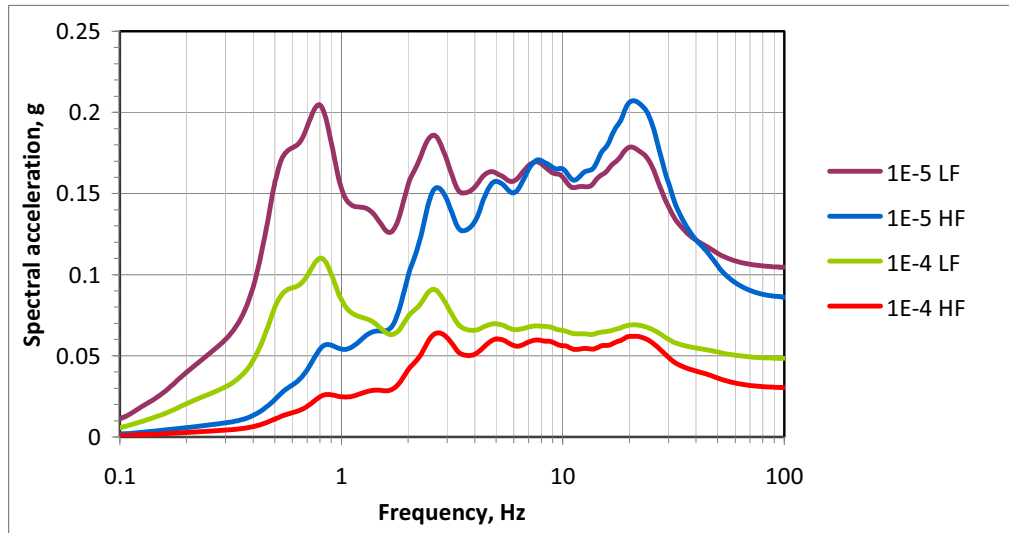


Figure 3JJ-209 HF and LF Horizontal 10<sup>-4</sup> and 10<sup>-5</sup> Site Spectra — FAR Soil Column

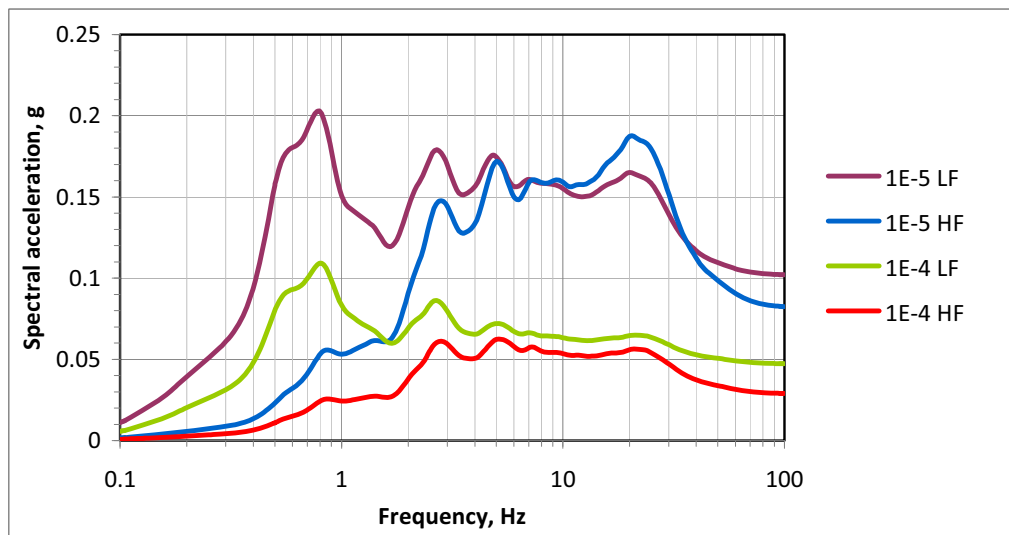
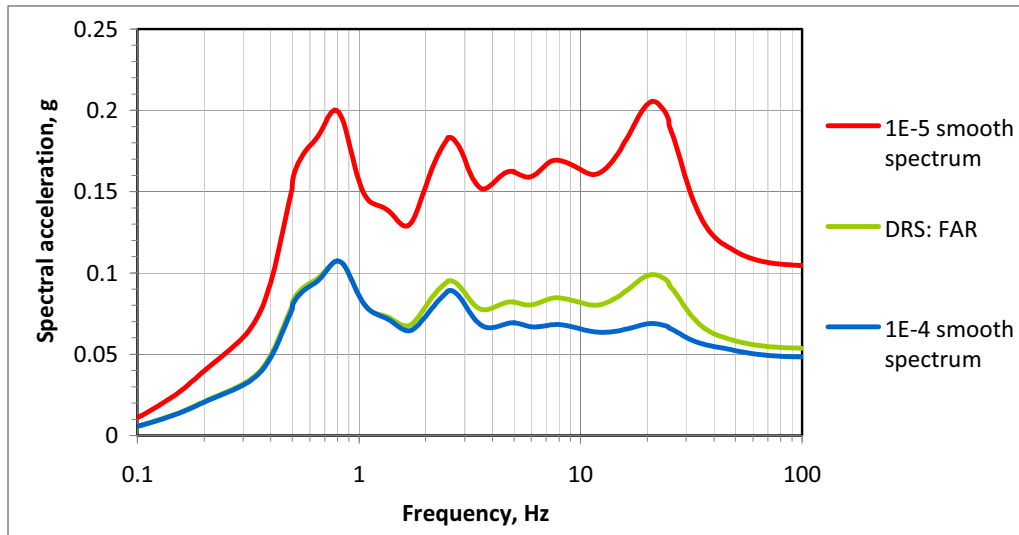
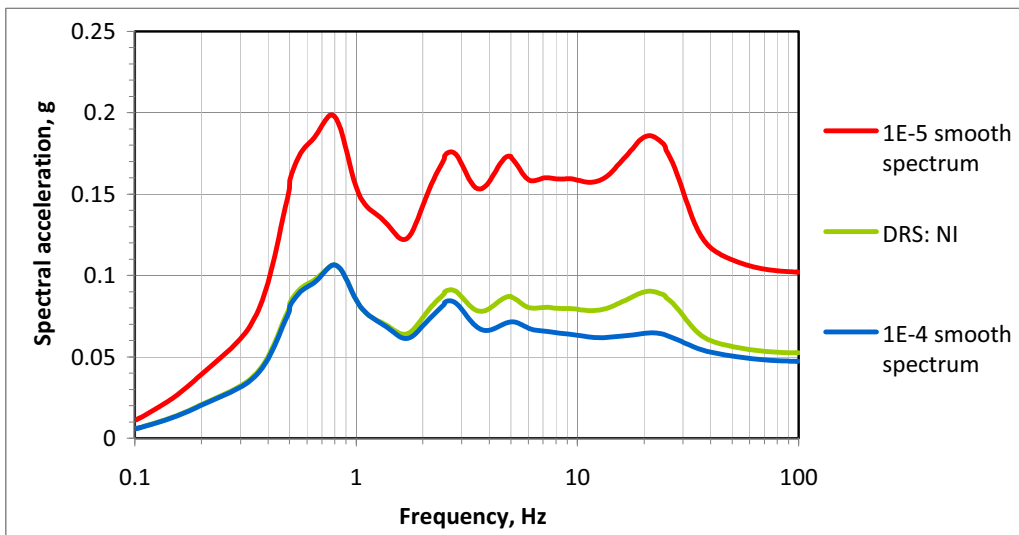


Figure 3JJ-210 HF and LF Horizontal 10<sup>-4</sup> and 10<sup>-5</sup> Site Spectra — NI Soil Column



**Figure 3JJ-211 Smoothed Horizontal  $10^{-4}$  and  $10^{-5}$  Site Spectra and DRS — FAR Soil Column**



**Figure 3JJ-212 Smoothed Horizontal  $10^{-4}$  and  $10^{-5}$  Site Spectra and DRS — NI Soil Column**



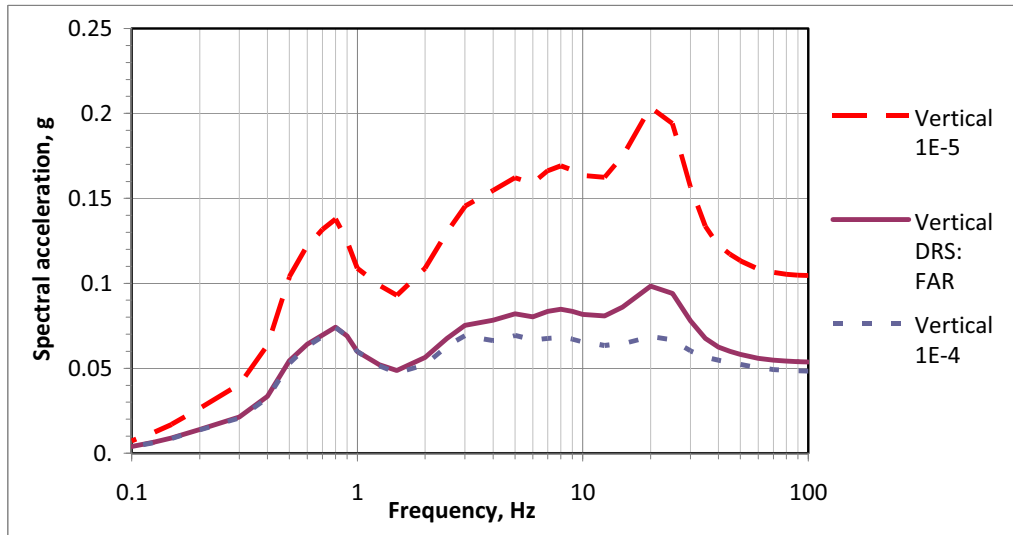


**Figure 3JJ-213 Smoothed Vertical  $10^{-4}$  and  $10^{-5}$  Site Spectra and DRS — FAR Soil Column**

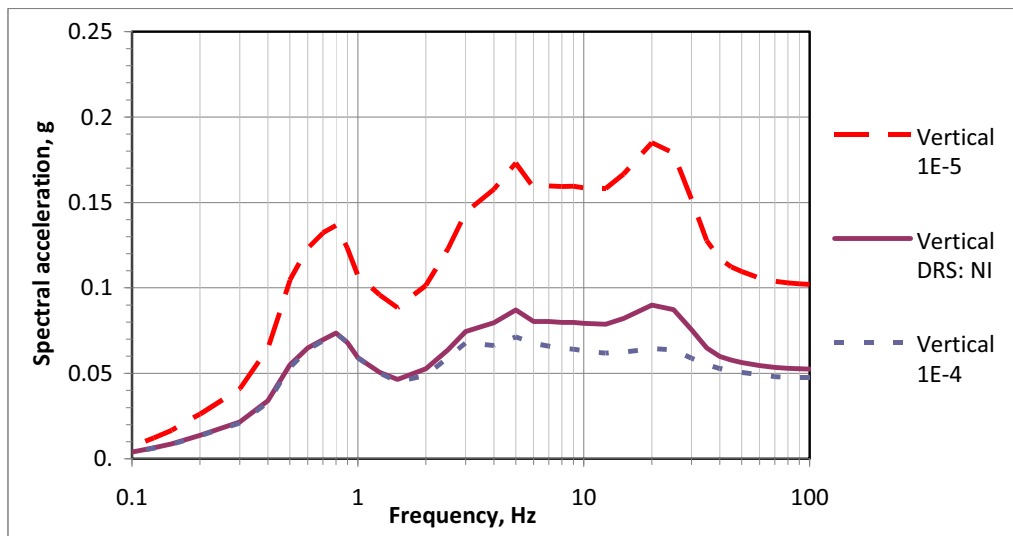


**Figure 3JJ-214 Smoothed Vertical  $10^{-4}$  and  $10^{-5}$  Site Spectra and DRS — NI Soil Column**

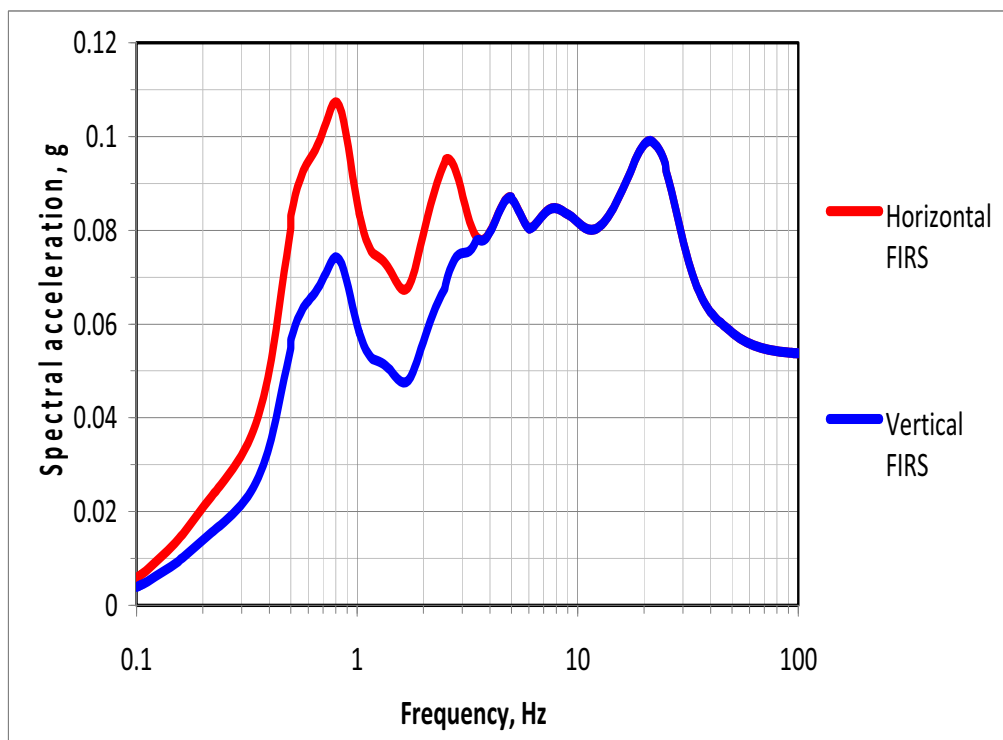


**Figure 3JJ-215 Recommended Horizontal and Vertical FIRS  
(Elevation –16 foot Horizon at Bottom of Nuclear Island Foundation)**

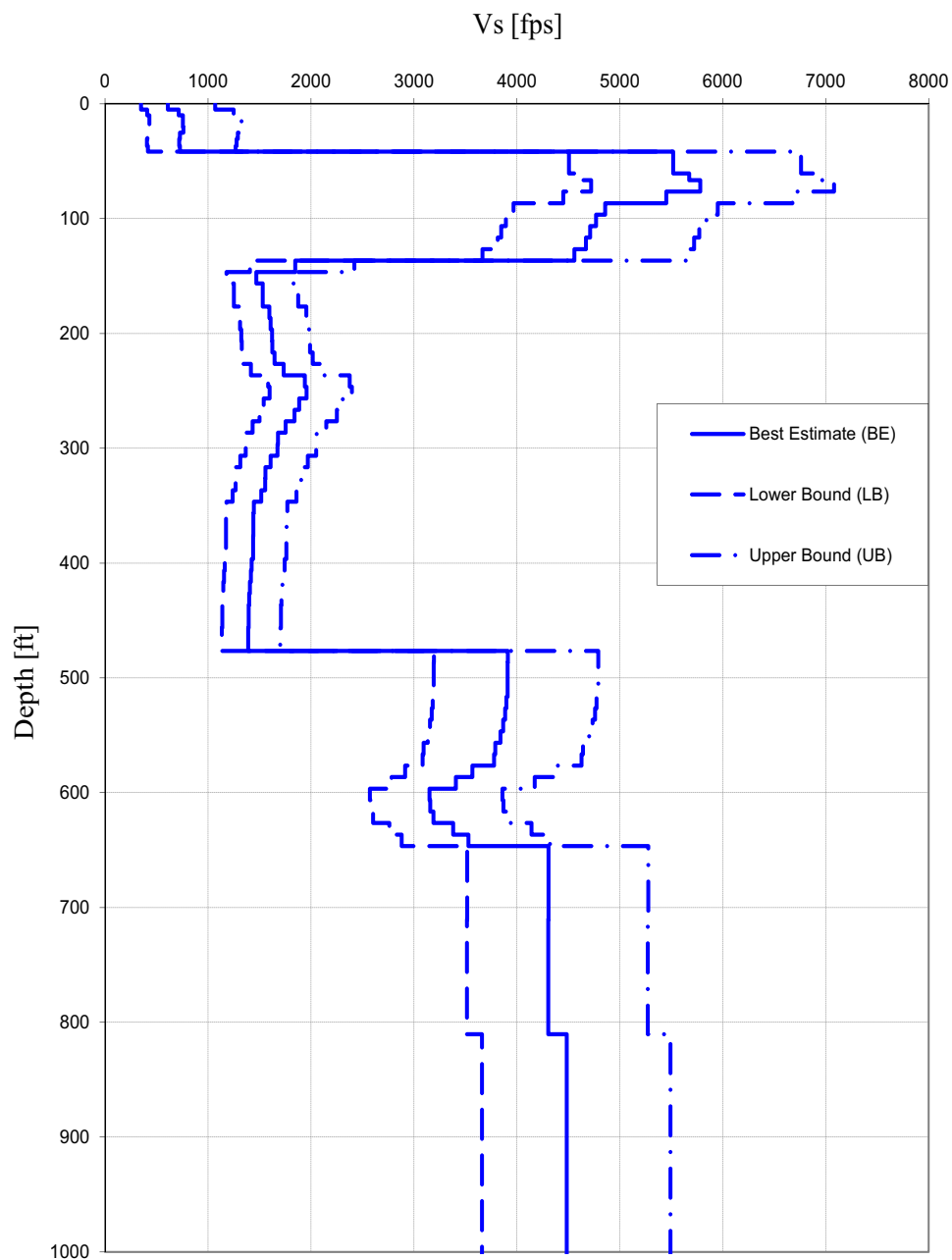


**Figure 3JJ-216 Recommended SSI Shear-Wave Velocity Profiles — NI Site Conditions (Upper 1000 feet — below 1000 feet depth is not shown)**

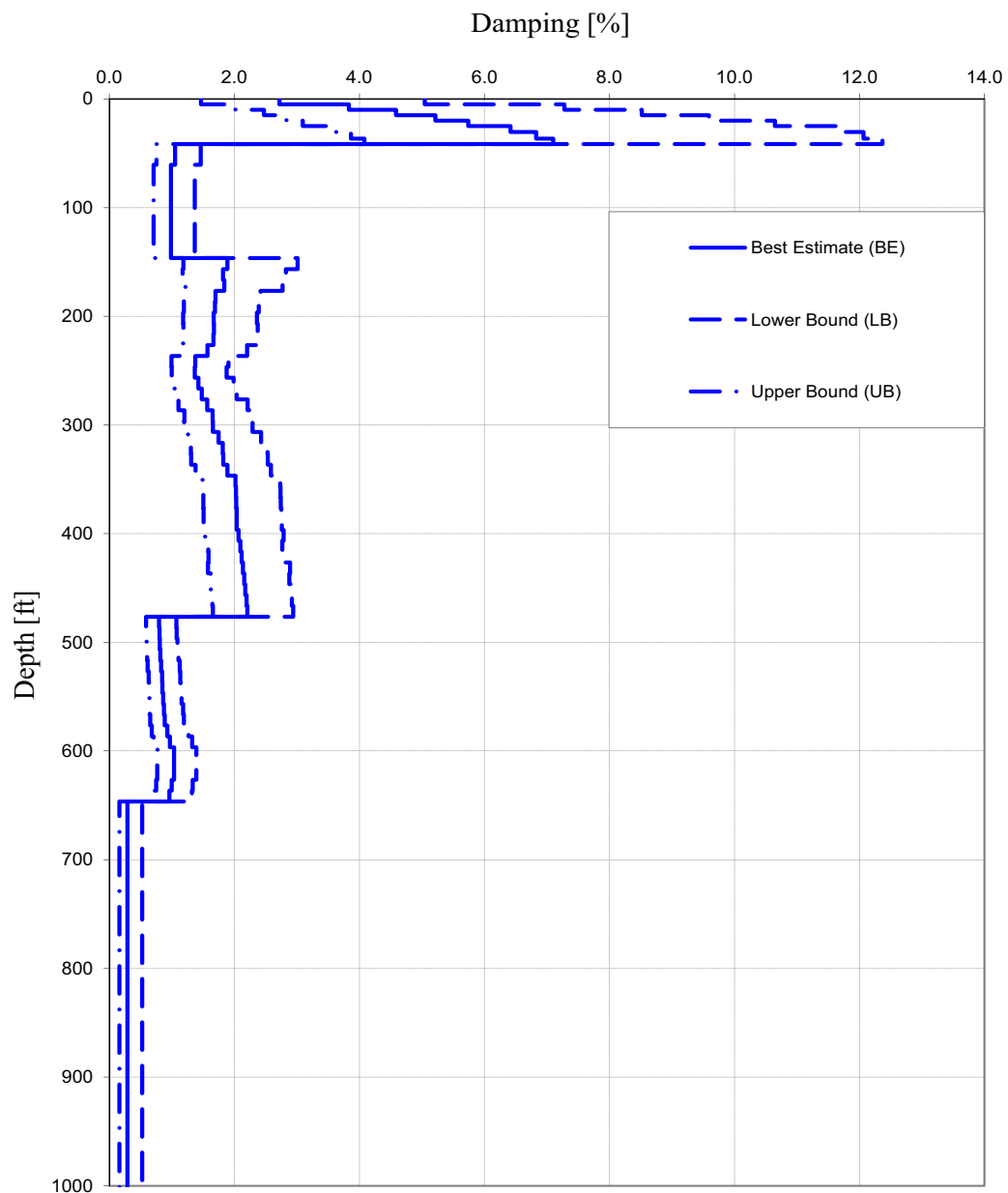


**Figure 3JJ-217 Recommended SSI Damping Profiles —  
NI Site Conditions (Upper 1000 feet — below 1000 feet depth is not shown)**

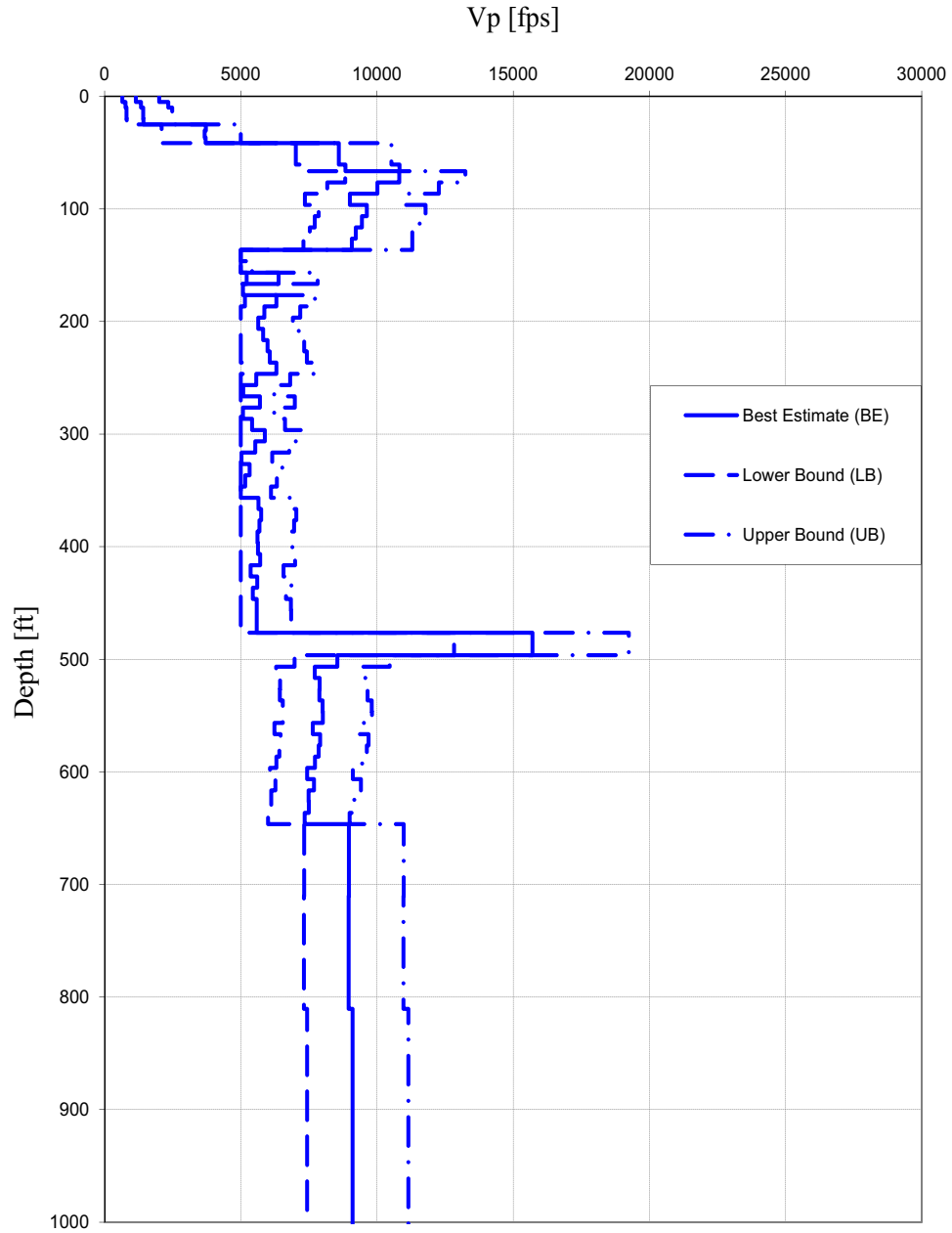


**Figure 3JJ-218 Recommended P-Wave Velocity Profiles — NI Site Conditions (Upper 1000 feet — below 1000 feet depth is not shown)**

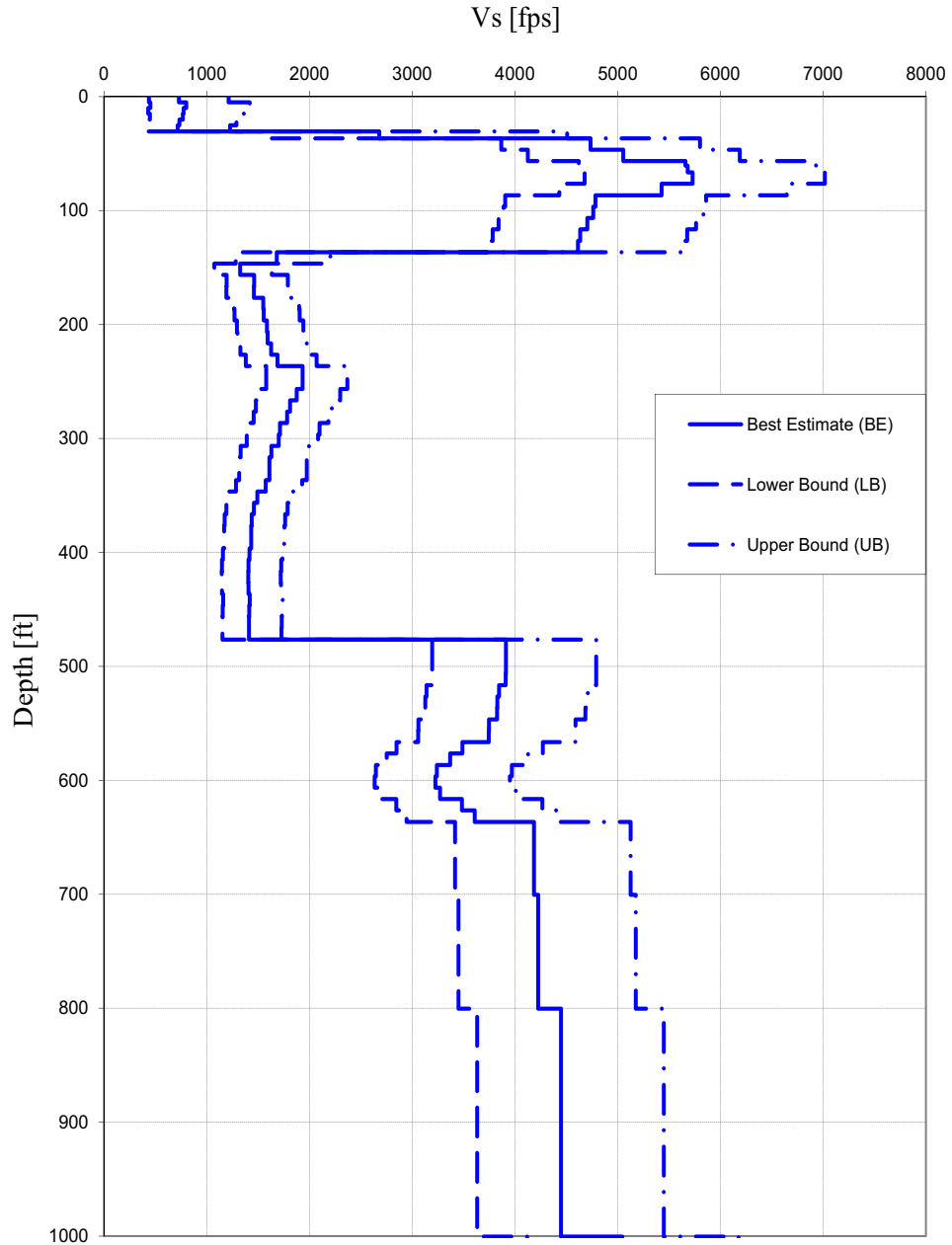


**Figure 3JJ-219 Recommended SSI Shear-Wave Velocity Profiles — FAR Site Conditions (Upper 1000 feet — below 1000 feet depth is not shown)**

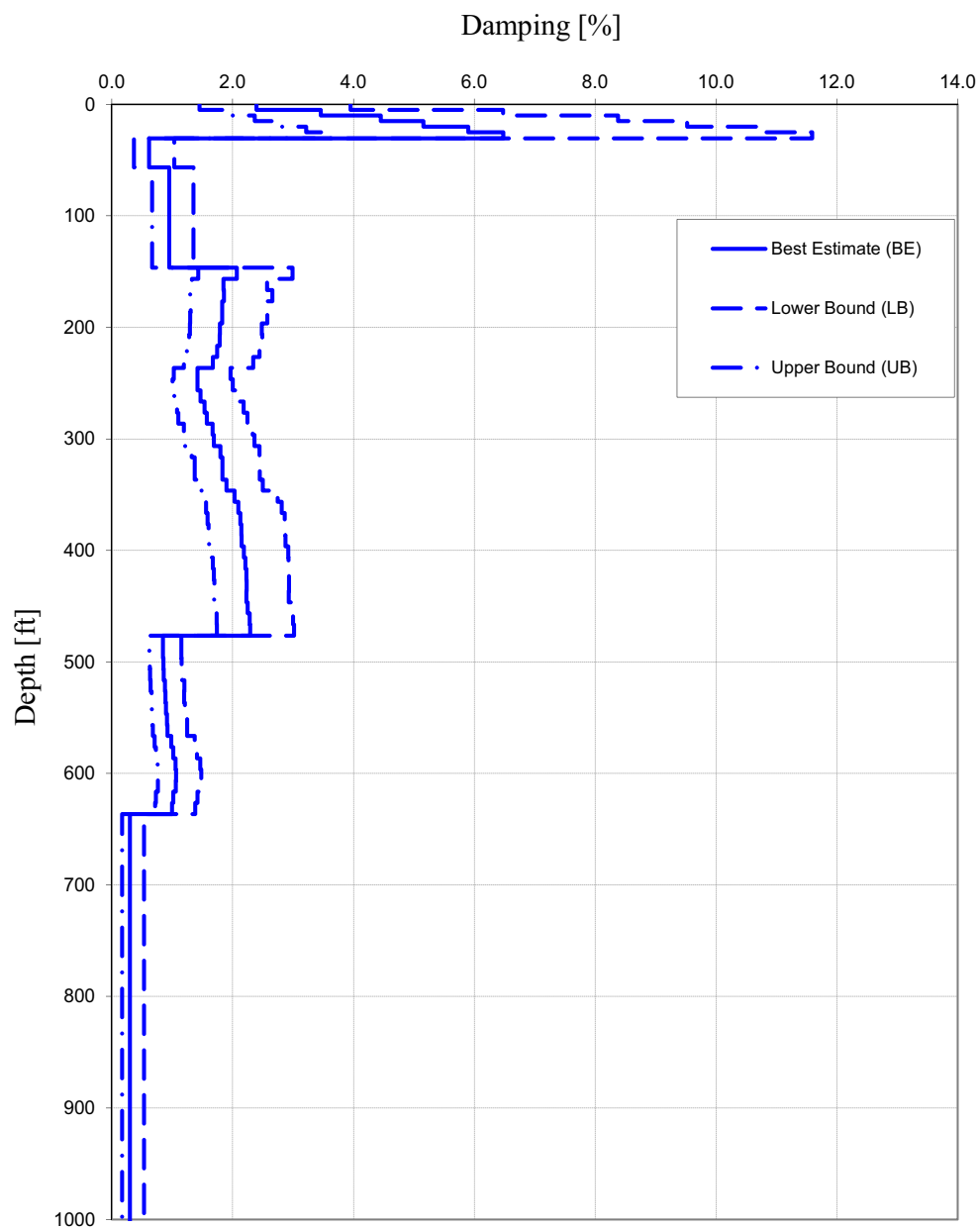


**Figure 3JJ-220 Recommended SSI Damping Profiles — FAR Site Conditions (Upper 1000 feet — below 1000 feet depth is not shown)**

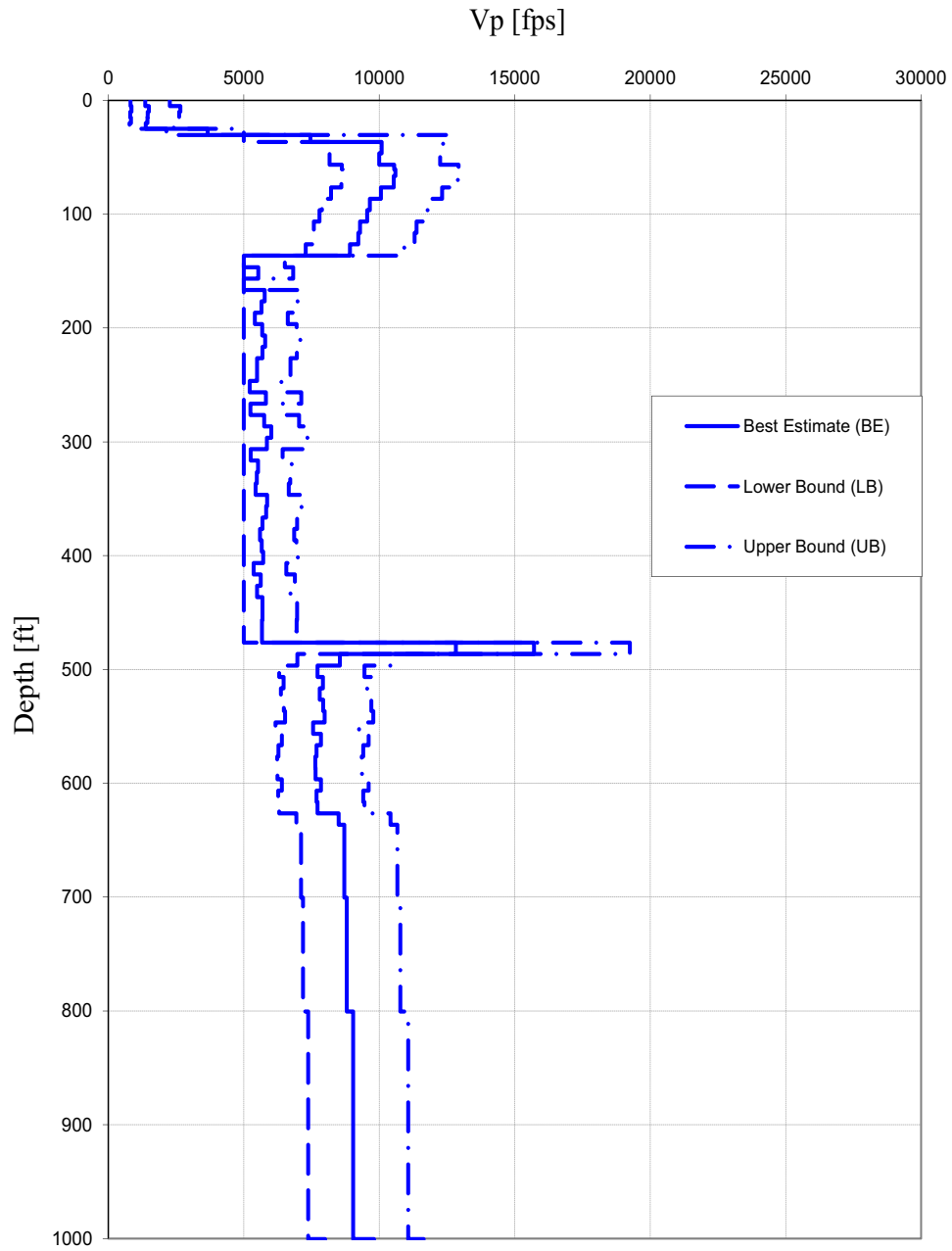


**Figure 3JJ-221 Recommended P-Wave Velocity Profiles — FAR Site Conditions (Upper 1000 feet — below 1000 feet depth is not shown)**



FPL: FIRS&RG1.60, TAP024-S, Run5

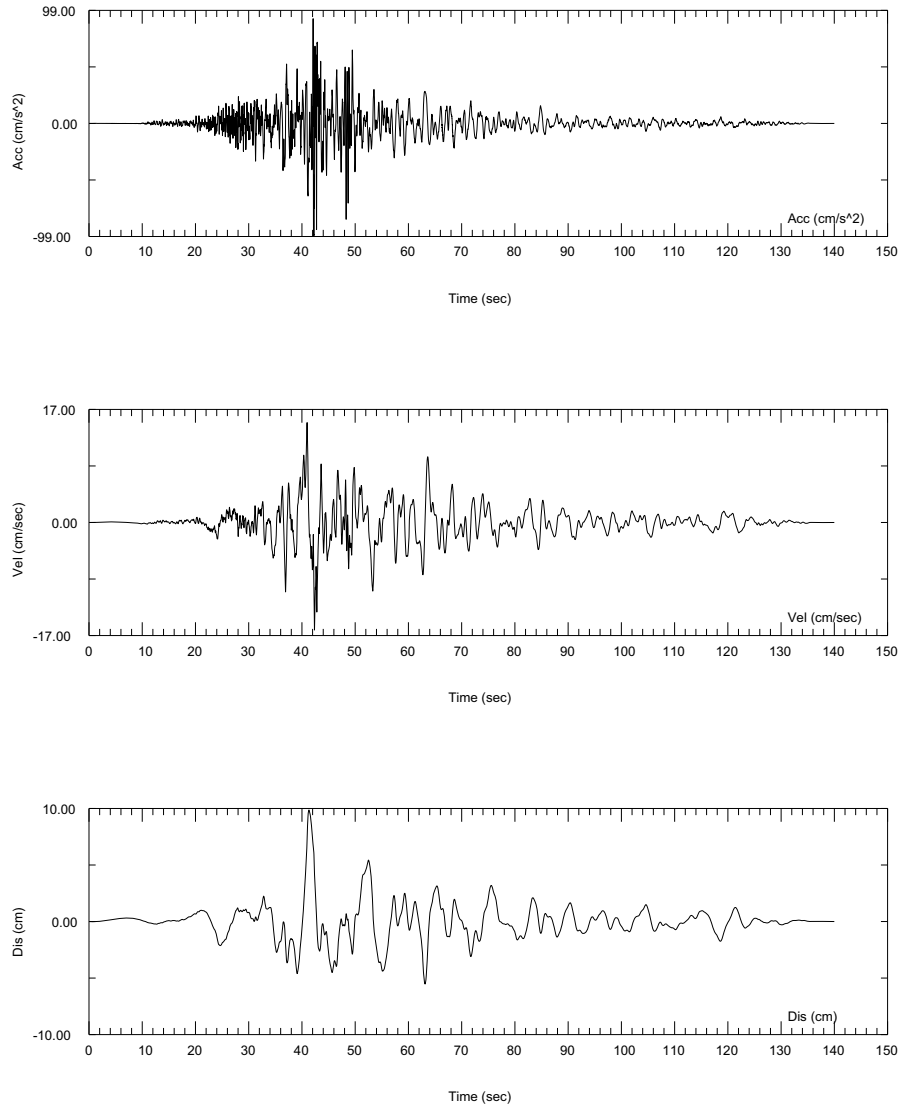


**Figure 3JJ-222a Final Spectrum-Compatible Acceleration, Velocity, and Displacement Time Histories for Horizontal 1 Case Before Constant Scale Factor of 1.01 is Applied**

FPL: FIRS&amp;RG1.60, TAP024-S

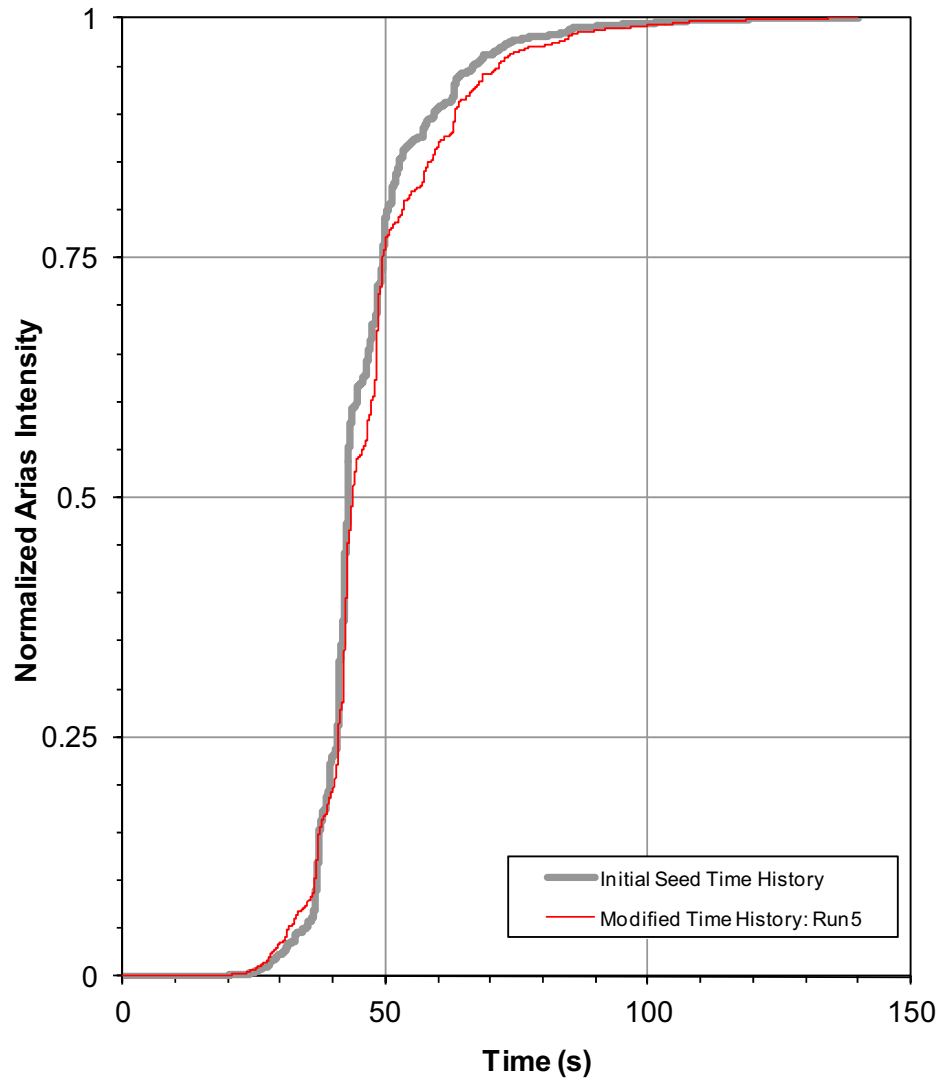


**Figure 3JJ-222b Comparison of Initial Seed Acceleration Normalized Arias Intensities Plot and Final Spectrum-Compatible Acceleration Normalized Arias Intensities Plot for Horizontal 1 Case Before Constant Scale Factor of 1.01 is Applied**

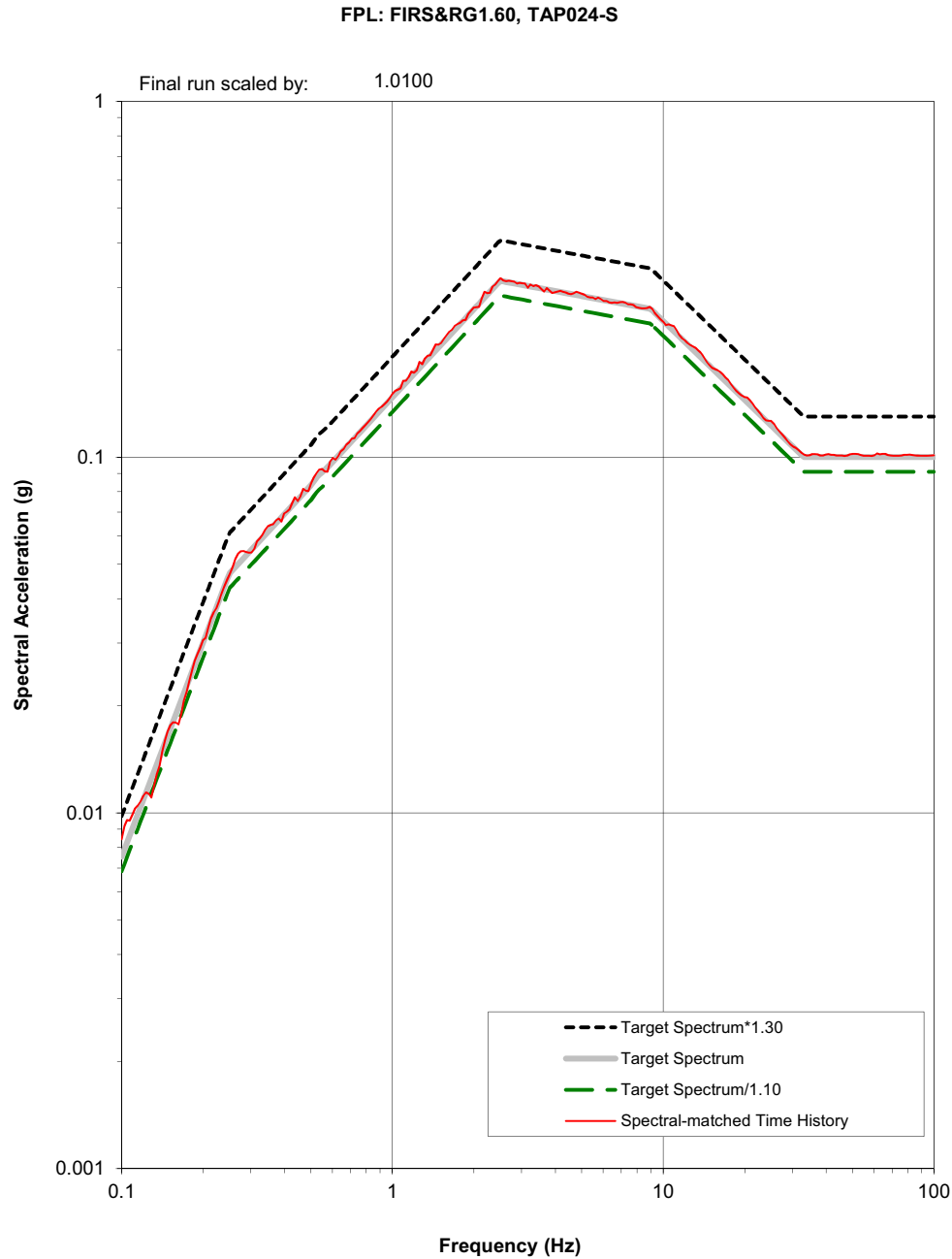


**Figure 3JJ-222c Comparison Between the Final Scaled Spectrum-Compatible Response Spectrum, Horizontal SSE ARS, and Upper and Lower Target Spectrum Bounds for Horizontal 1 Case With the Constant Scale Factor of 1.01 Applied**

FPL: FIRS&RG1.60, TAP024-W, Run6

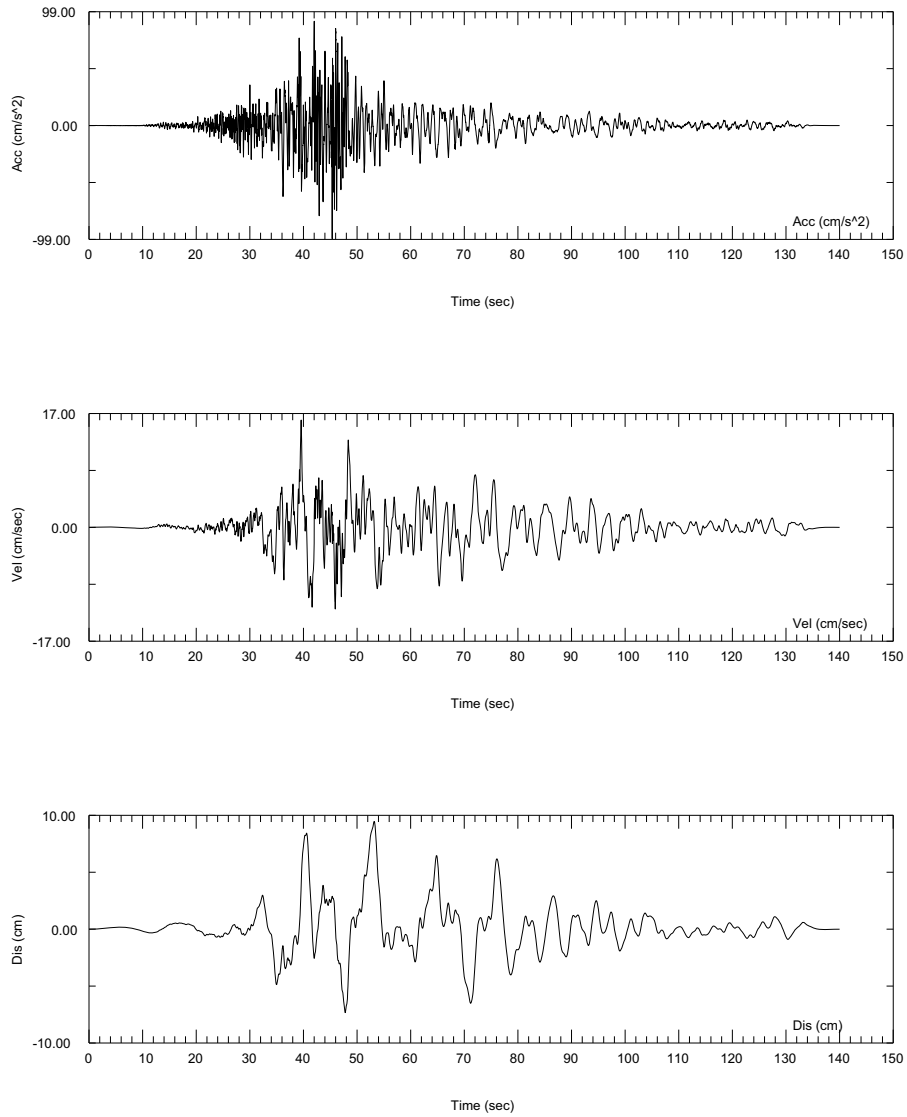


**Figure 3JJ-223a Final Spectrum-Compatible Acceleration, Velocity, and Displacement Time Histories for Horizontal 2 Case Before Constant Scale Factor of 1.015 is Applied**

FPL: FIRS&amp;RG1.60, TAP024-W

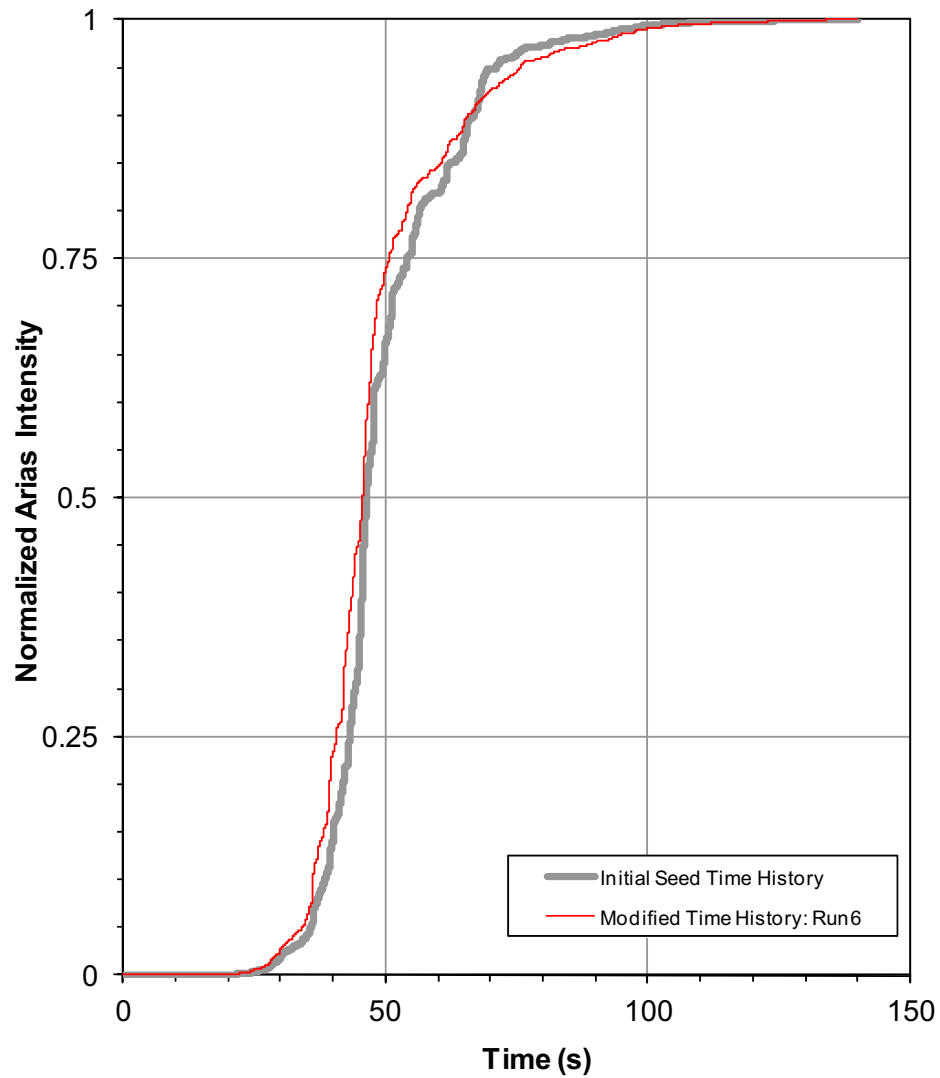


**Figure 3JJ-223b Comparison of Initial Seed Acceleration Normalized Arias Intensities Plot and Final Spectrum-Compatible Acceleration Normalized Arias Intensities Plot for Horizontal 2 Case Before Constant Scale Factor of 1.015 is Applied**

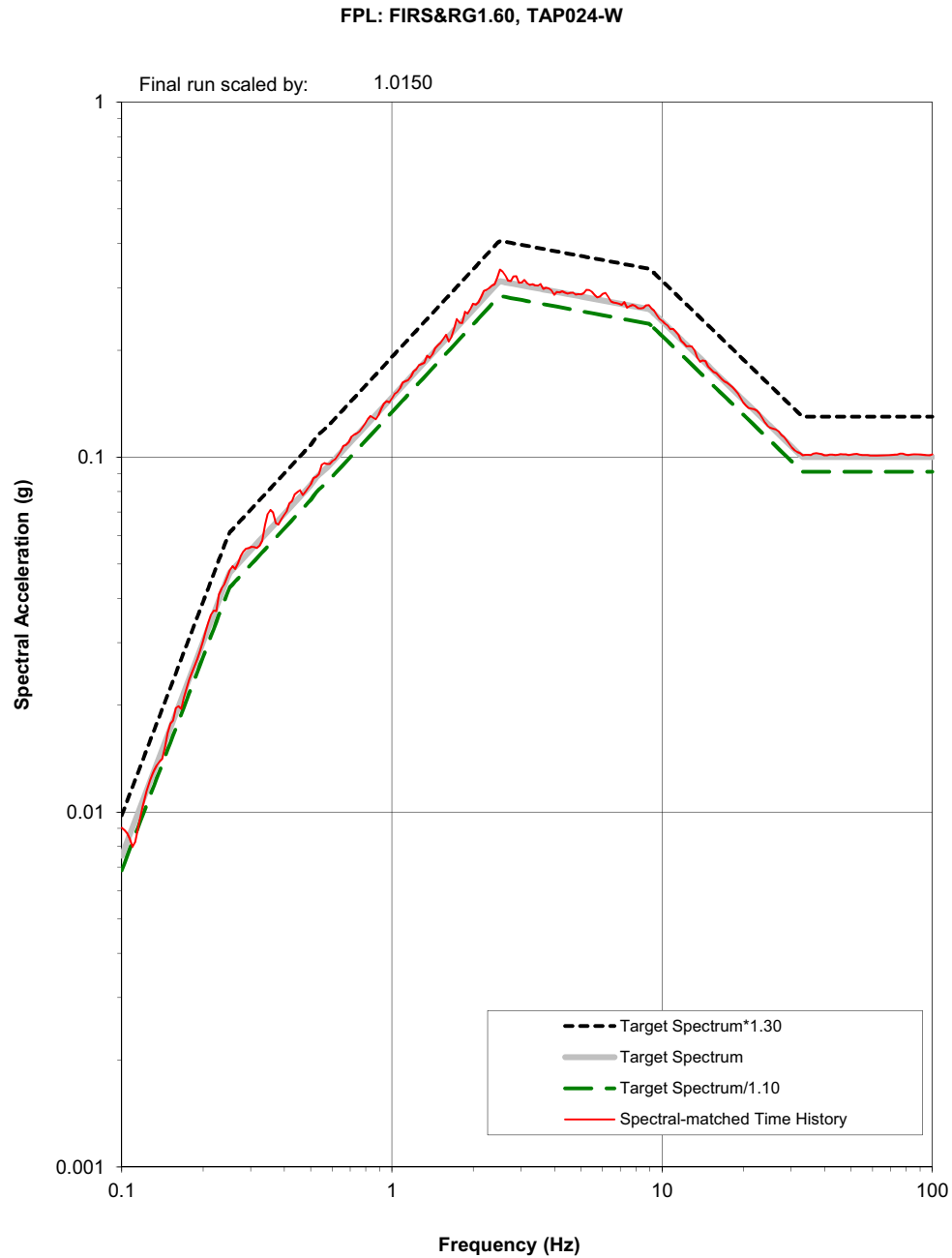


**Figure 3JJ-223c Comparison Between the Final Scaled Spectrum-Compatible Response Spectrum, Horizontal SSE ARS, and Upper and Lower Target Spectrum Bounds for Horizontal 2 Case With the Constant Scale Factor of 1.015 Applied**

FPL: FIRS&RG1.60, TAP024-V, Run5

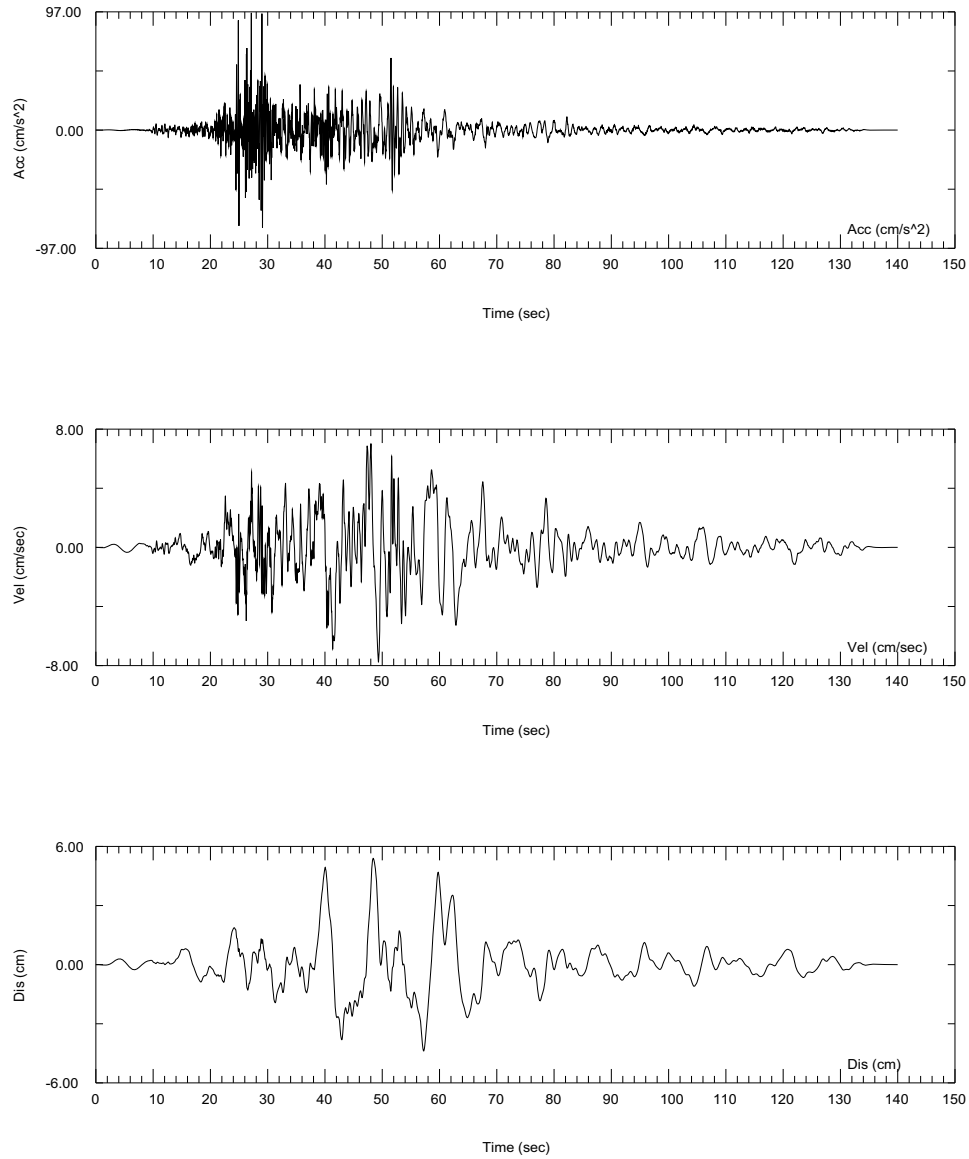


**Figure 3JJ-224a Final Spectrum-Compatible Acceleration, Velocity, and Displacement Time Histories for Vertical Case Before Constant Scale Factor of 1.015 is Applied**

FPL: FIRS&amp;RG1.60, TAP024-V

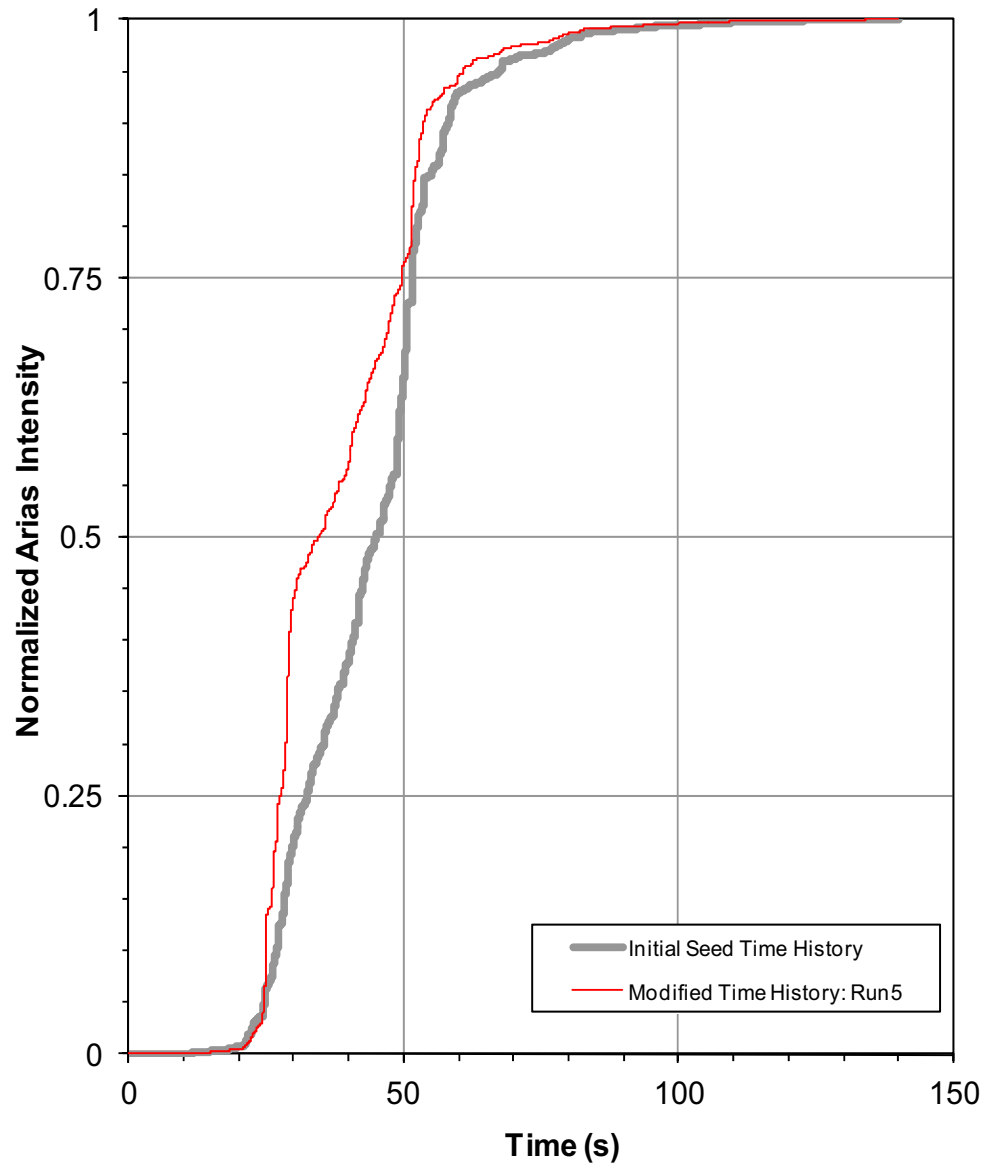


**Figure 3JJ-224b Comparison of Initial Seed Acceleration Normalized Arias Intensities Plot and Final Spectrum-Compatible Acceleration Normalized Arias Intensities Plot for Vertical Case Before Constant Scale Factor of 1.015 is Applied**



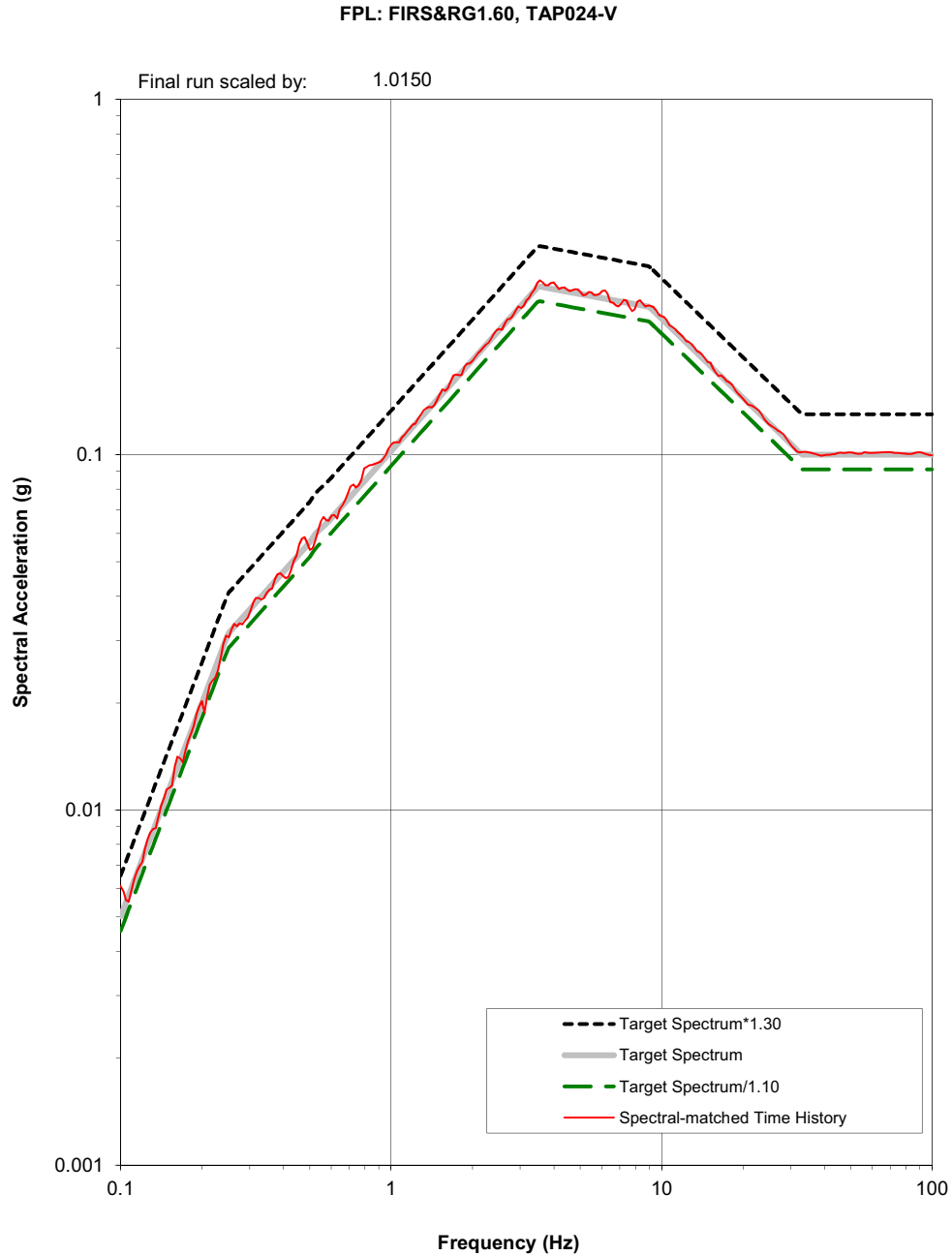


**Figure 3JJ-224c Comparison Between the Final Scaled Spectrum-Compatible Response Spectrum, Vertical SSE ARS, and Upper and Lower Target Spectrum Bounds for Vertical Case With the Constant Scale Factor of 1.015 Applied**

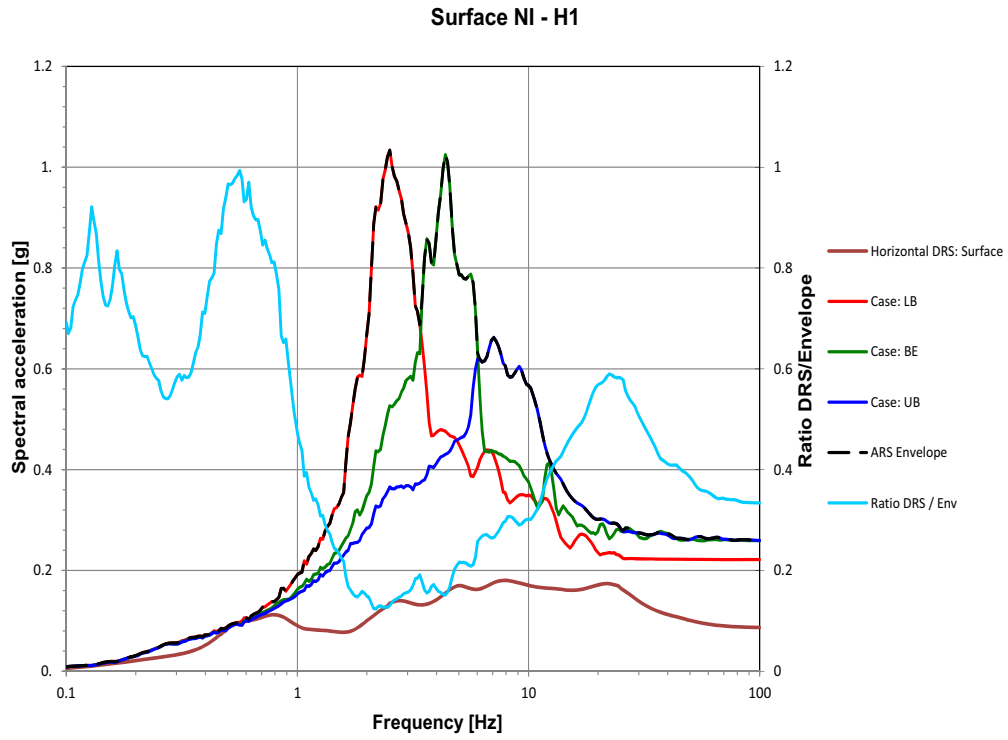


**Figure 3JJ-225 5% Damping ARS at Ground Surface —Direction H1 — NI Site Condition**

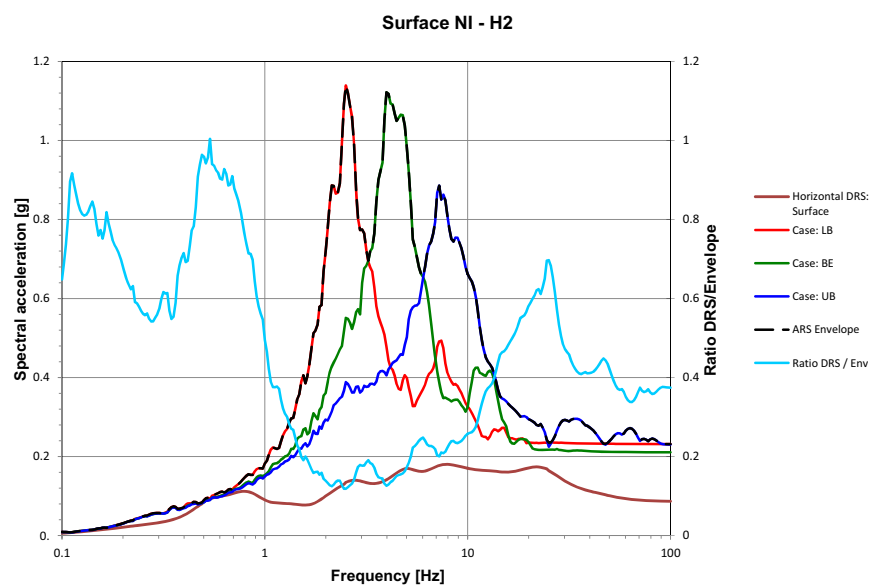


**Figure 3JJ-226 5% Damping ARS at Ground Surface — Direction H2 —NI Site Condition**

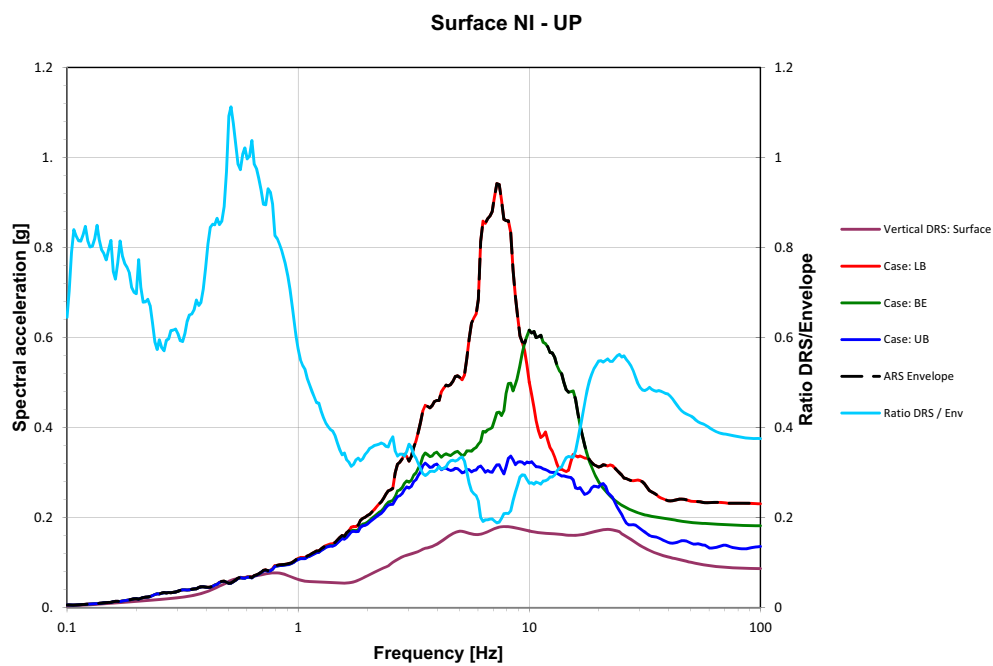


**Figure 3JJ-227 5% Damping ARS at Ground Surface —Direction UP—NI Site Condition**

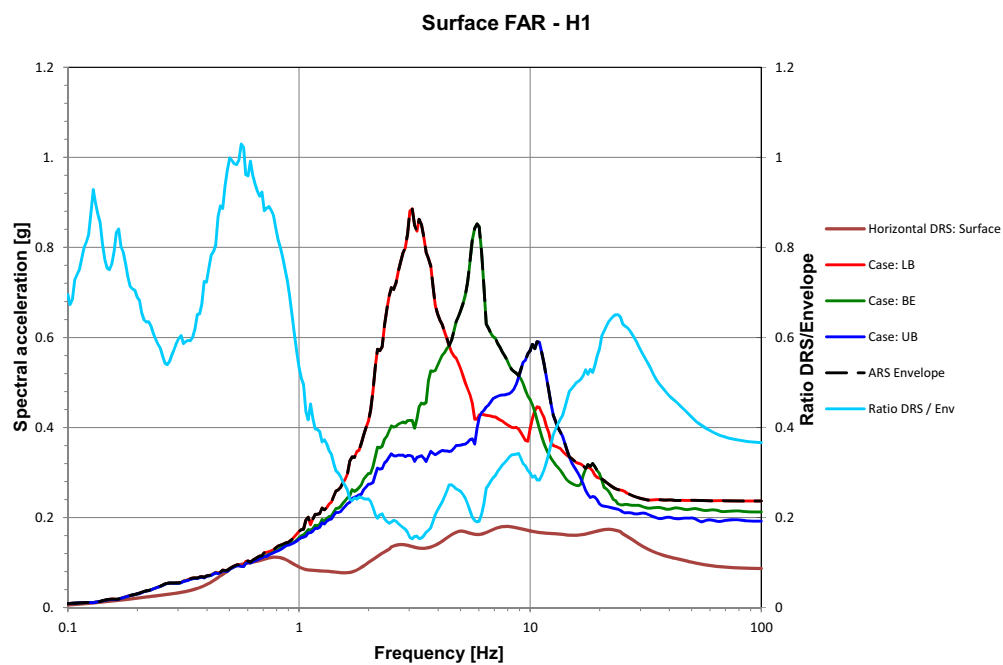


**Figure 3JJ-228 5% Damping ARS at Ground Surface —Direction H1—FAR Site Condition**

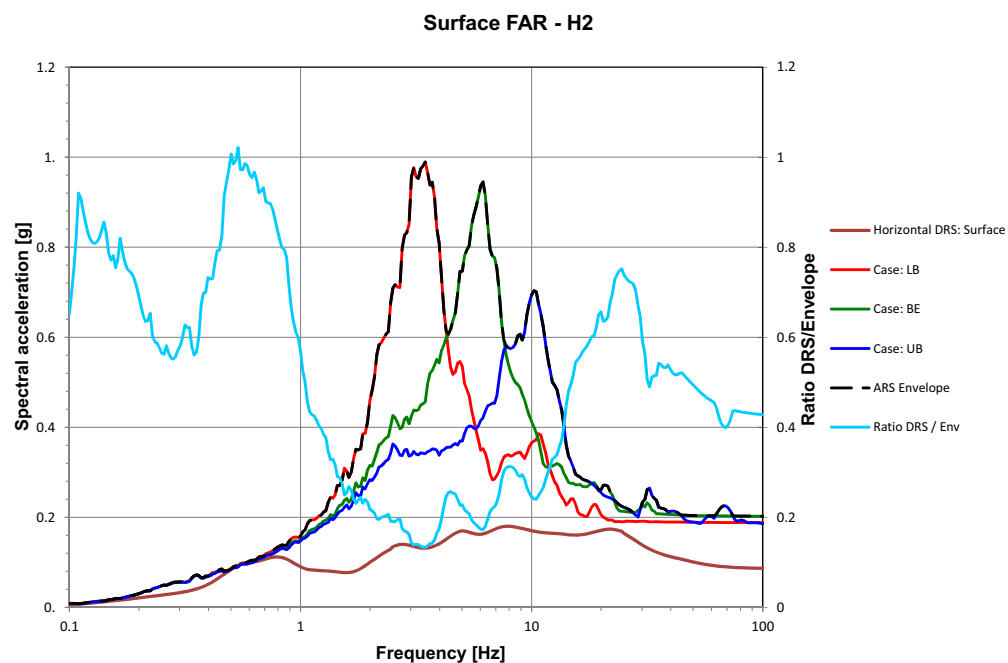


**Figure 3JJ-229 5% Damping ARS at Ground Surface —Direction H2—FAR Site Condition**

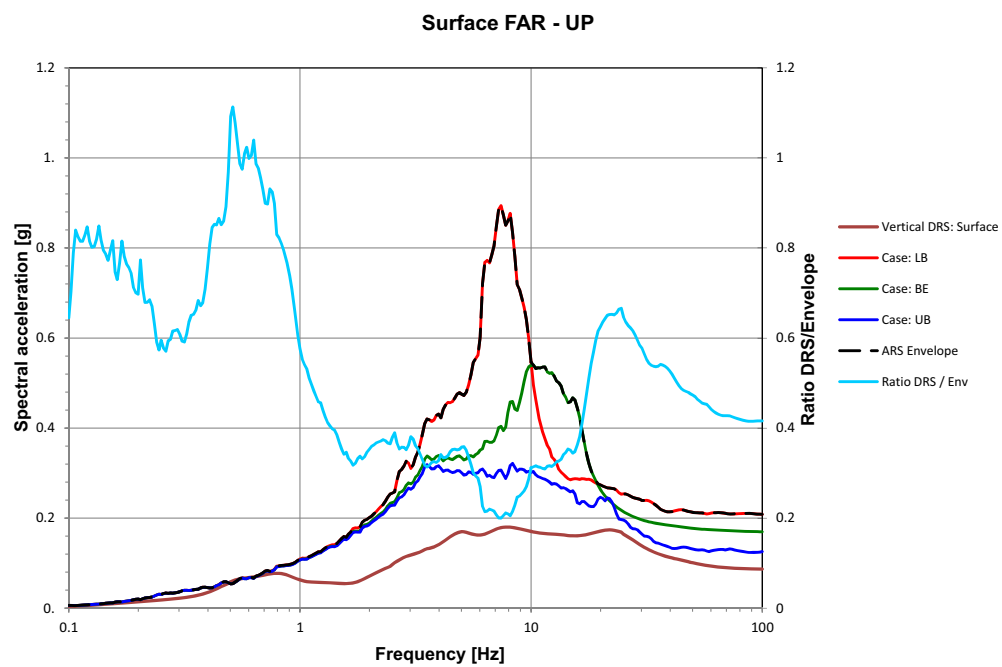


**Figure 3JJ-230 5% Damping ARS at Ground Surface —Direction UP—FAR Site Condition**

**Figure 3JJ-231**  
**Not Used**



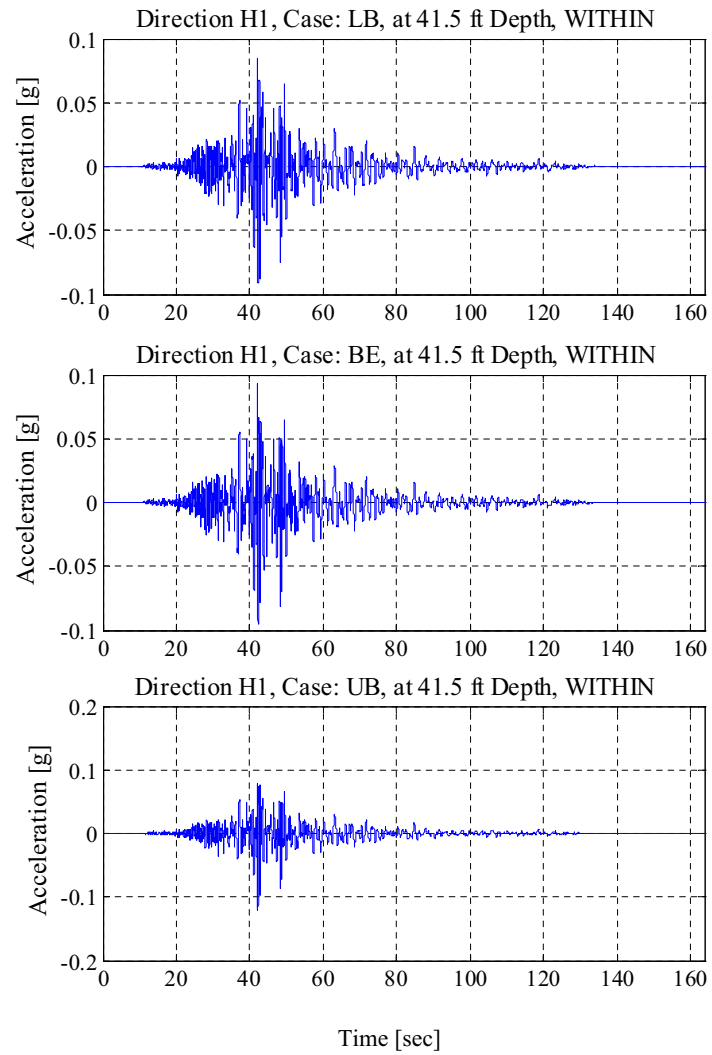


**Figure 3JJ-232 SSI Input “Within” Acceleration Time History — Direction H1 — NI Site Condition Time [sec]**

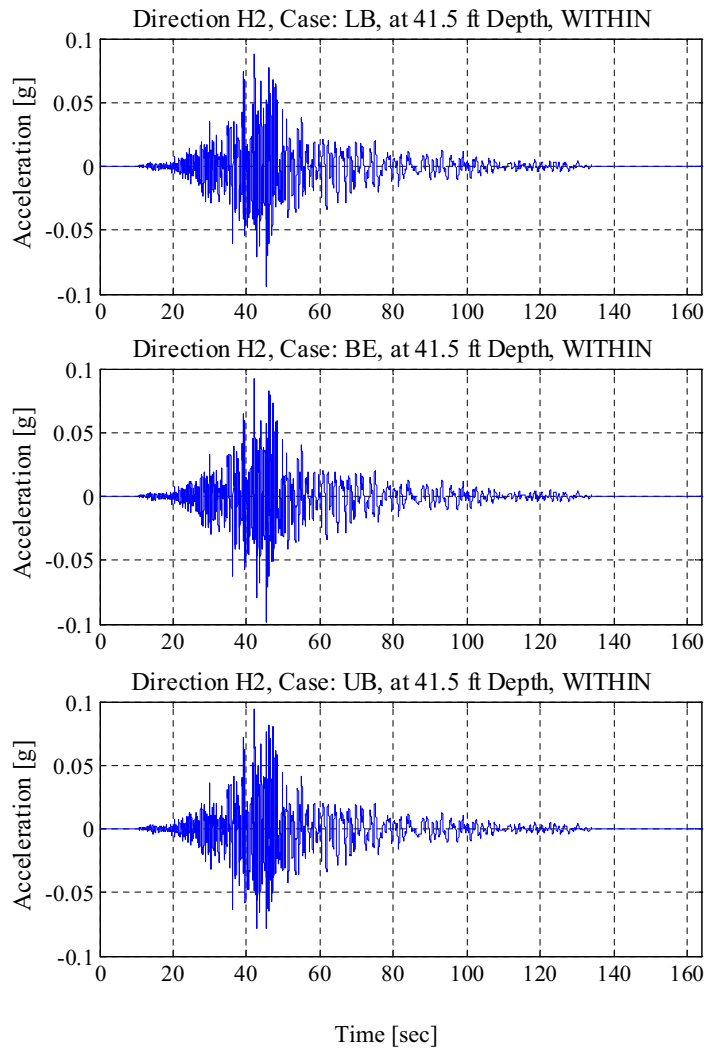


**Figure 3JJ-233 SSI Input “Within” Acceleration Time History — Direction H2 — NI Site Condition Time [sec]**

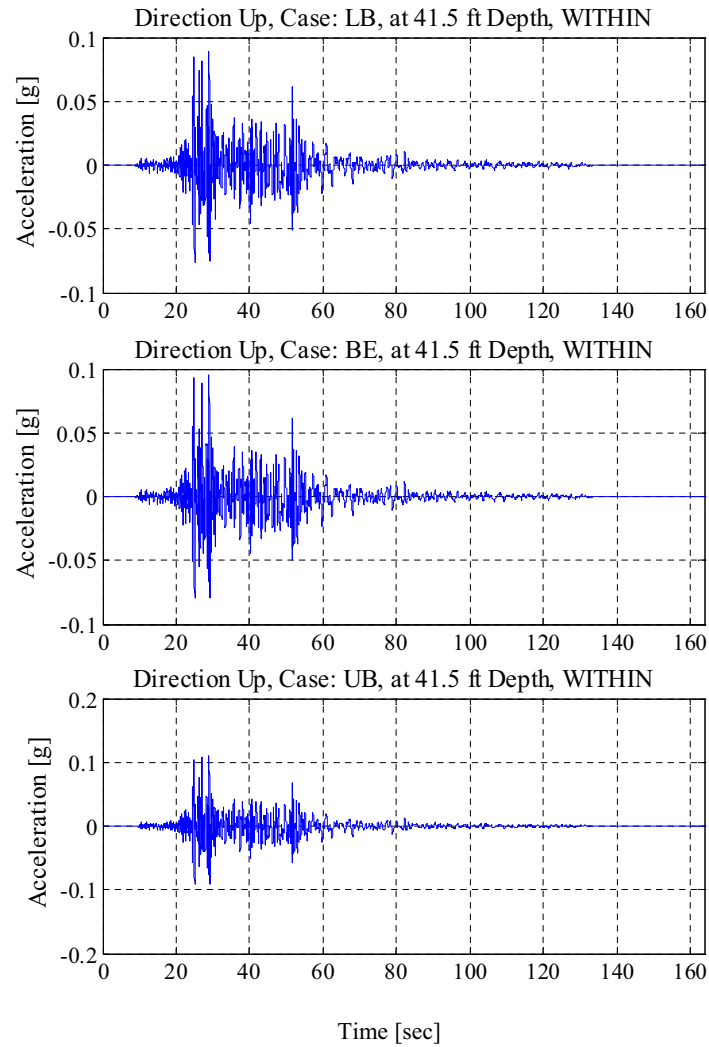


**Figure 3JJ-234 SSI Input “Within” Acceleration Time History —  
Direction UP — NI Site Condition Time [sec]**

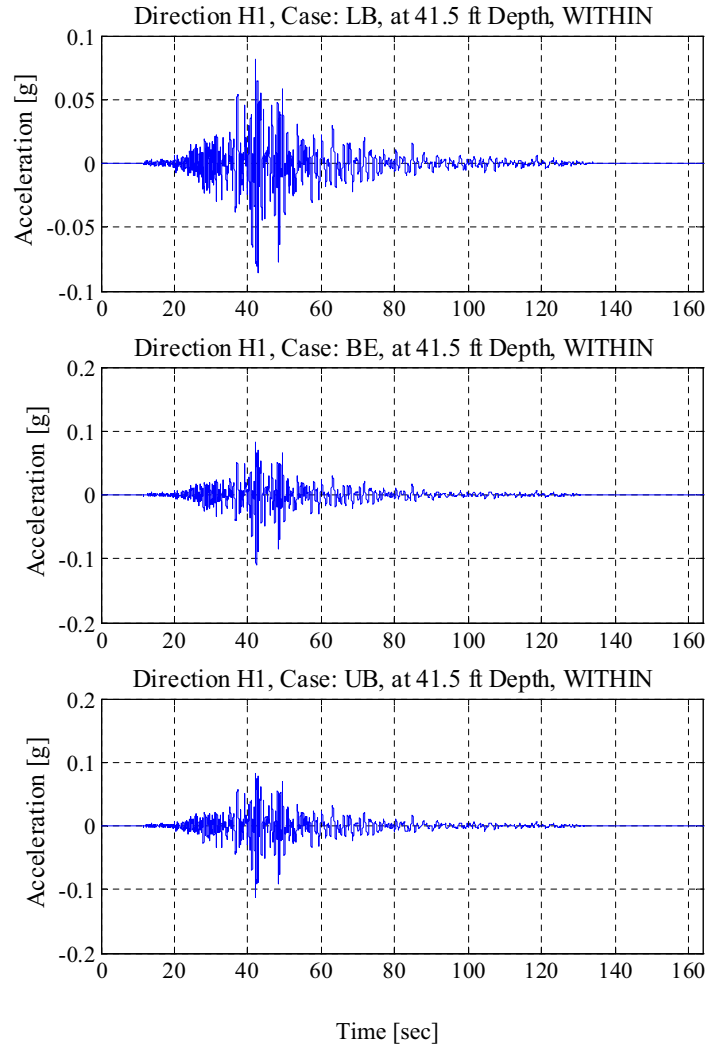


**Figure 3JJ-235 SSI Input “Within” Acceleration Time History — Direction H1 — FAR Site Condition Time [sec]**

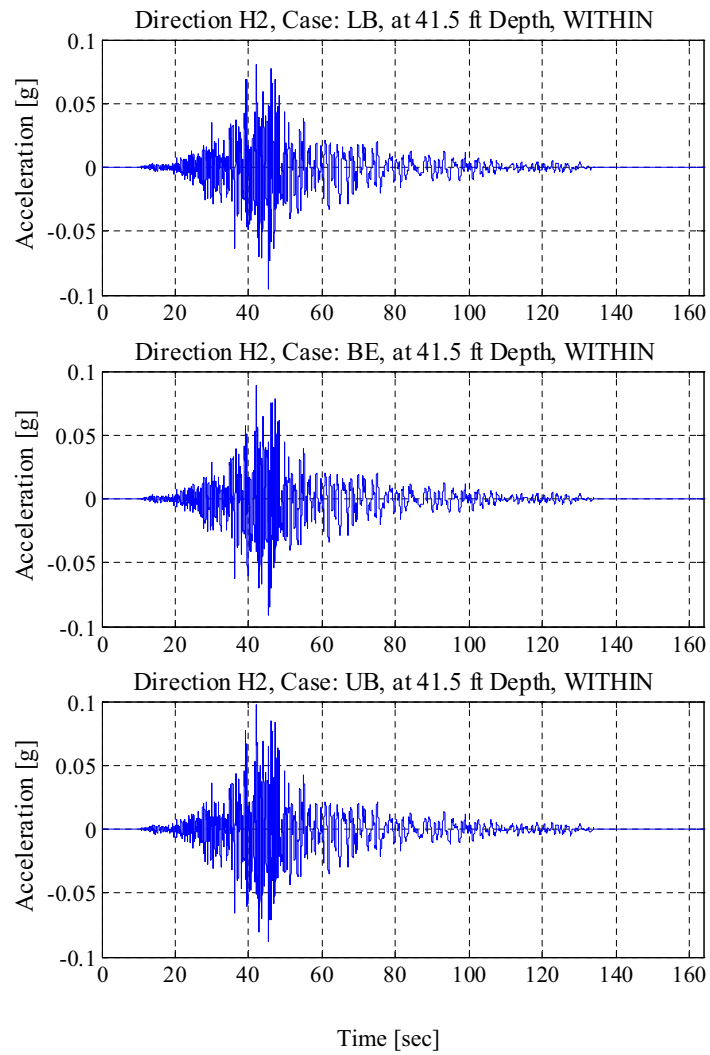


**Figure 3JJ-236 SSI Input “Within” Acceleration Time History — Direction H2 — FAR Site Condition Time [sec]**

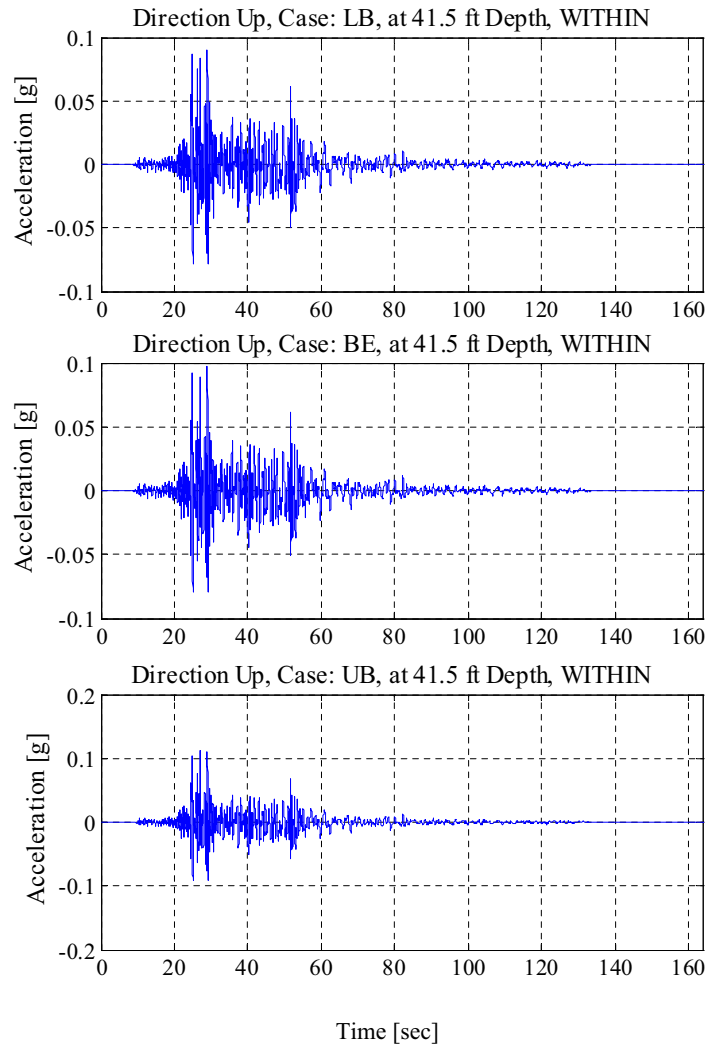


**Figure 3JJ-237 SSI Input “Within” Acceleration Time History — Direction UP — FAR Site Condition**

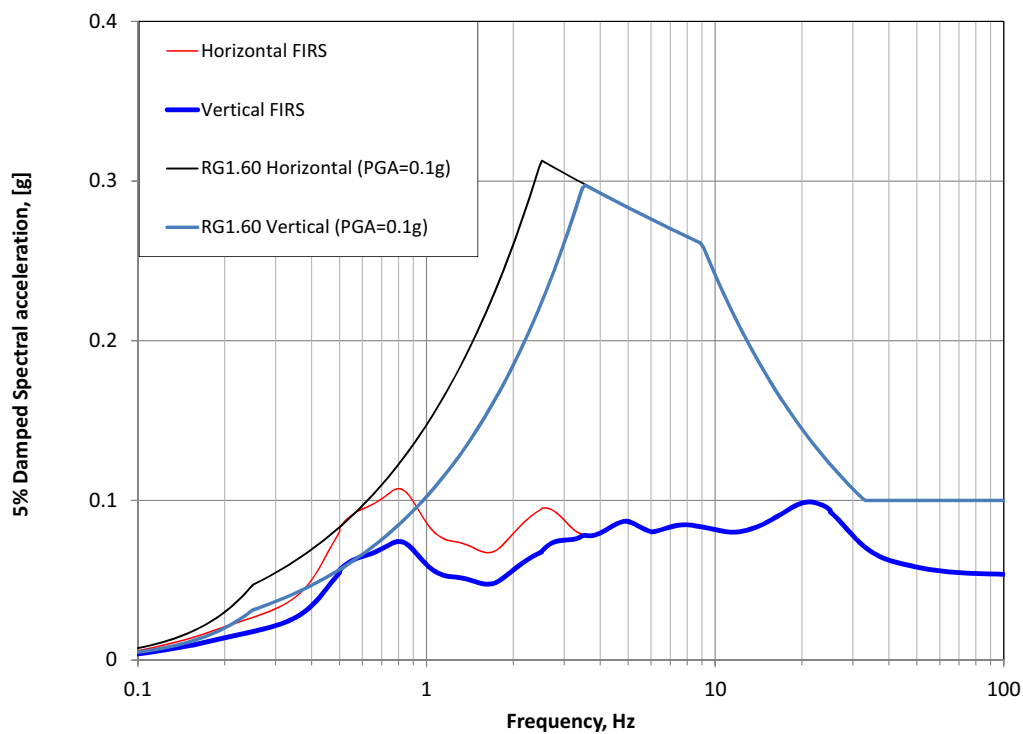


**Figure 3JJ-238 5% Damped ARS for FIRS and RG 1.60 Scaled to a PGA of 0.1 g (Elevation –16 Foot Horizon at Bottom of Nuclear Island Foundation)**

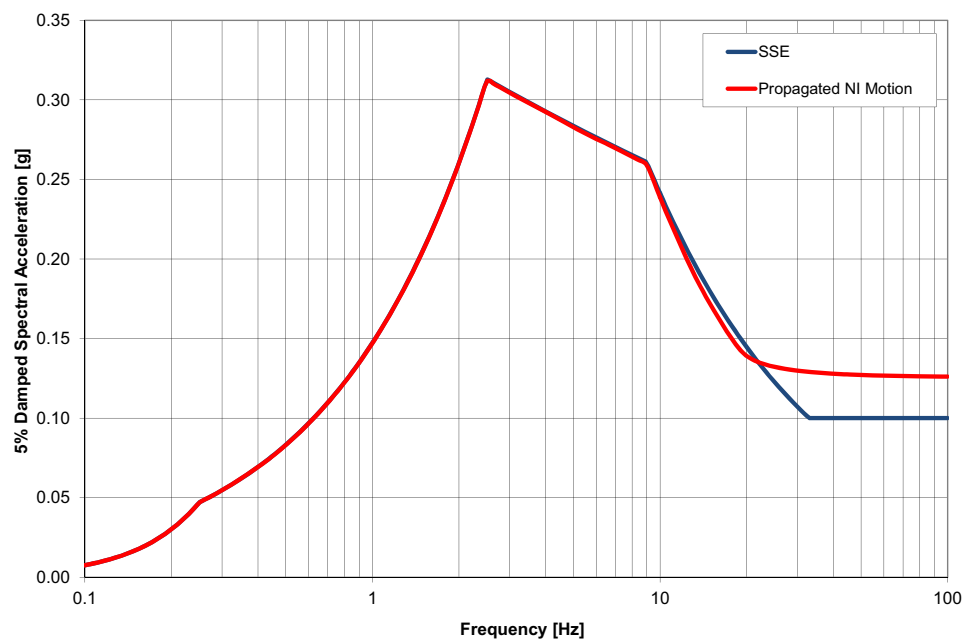


**Figure 3JJ-239 Propagated Motion at Founding Level — NI Soil Column  
(Elevation –16-Foot Horizon at Bottom of Nuclear Island Foundation)**



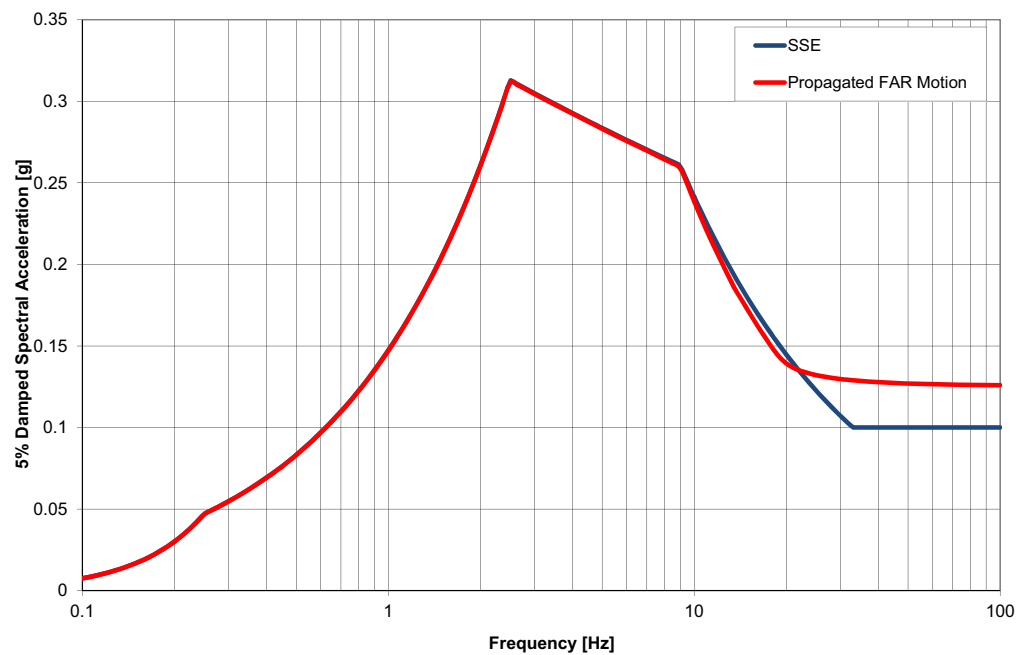


**Figure 3JJ-240 Propagated Motion at Foundation Level — FAR Soil Column (Elevation -16-Foot Horizon at Bottom of Nuclear-Island Foundation)**

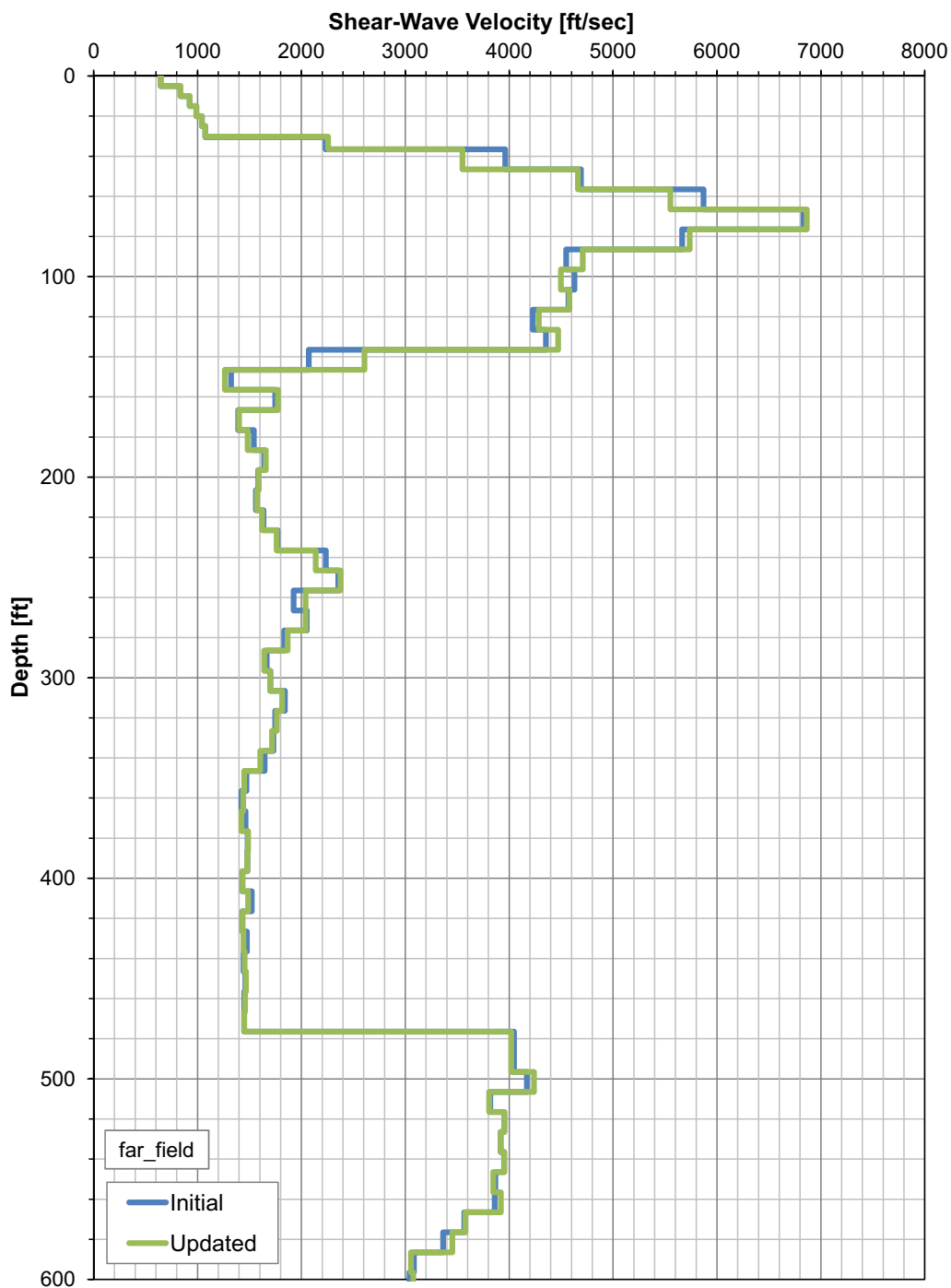


**Figure 3JJ-241 Comparison of Best-Estimate S-Wave Velocity Profile for the FAR Profile Provided by the Three Sources (Upper 600 feet - below 600 feet is not shown)**

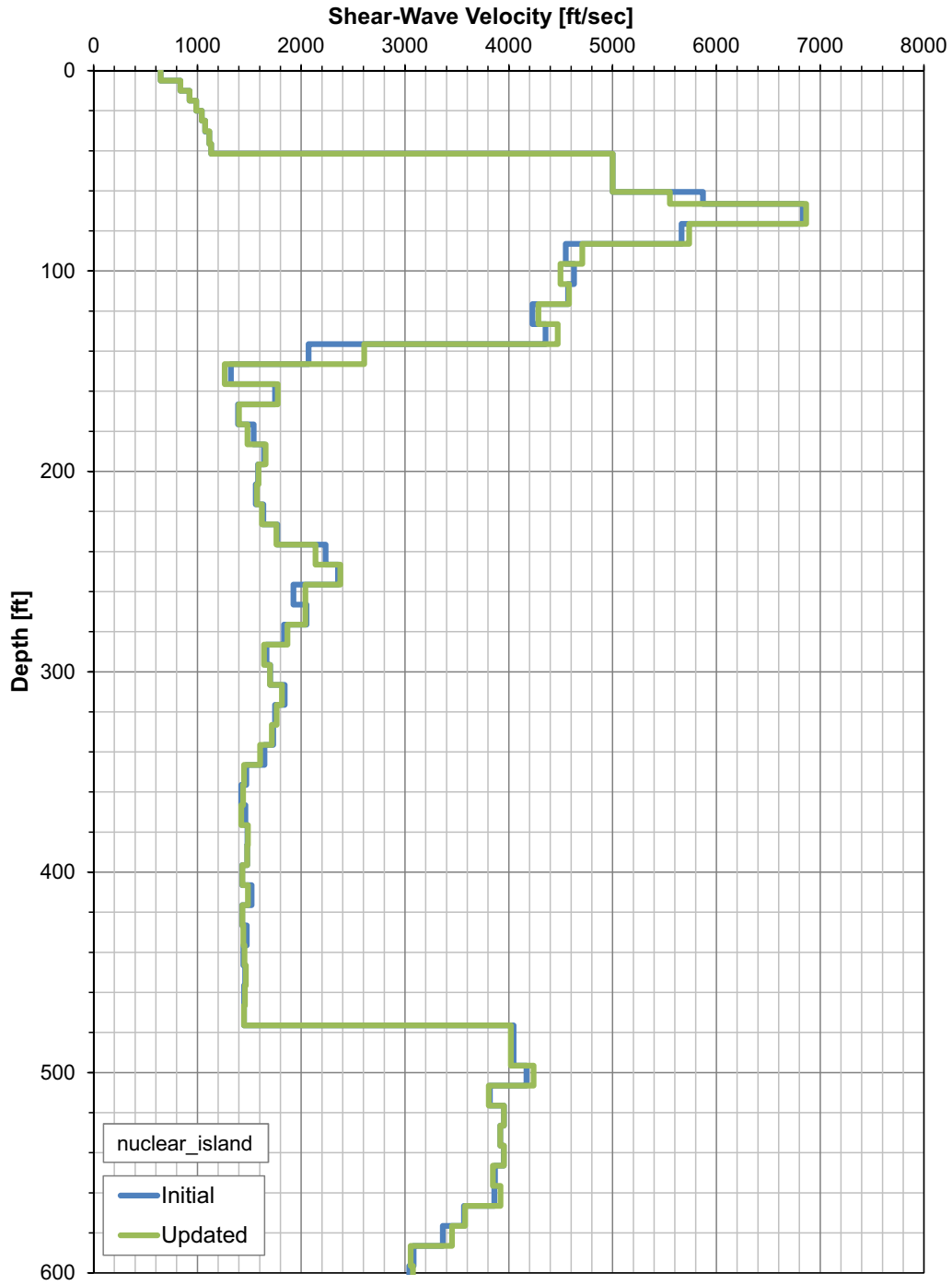


**Figure 3JJ-242 Comparison of Best-Estimate S-Wave Velocity Profiles for the NI Profile Provided by the Three Sources (Upper 600 feet - below 600 feet is not shown)**

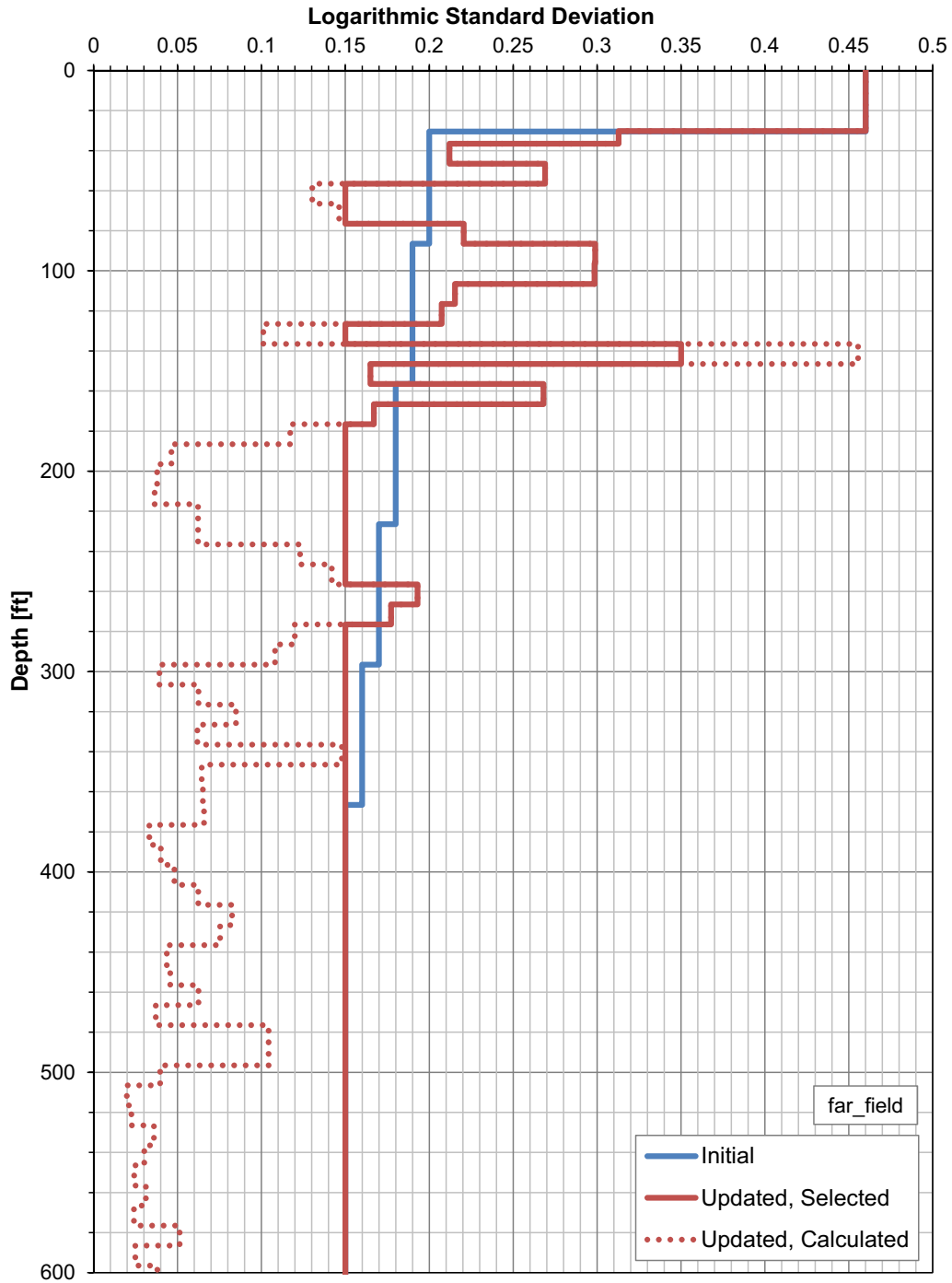


**Figure 3JJ-243 Comparison of Logarithmic Standard Deviation of the S-Wave Velocity for the FAR Profile Provided by the Two Sources (Upper 600 feet - below 600 feet is not shown)**

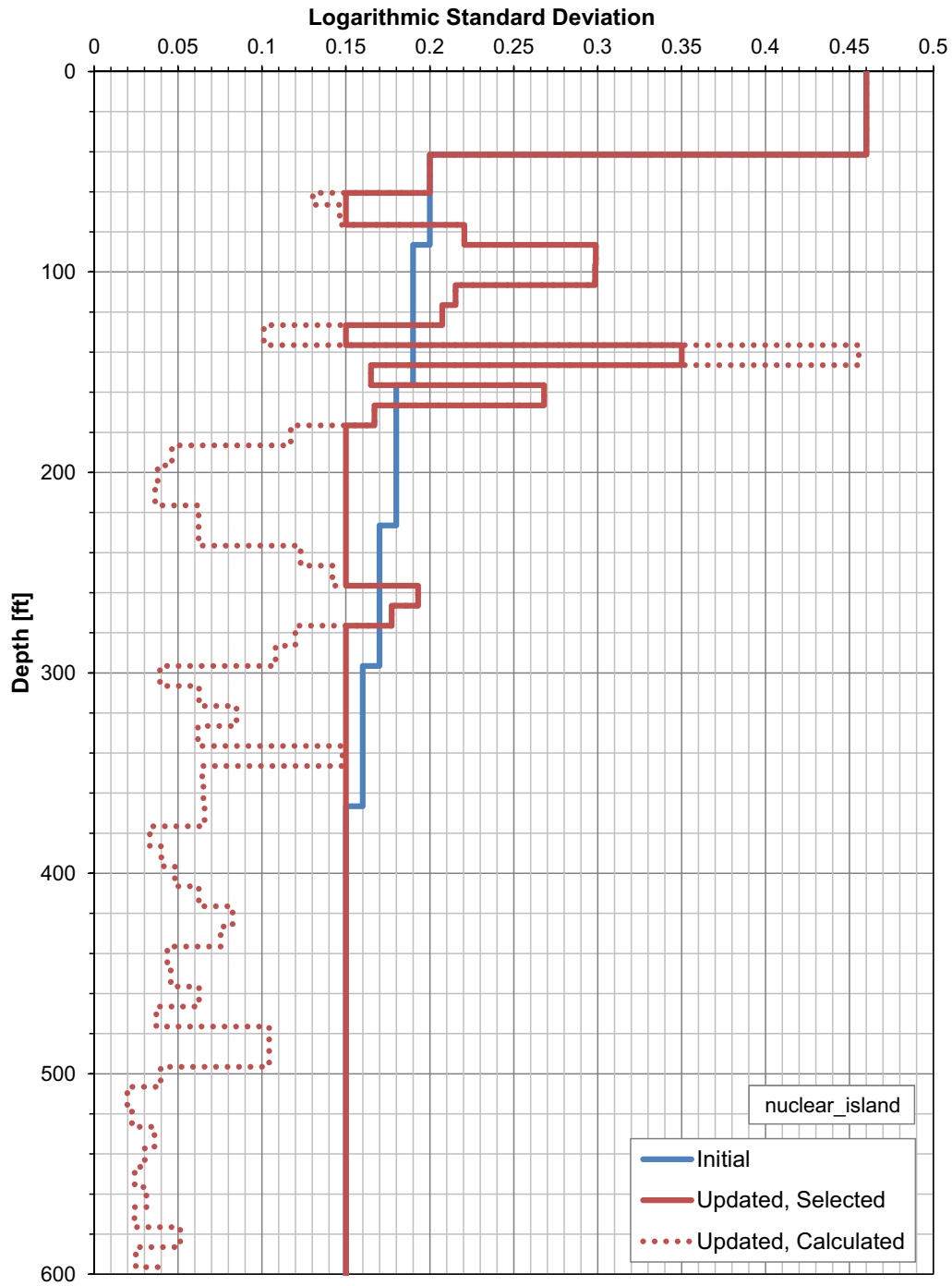


**Figure 3JJ-244 Comparison of Logarithmic Standard Deviation of the S-Wave Velocity for the NI Profile Provided by the Three Sources (Upper 600 feet - below 600 feet is not shown)**

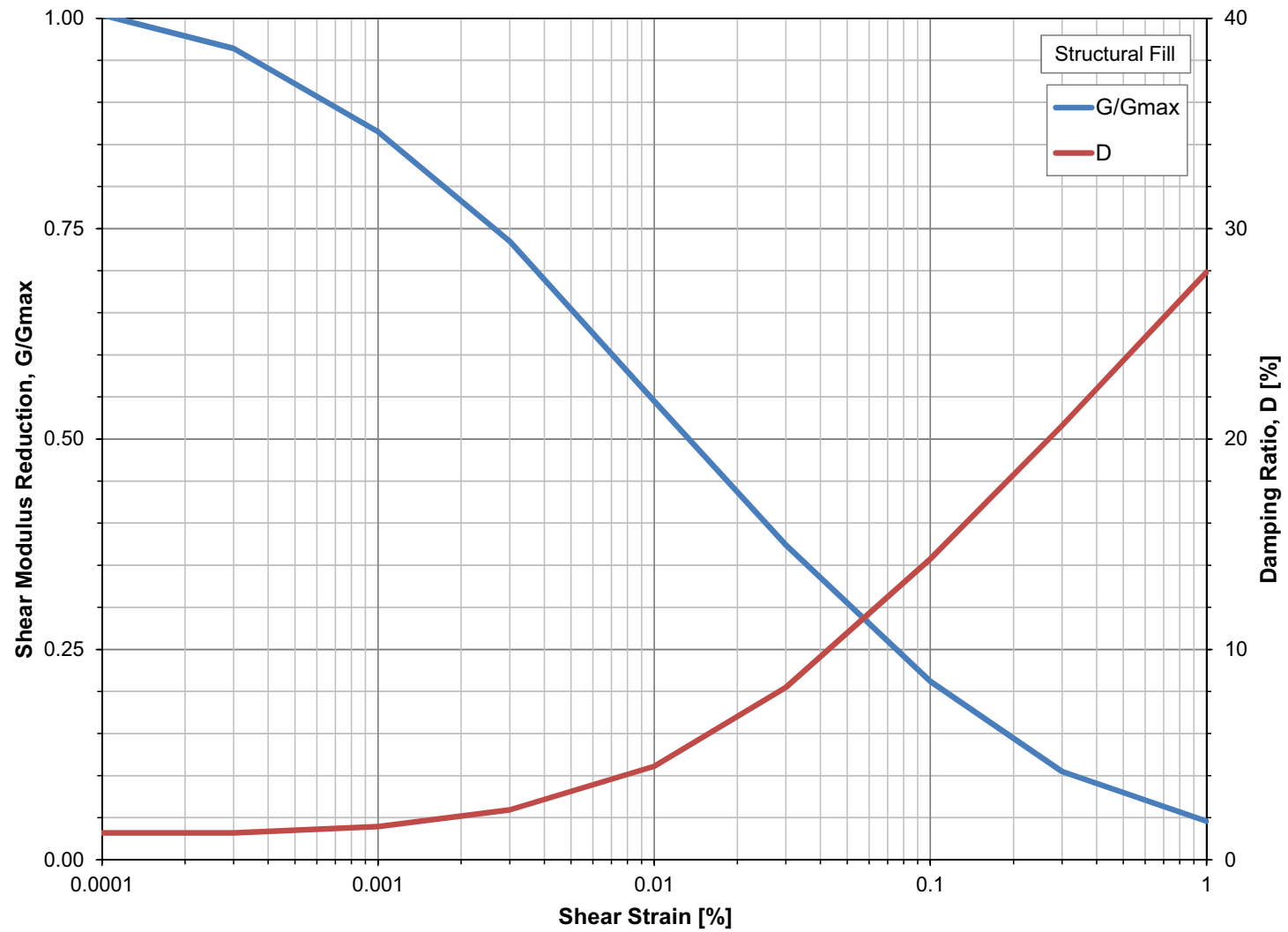


Figure 3JJ-245 Nonlinear Curves for the Structural Fill

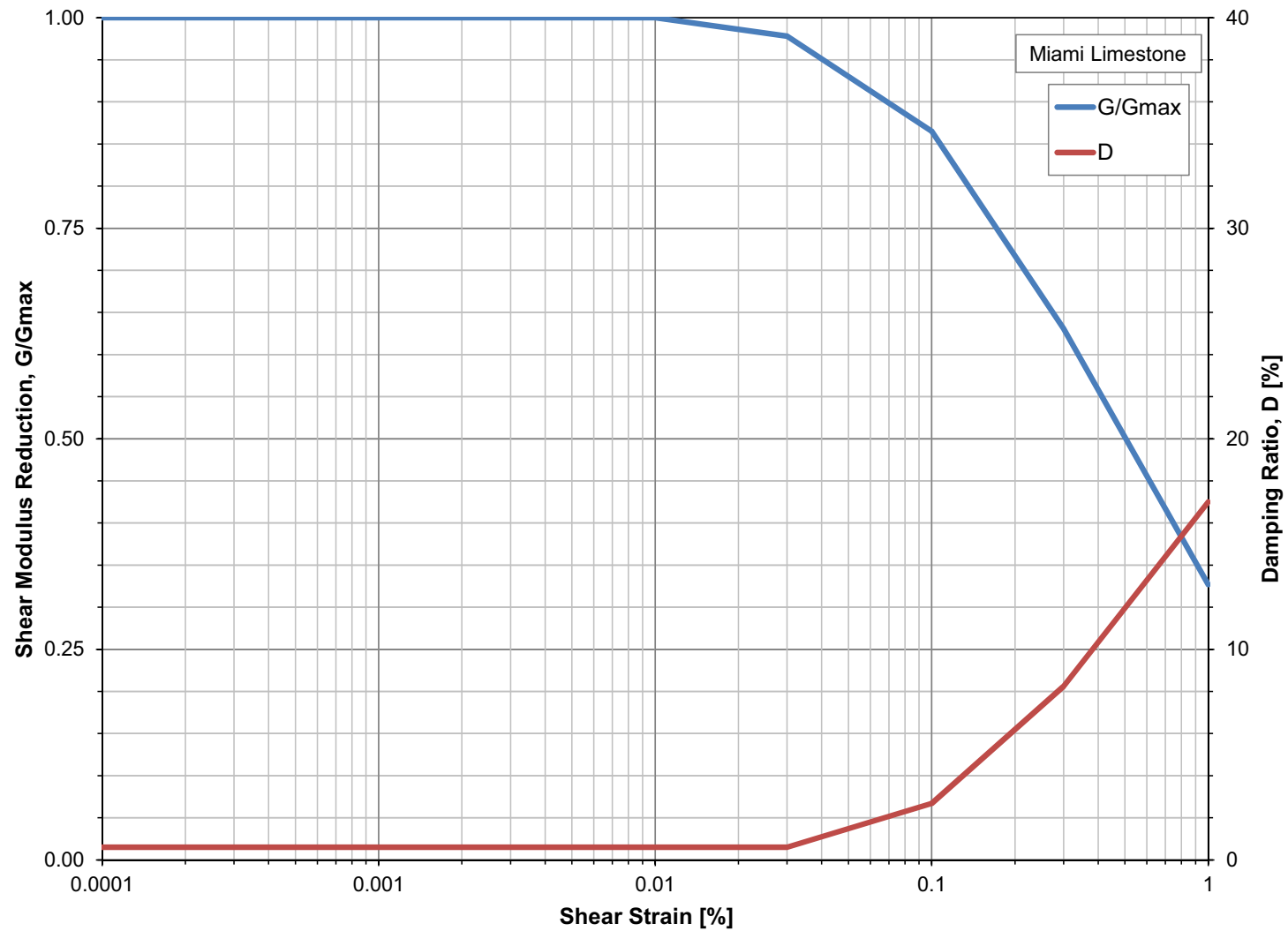


Figure 3JJ-246 Nonlinear Curves for the Miami Limestone

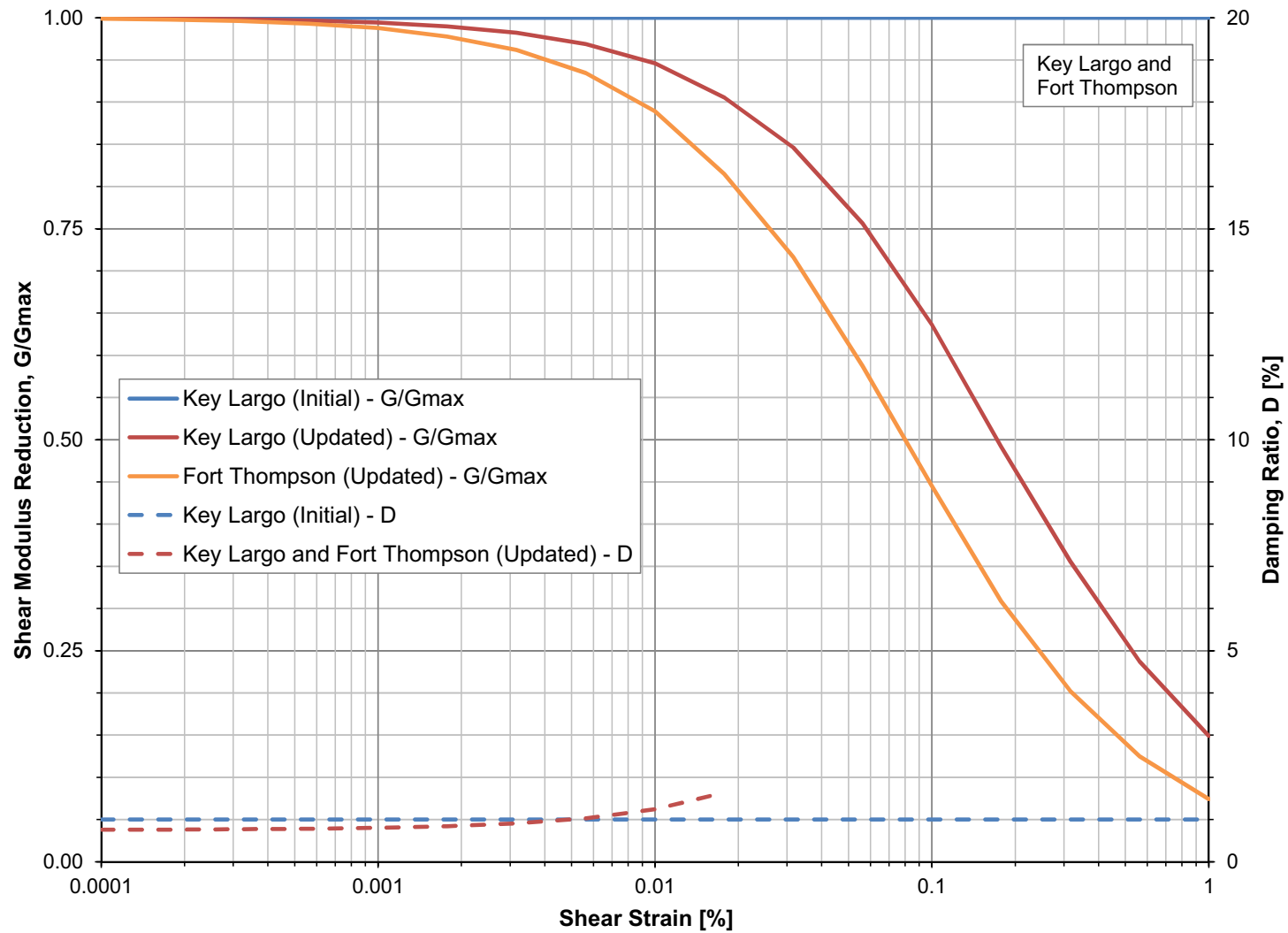
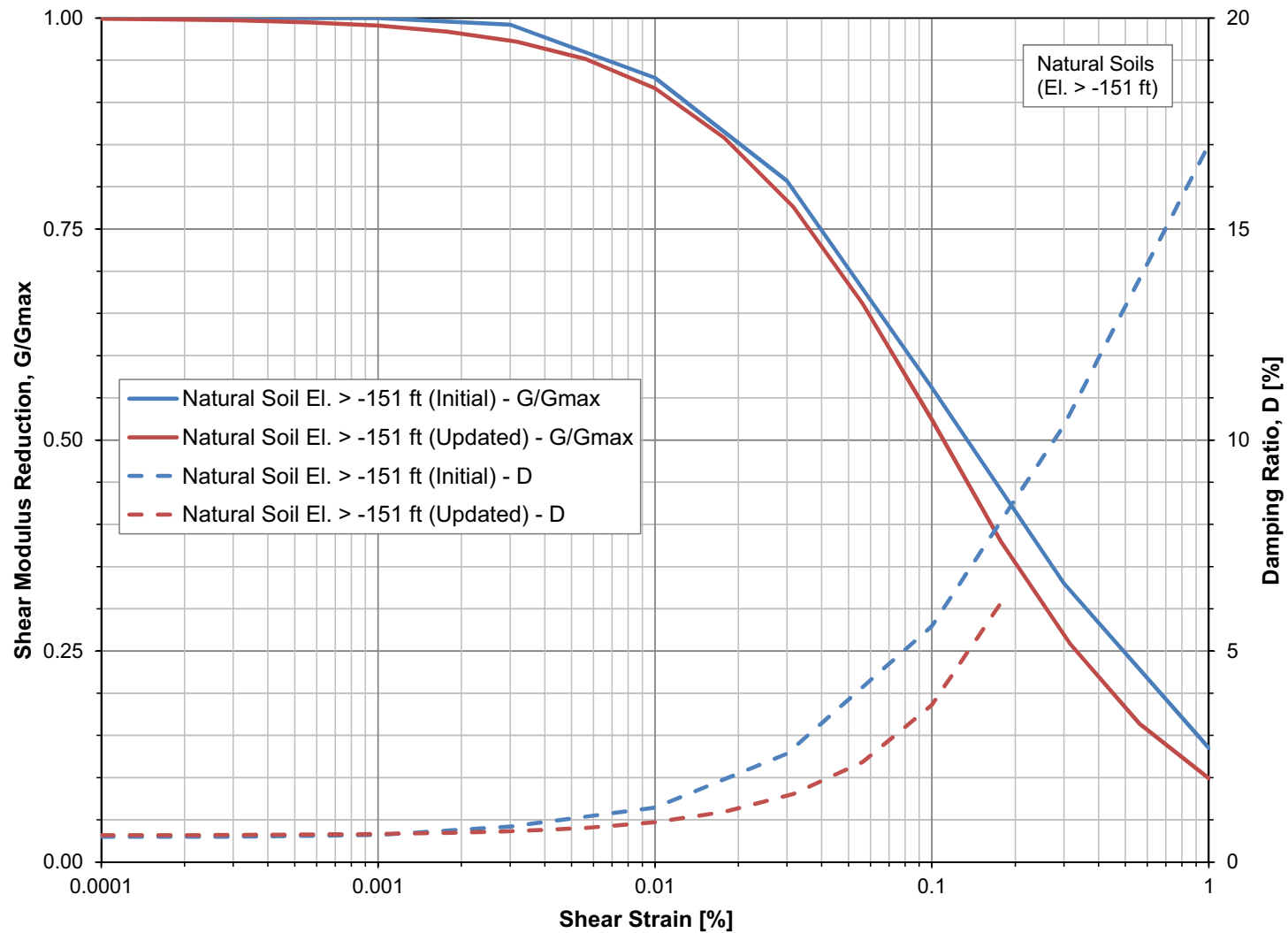
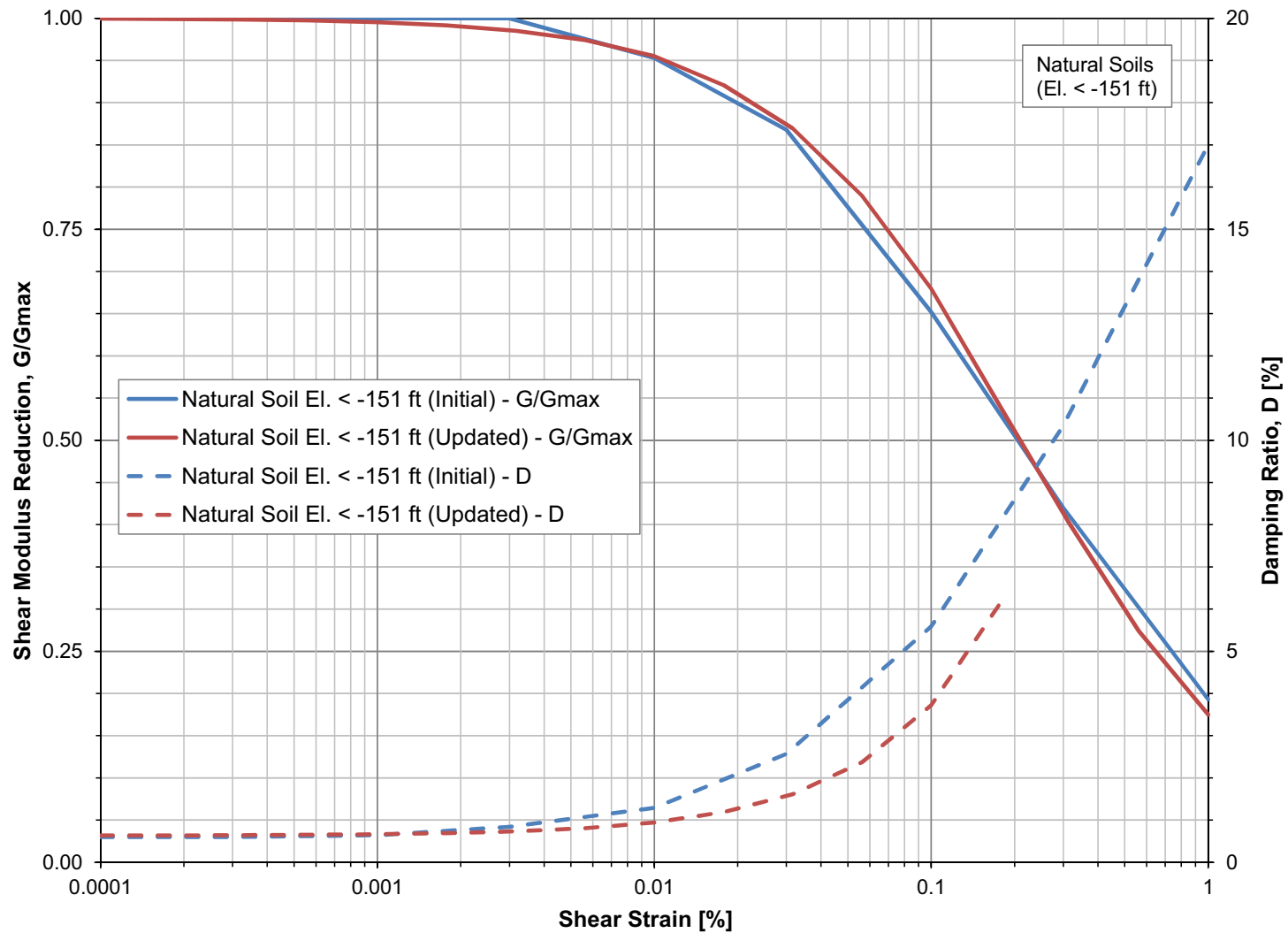


Figure 3JJ-247 Nonlinear Curves for Key Largo and Fort Thompson Formations





**Figure 3JJ-248 Nonlinear Curves for the Natural Soil (El. >-151 feet)**



**Figure 3JJ-249 Nonlinear Curves for the Natural Soil (El. <-151 feet)**

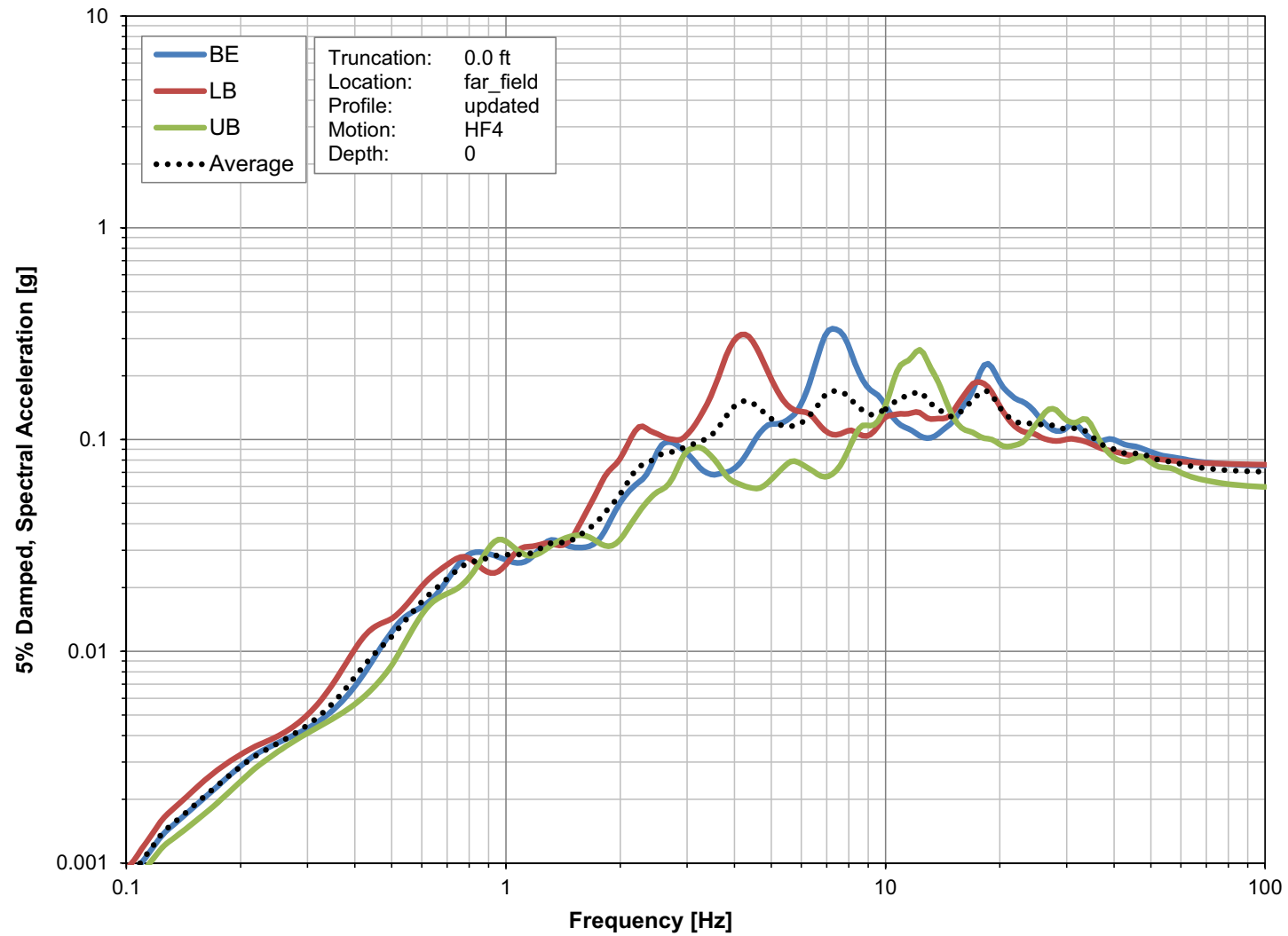


Figure 3JJ-250 Surface ARS for the “Updated” Site Column with the HF4 Input Motion

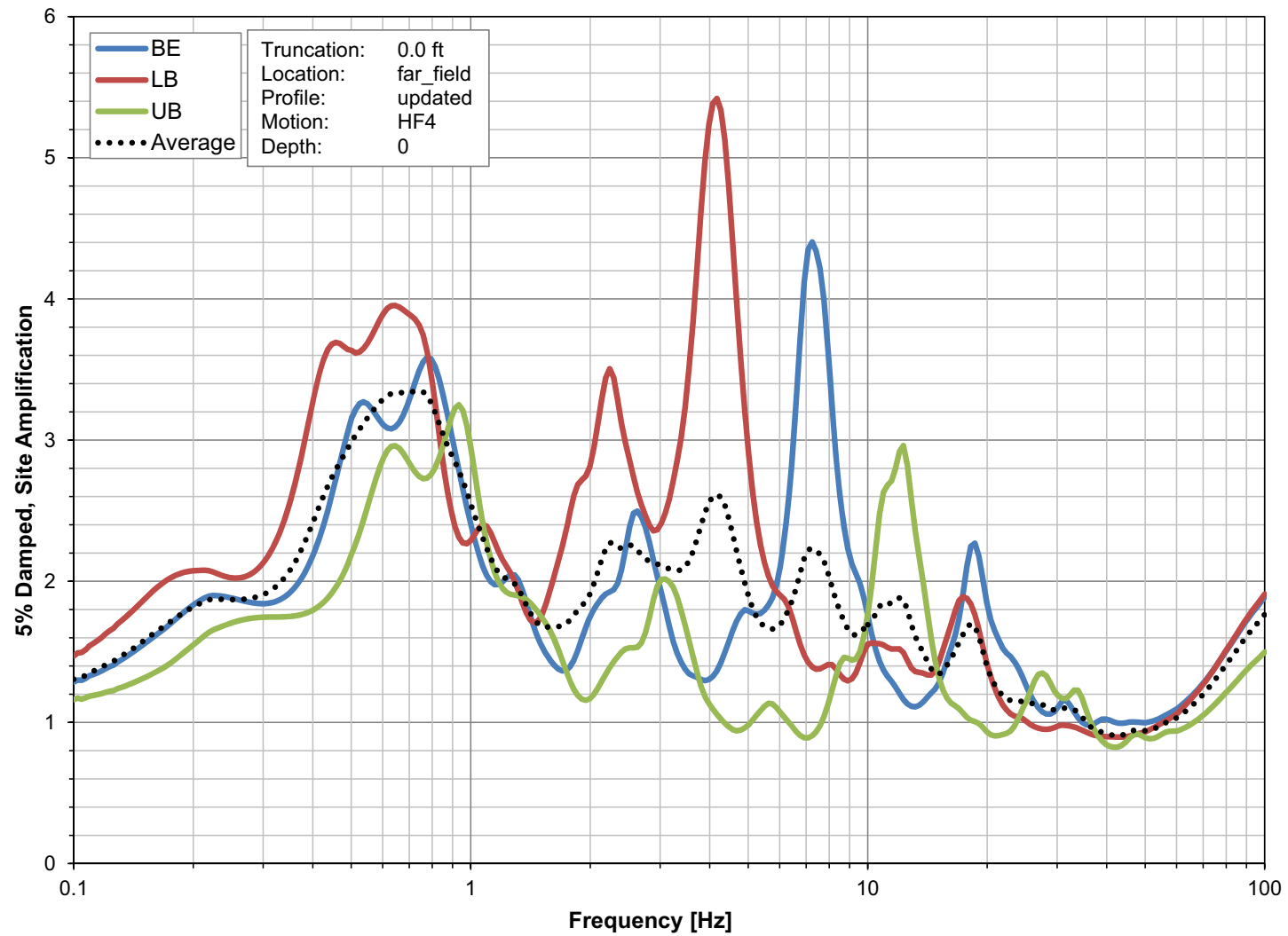


Figure 3JJ-251 Surface Site Amplification for the “Updated” Site Column with the HF4 Input Motion

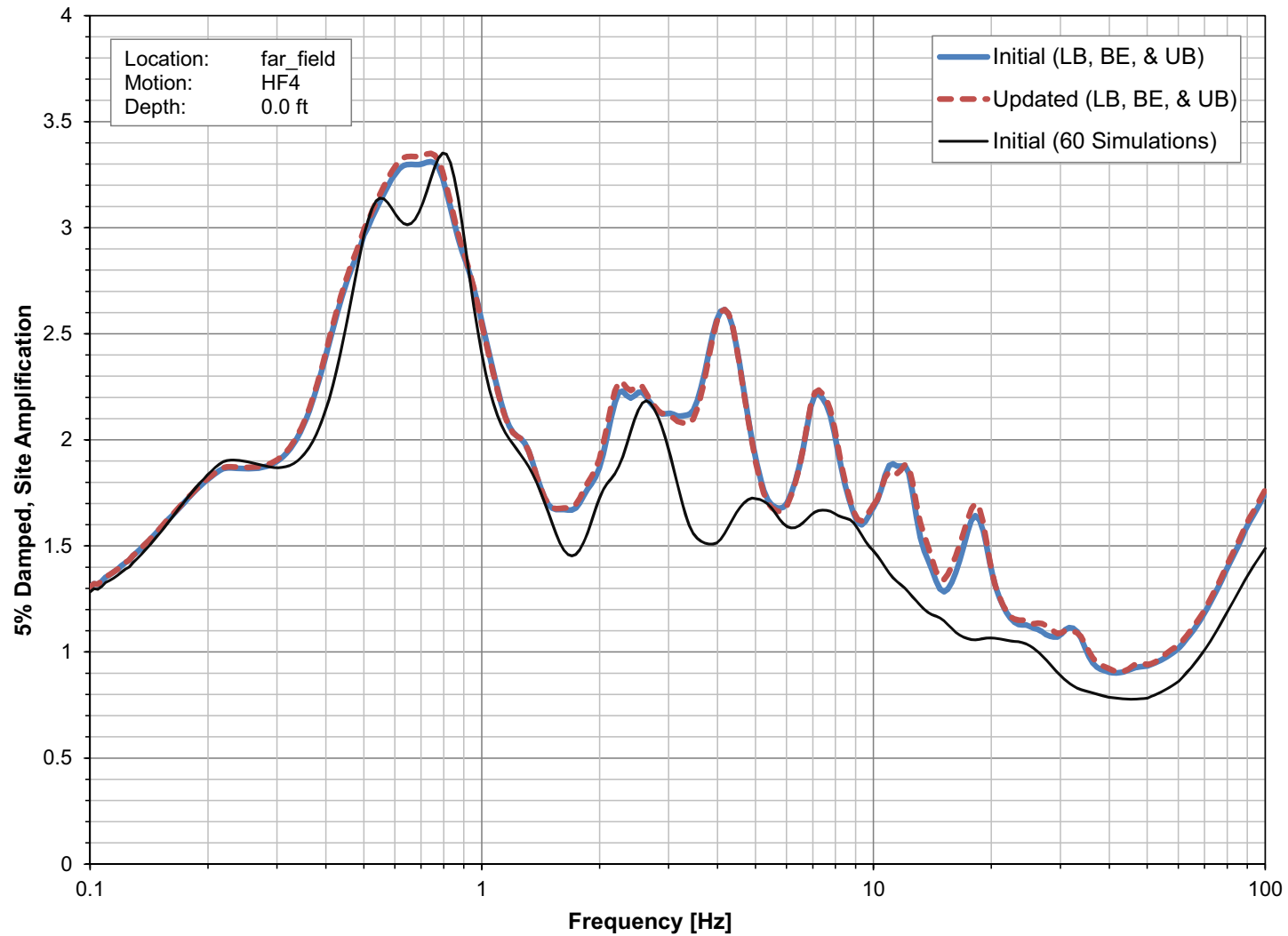
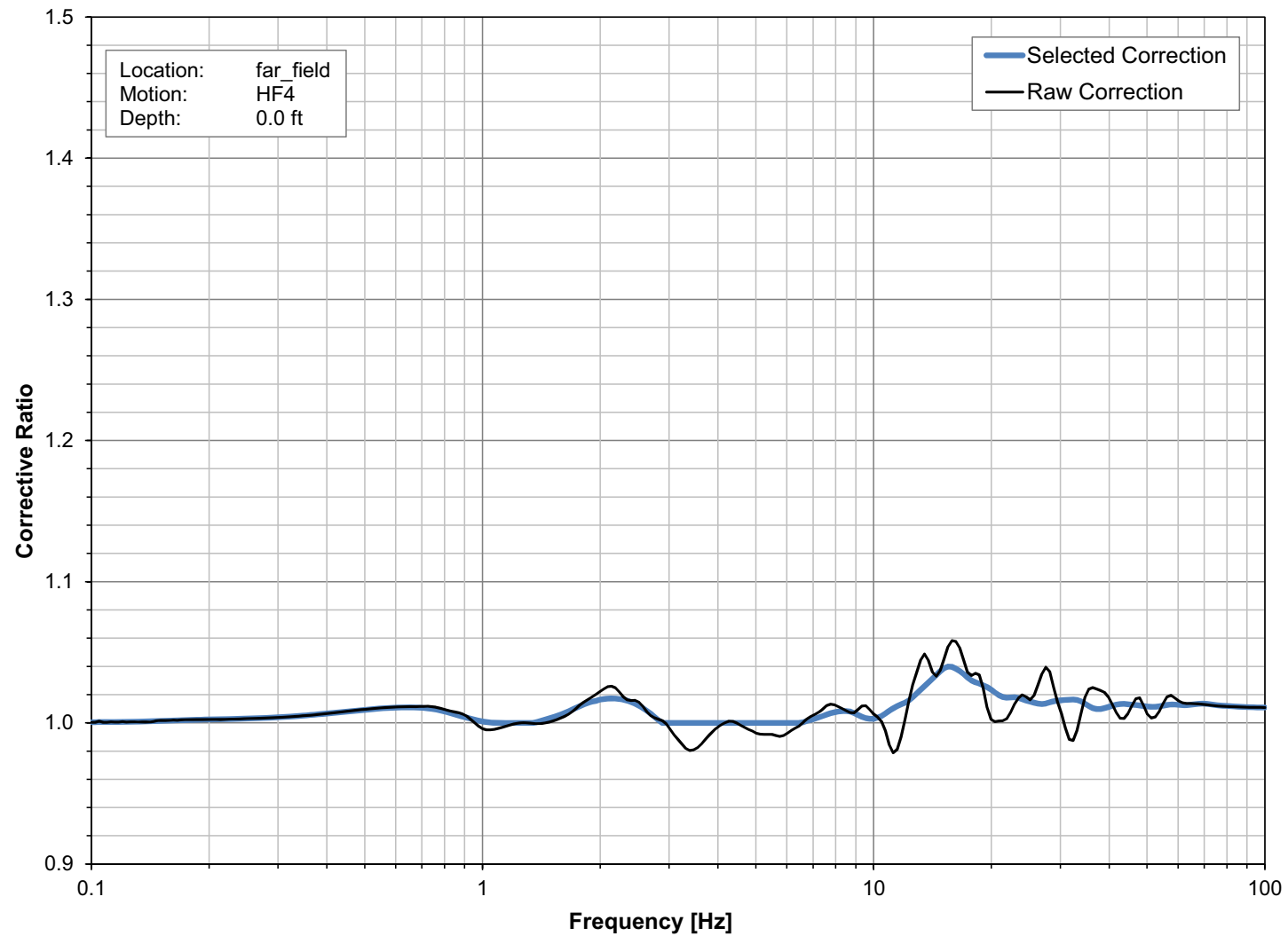


Figure 3JJ-252 Surface Site Amplification with the HF4 Input Motion



**Figure 3JJ-253 Corrective Ratio for the Surface Site Amplification for the FAR Site Column and the HF4 Input Motion**

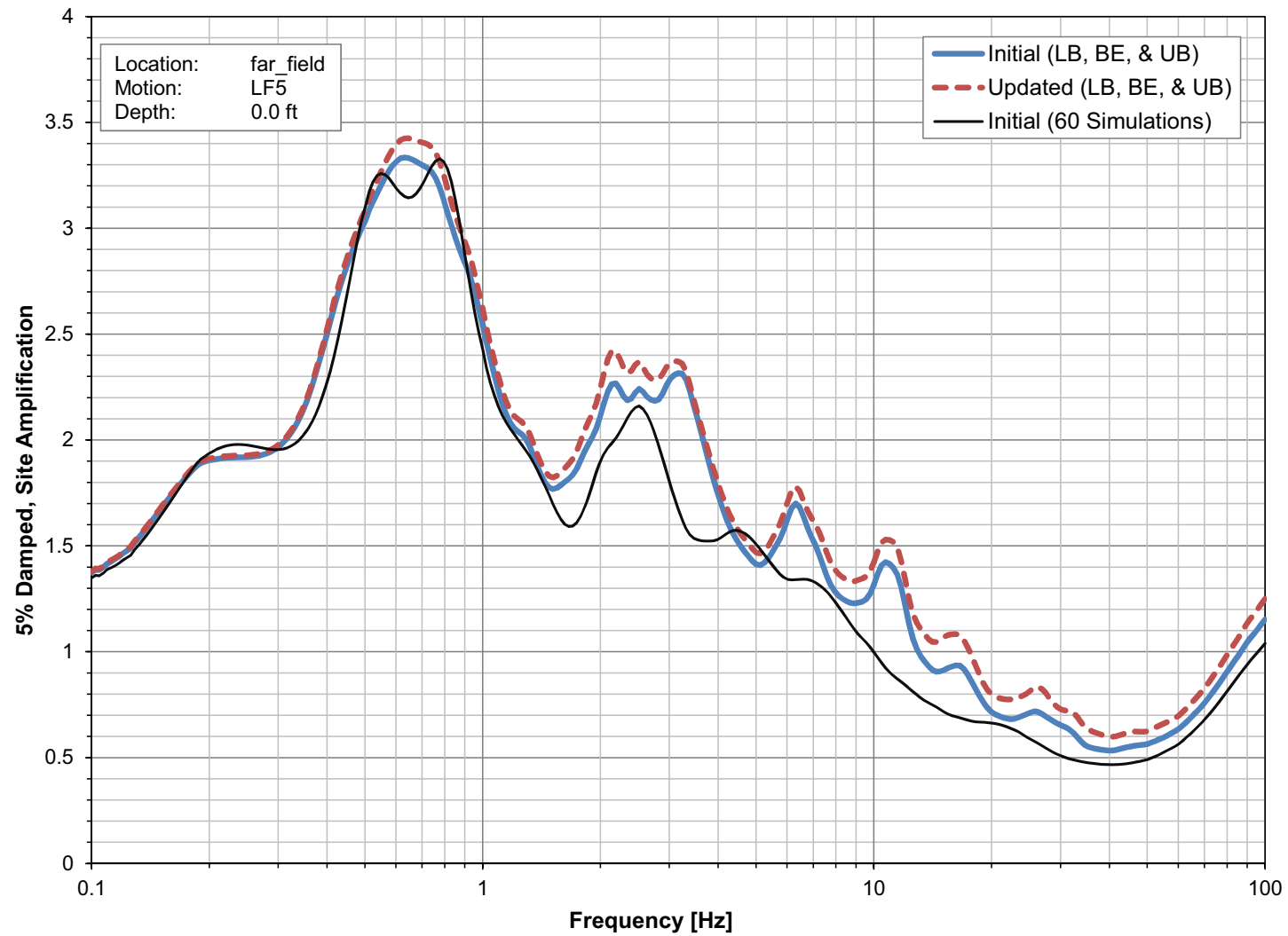
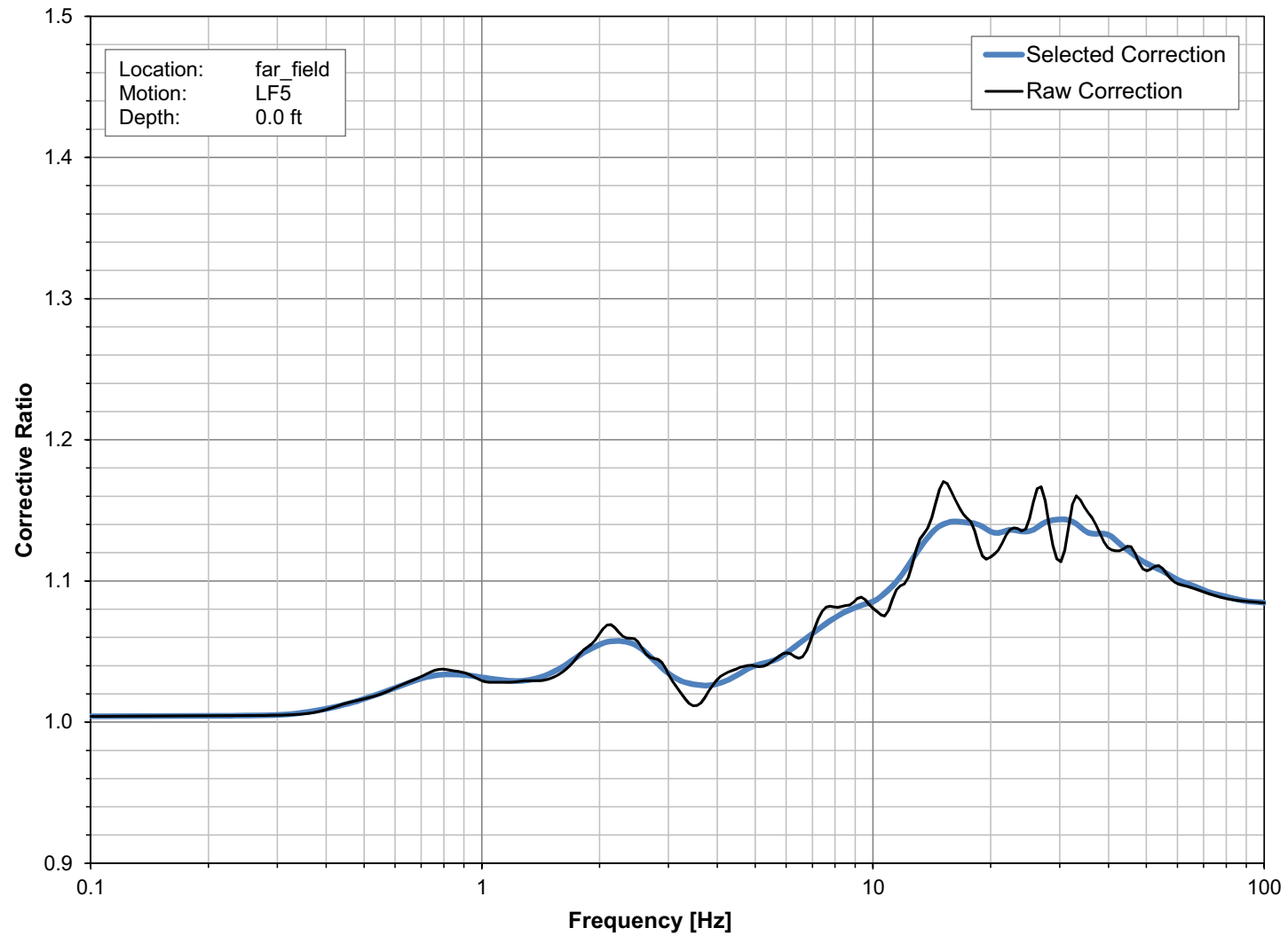


Figure 3JJ-254 Surface Site Amplification with the LF5 Input Motion



**Figure 3JJ-255 Corrective Ratio for the Surface Site Amplification for the FAR Site Column and the LF5 Input Motion**



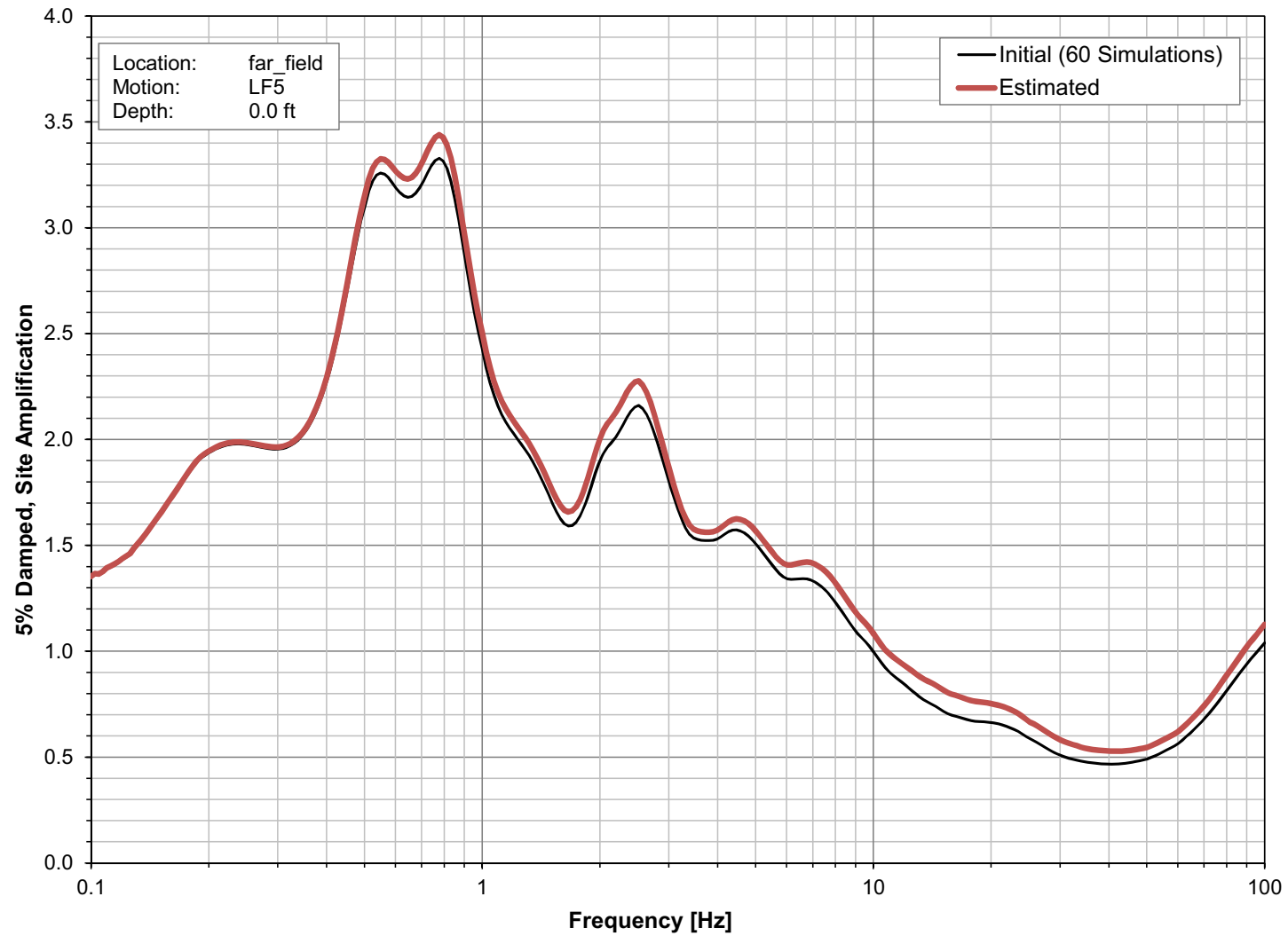


Figure 3JJ-256 Sensitivity Surface Site Amplification for the FAR Site Column and the LF5 Input Motion

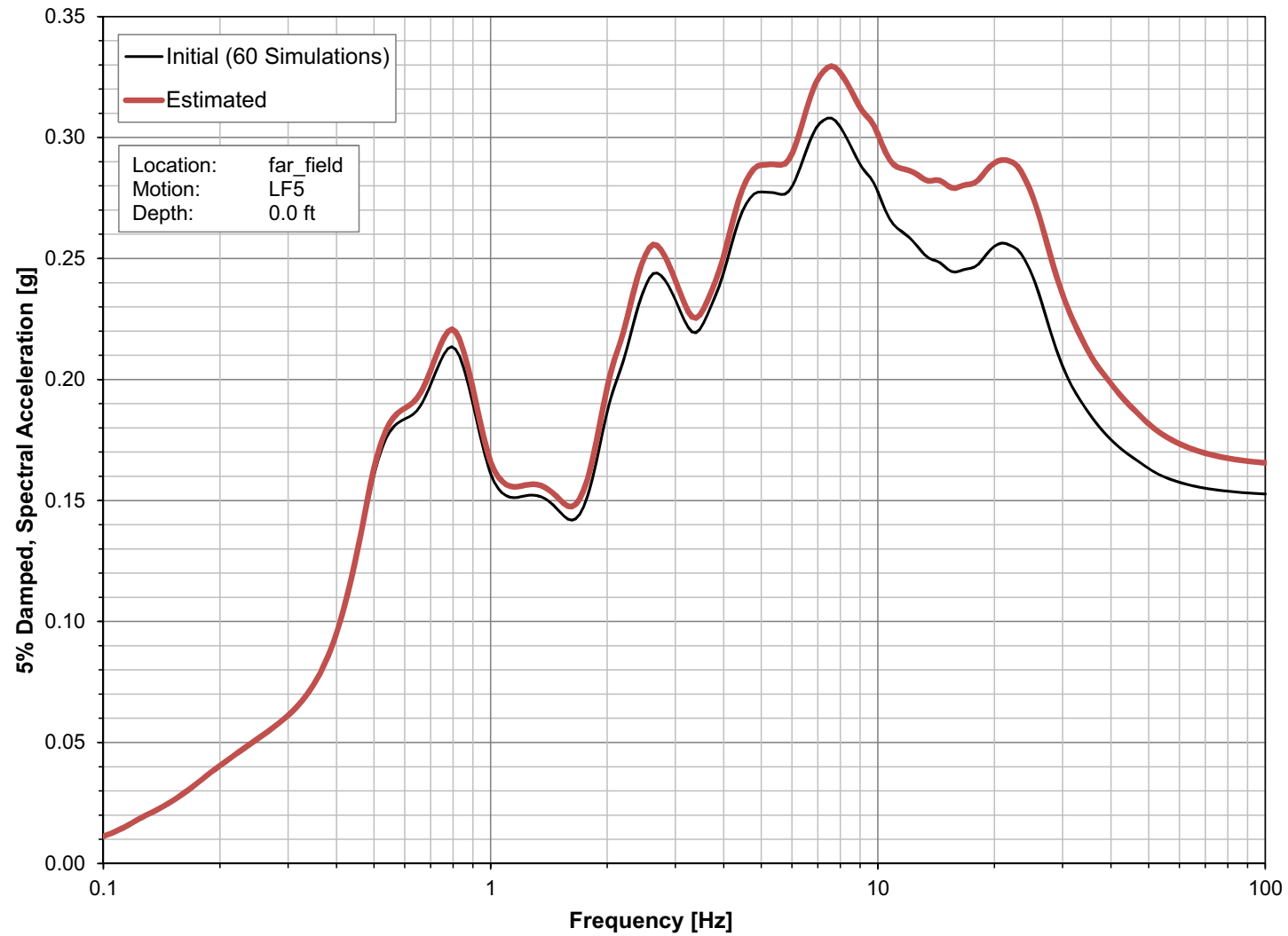
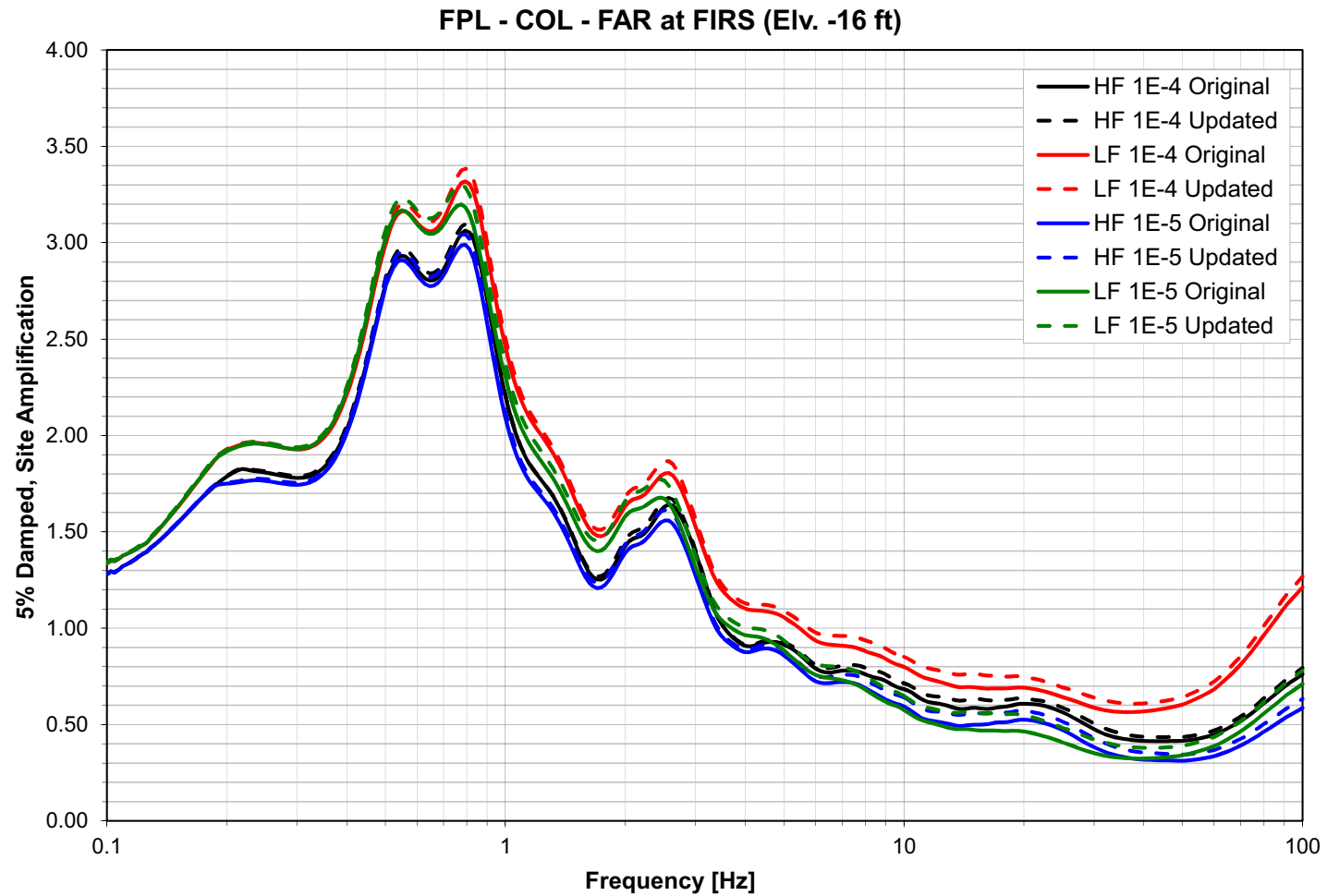
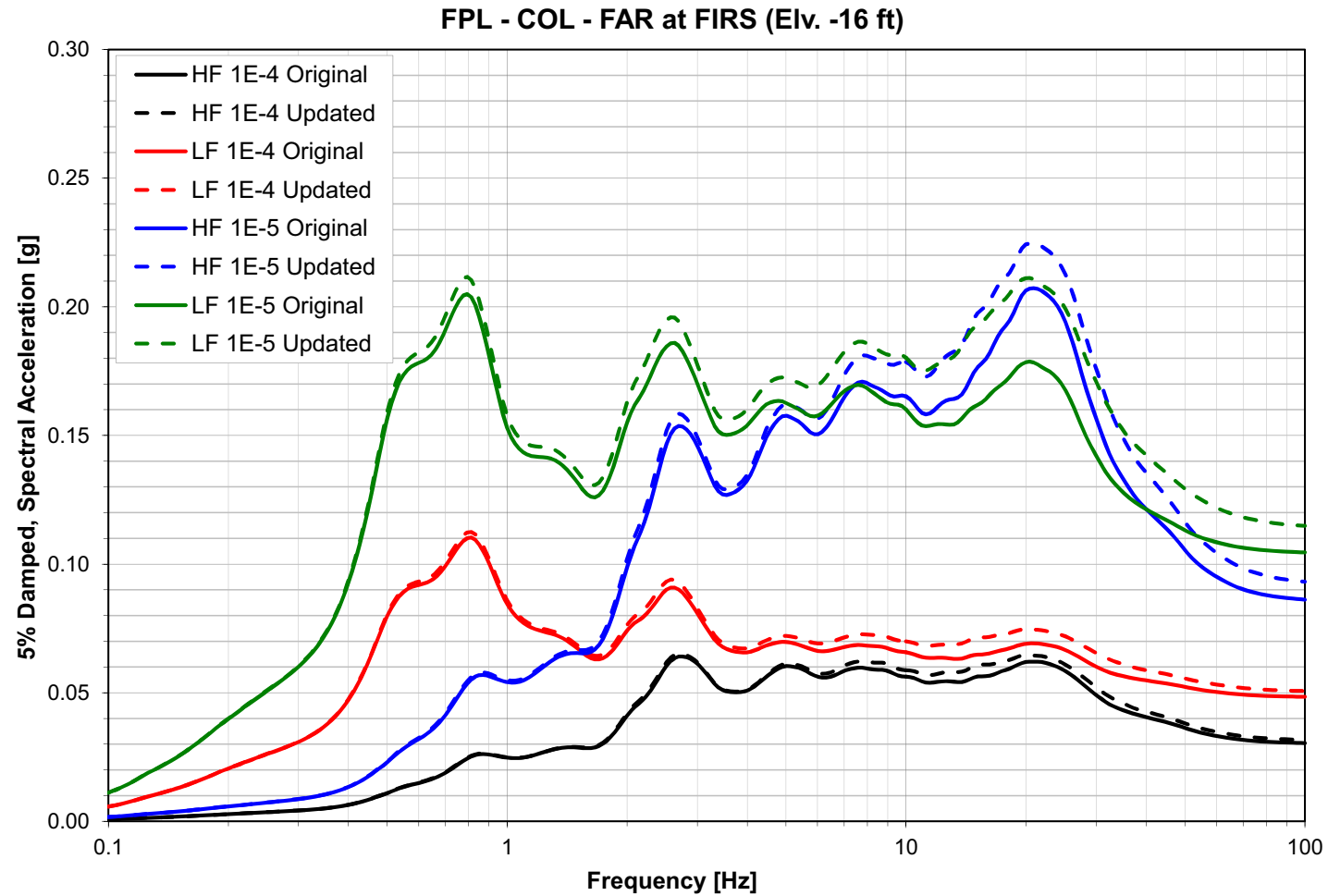


Figure 3JJ-257 Sensitivity Surface ARS for the FAR Site Column and the LF5 Input Motion



**Figure 3JJ-258 Comparison of the Site Amplification for the NI Foundation  
Between the Sensitivity and the Initial Analyses (FAR Profile)**



**Figure 3JJ-259 Comparison of the ARS for the NI Foundation Between the Sensitivity and the Initial Analysis (FAR Profile)**

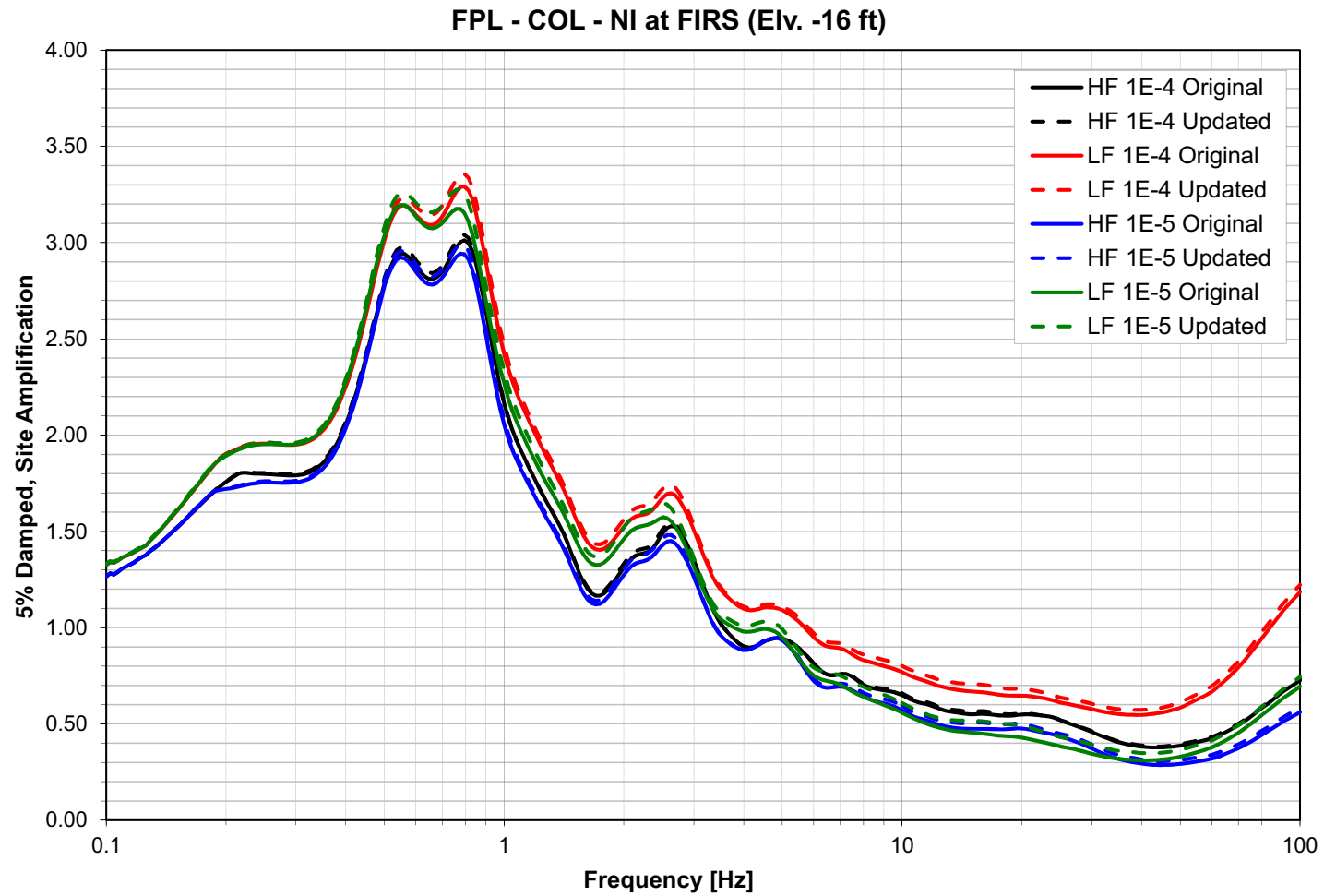


**Figure 3JJ-260 Comparison of the Site Amplification for the NI Foundation  
Between the Sensitivity and the Initial Analysis (NI Profile)**

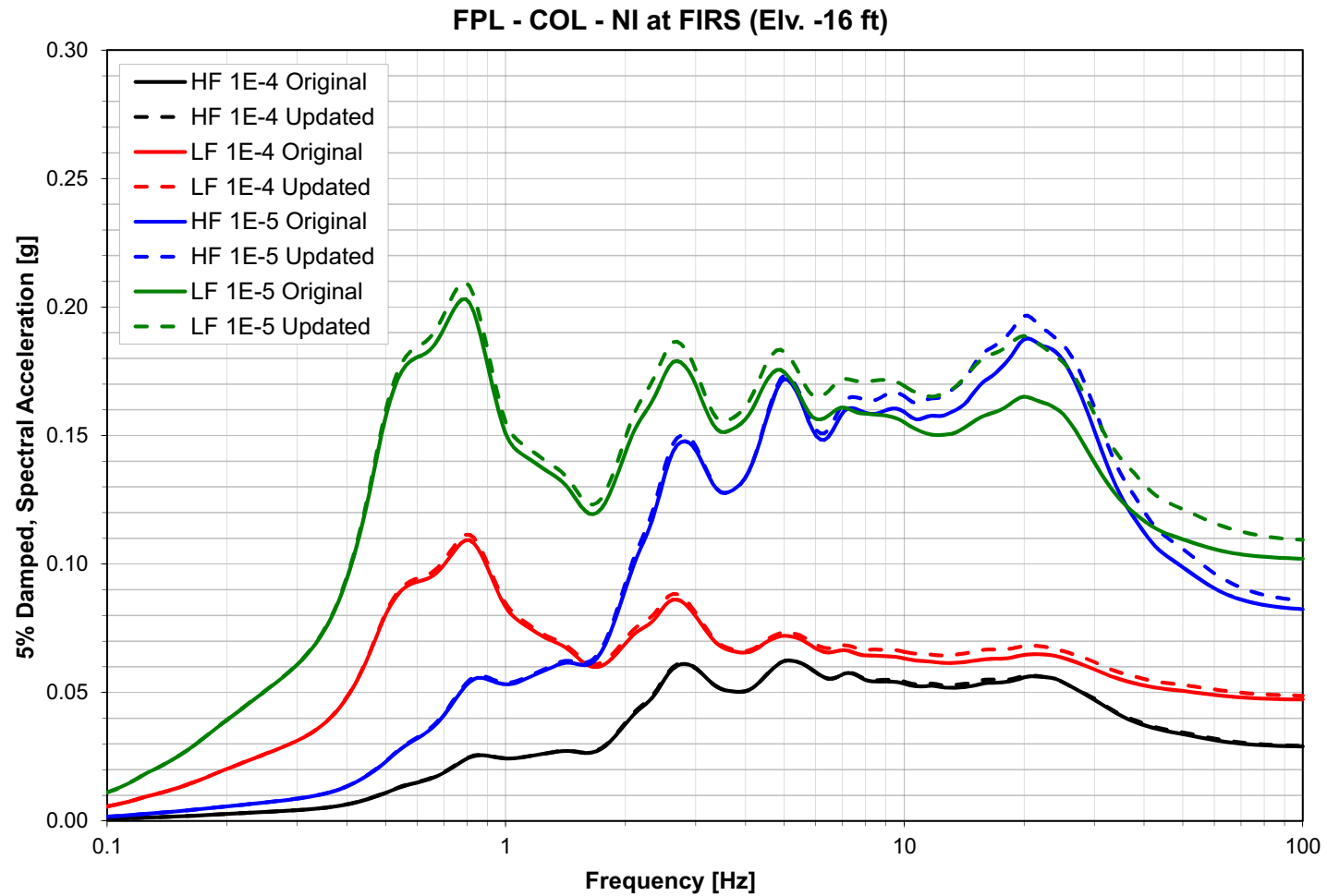


**Figure 3JJ-261 Comparison of the ARS for the NI Foundation Between the Sensitivity and the Initial Analysis (NI Profile)**

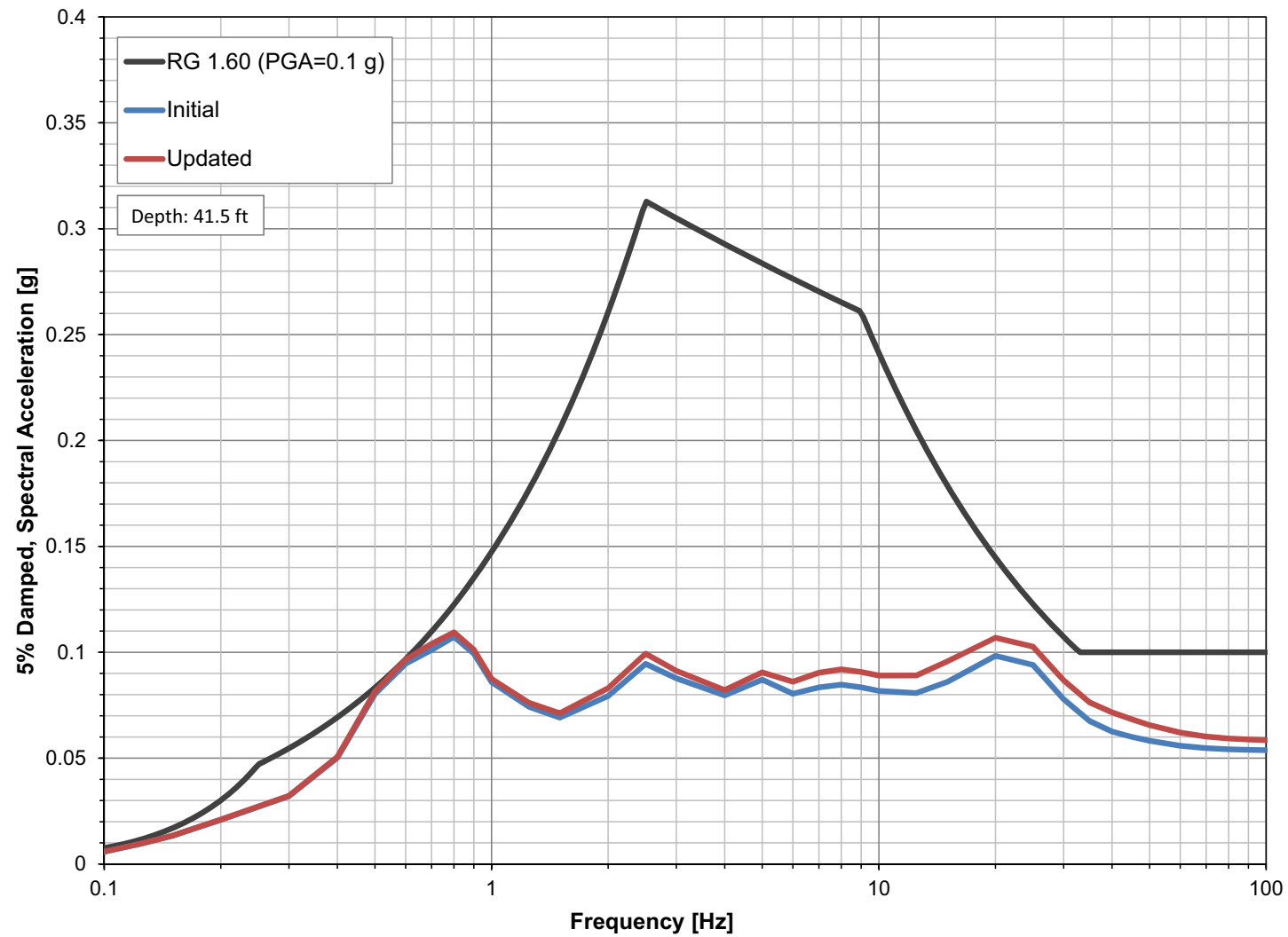
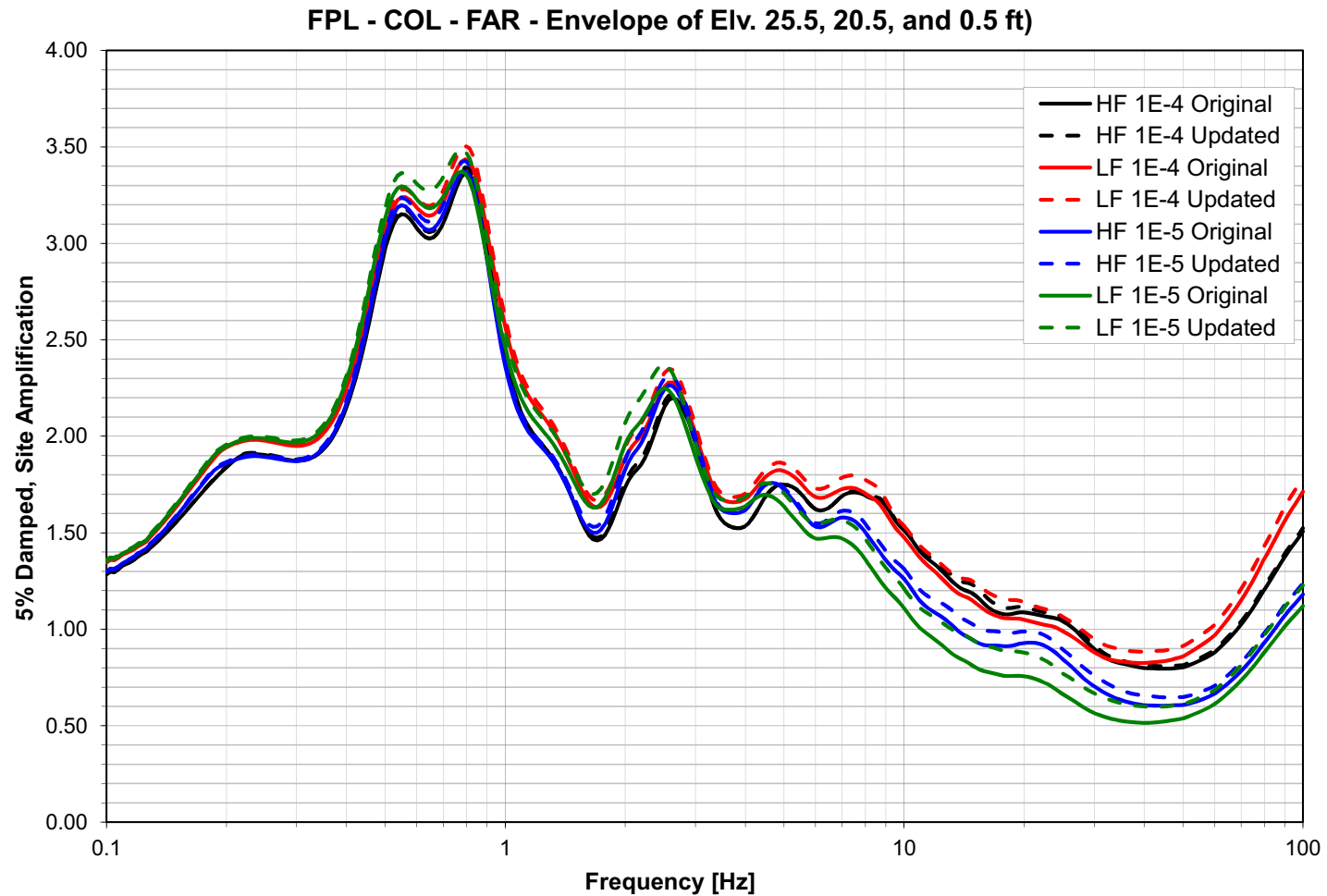
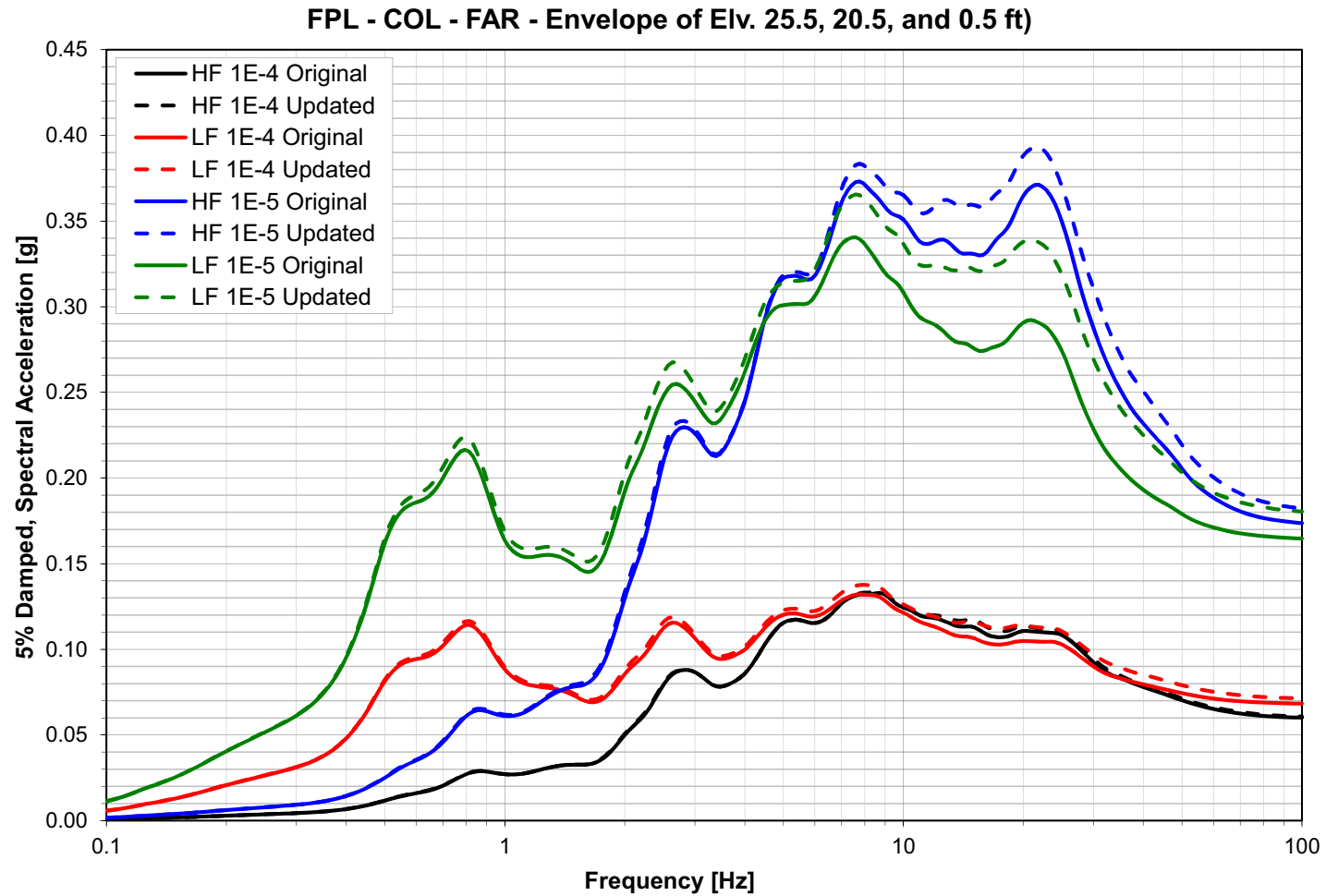


Figure 3JJ-262 Comparison Between the NI FIRS Computed with the Sensitivity Analysis and the Initial Analysis (NI Profile)



**Figure 3JJ-263 Comparison of the Enveloped Site Amplification for the Surface DRS  
Between the Sensitivity and the Initial Analysis (FAR Profile)**





**Figure 3JJ-264 Comparison of the Enveloped ARS for the Surface DRS  
Between the Sensitivity and the Initial Analysis (FAR Profile)**

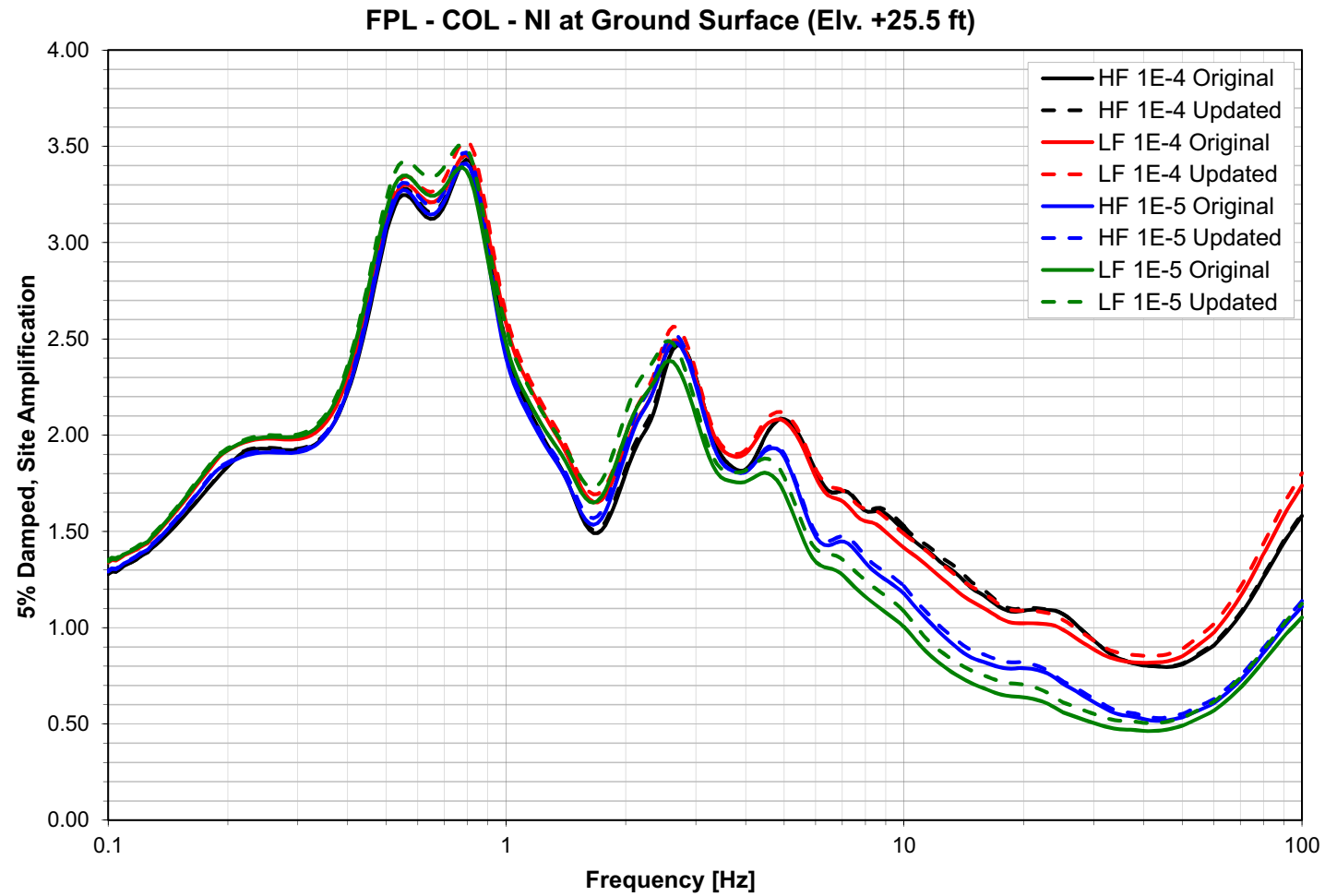


**Figure 3JJ-265 Comparison of the Site Amplification for the Surface DRS  
Between the Sensitivity and the Initial Analysis (NI Profile)**

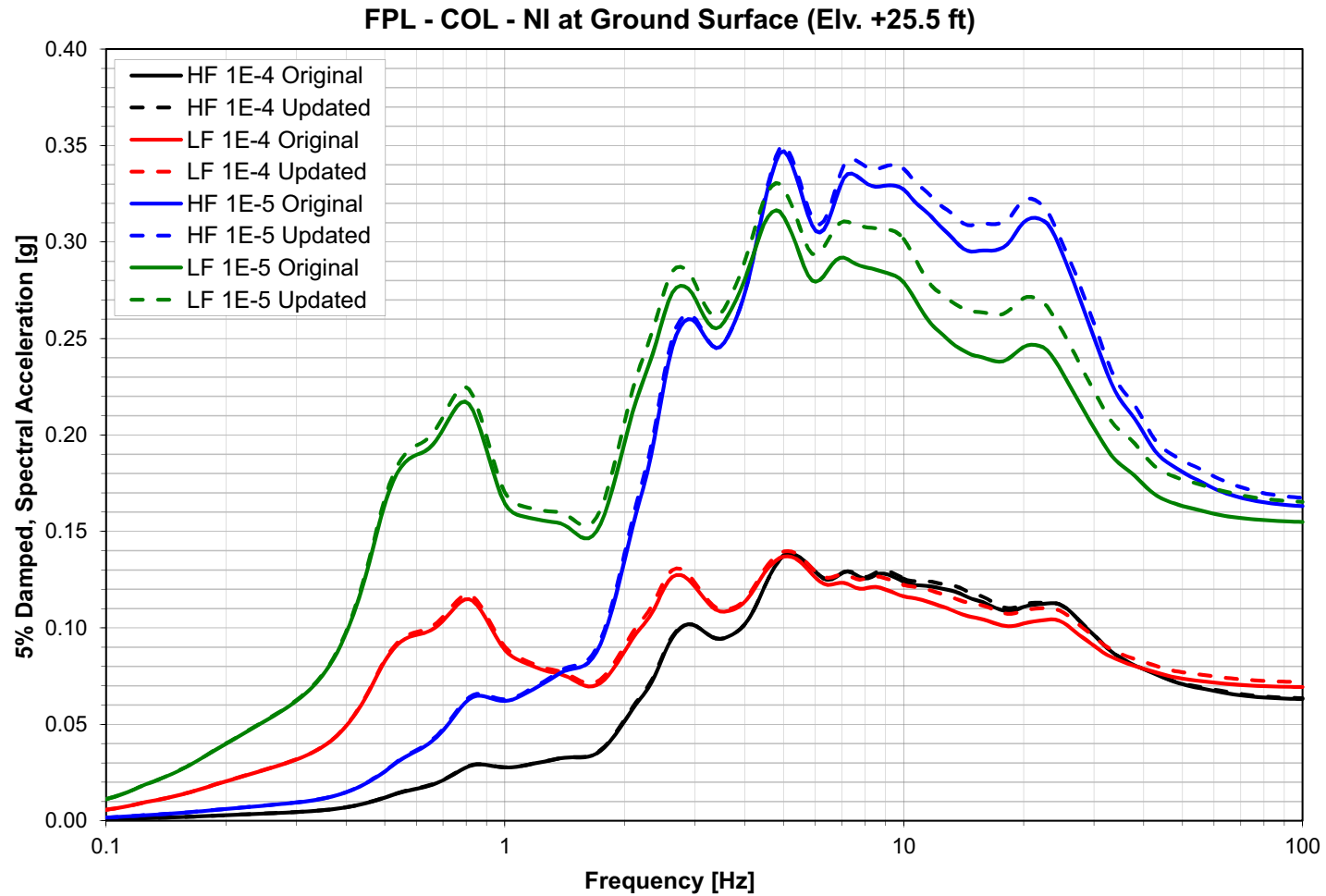


**Figure 3JJ-266 Comparison of the ARS for the Surface DRS Between the Sensitivity and the Initial Analysis (NI profile)**

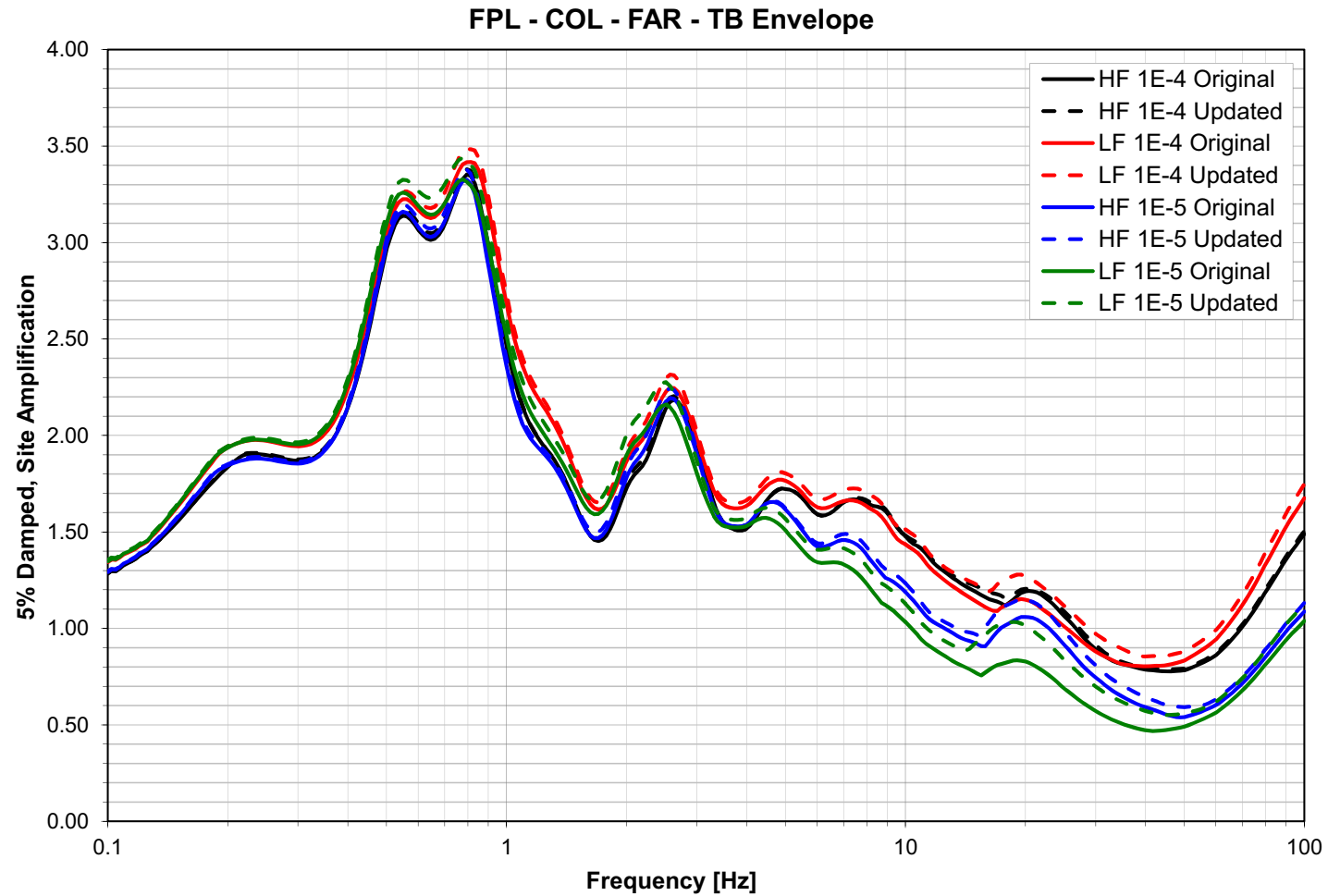


**Figure 3JJ-267 Comparison of the Enveloped Site Amplification for the Turbine Building FIRS Between the Sensitivity and Initial Analyses (FAR Profile)**

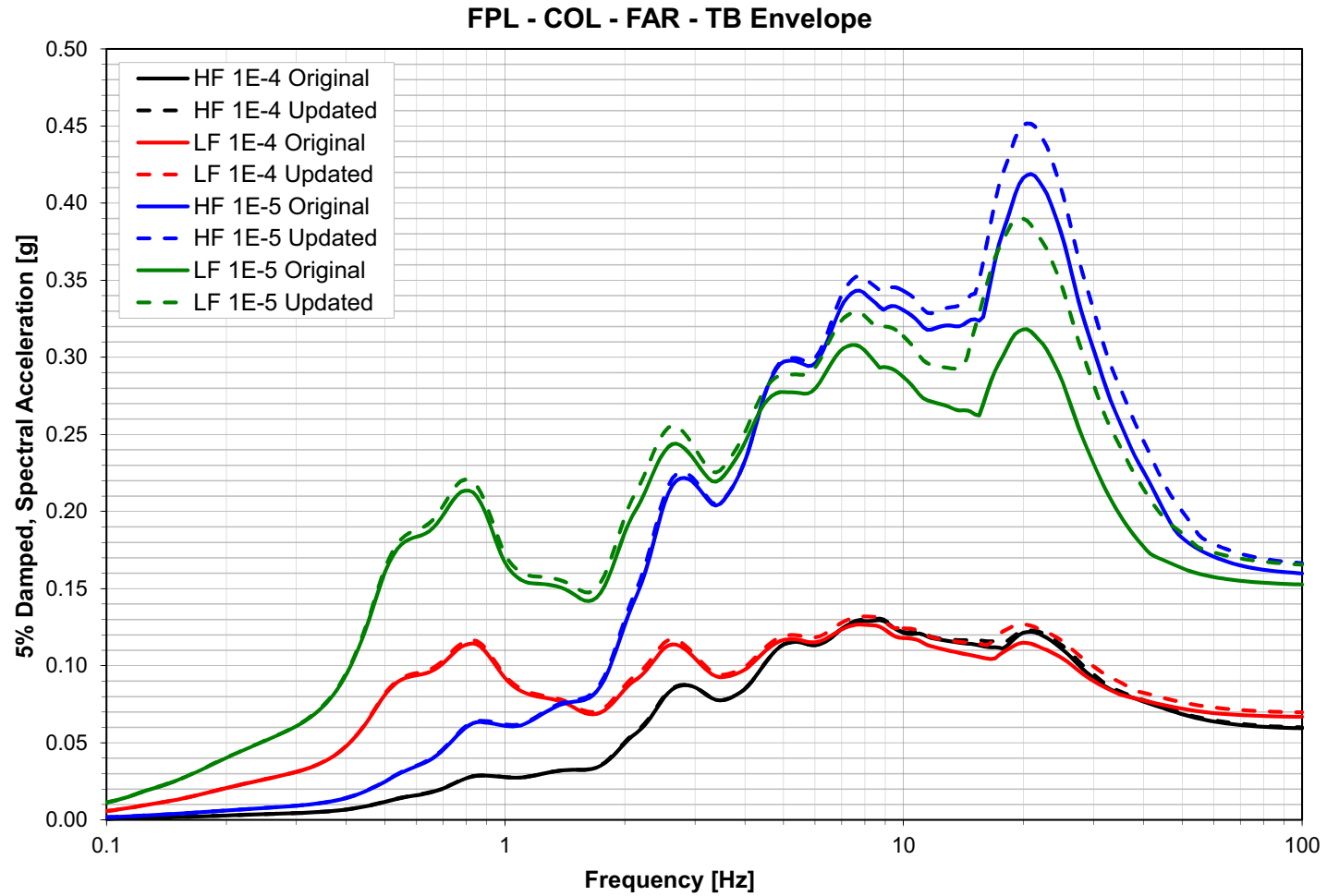


**Figure 3JJ-268 Comparison of the Enveloped ARS for the Turbine Building FRS Between the Sensitivity and Initial Analyses (FAR Profile)**

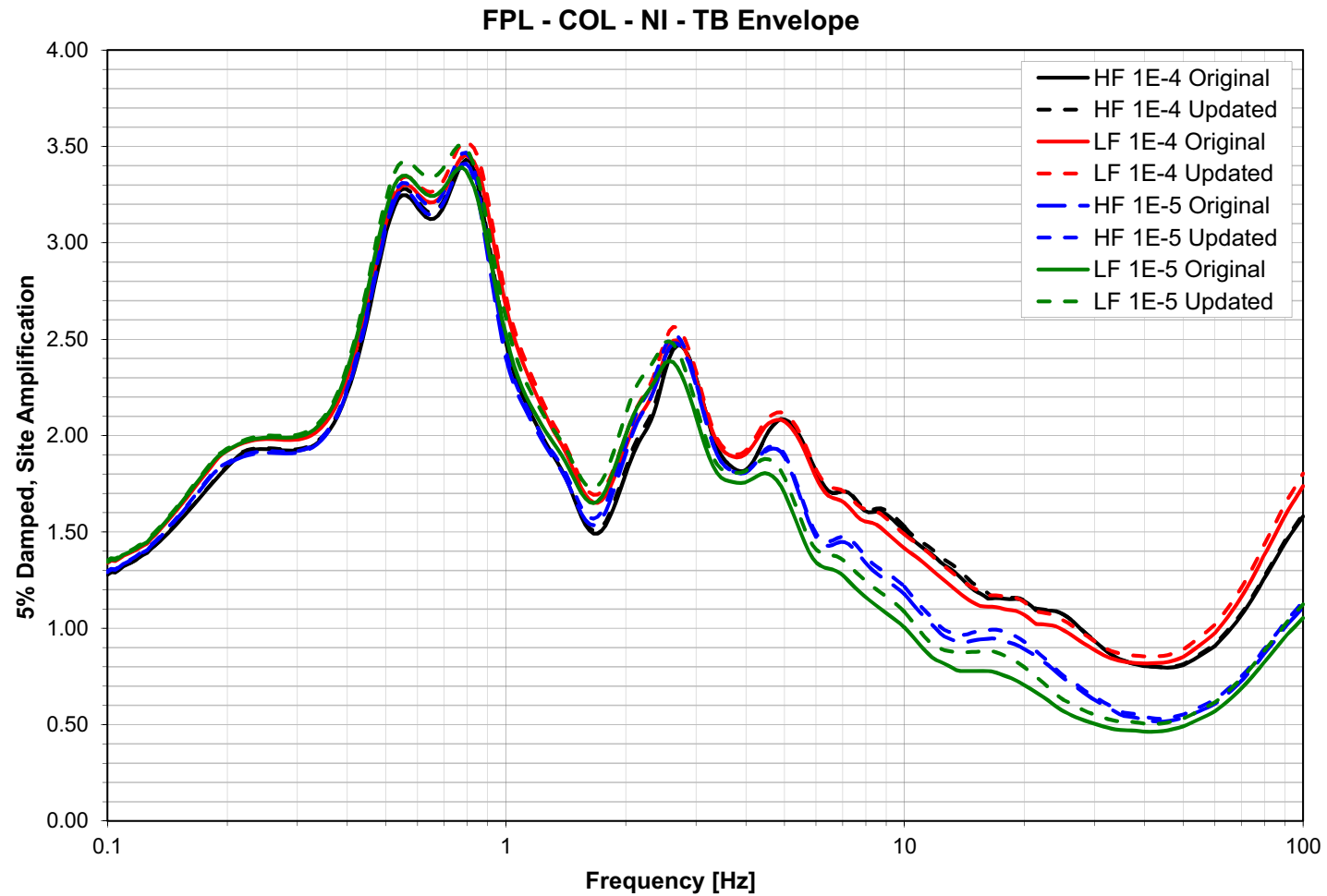


**Figure 3JJ-269 Comparison of the Enveloped Site Amplification for the Turbine Building FIRS Between the Sensitivity and Initial Analyses (NI Profile)**

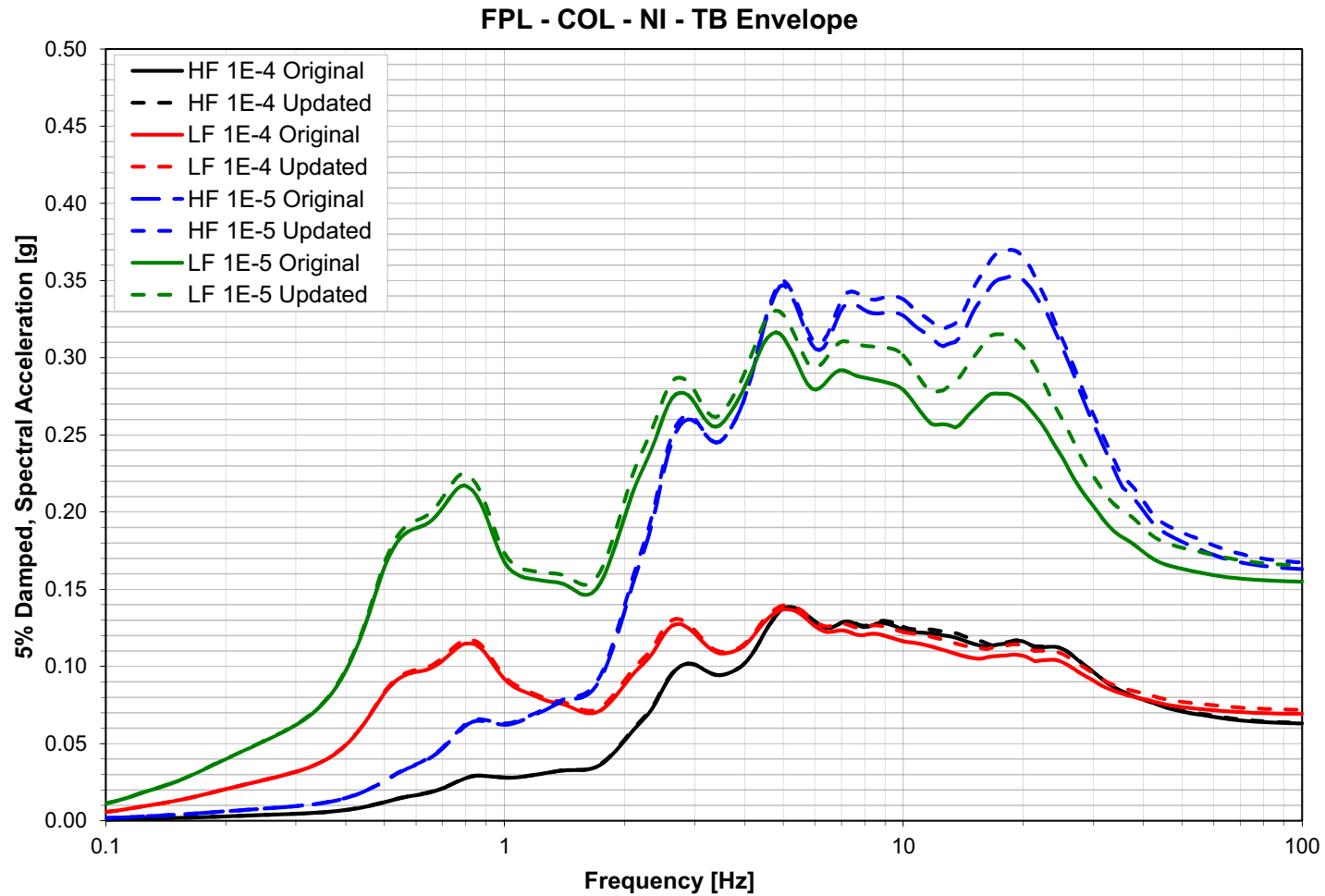


**Figure 3JJ-270 Comparison of the Enveloped ARS for the Turbine Building FIRS  
Between the Sensitivity and the Initial Analysis (NI Profile)**

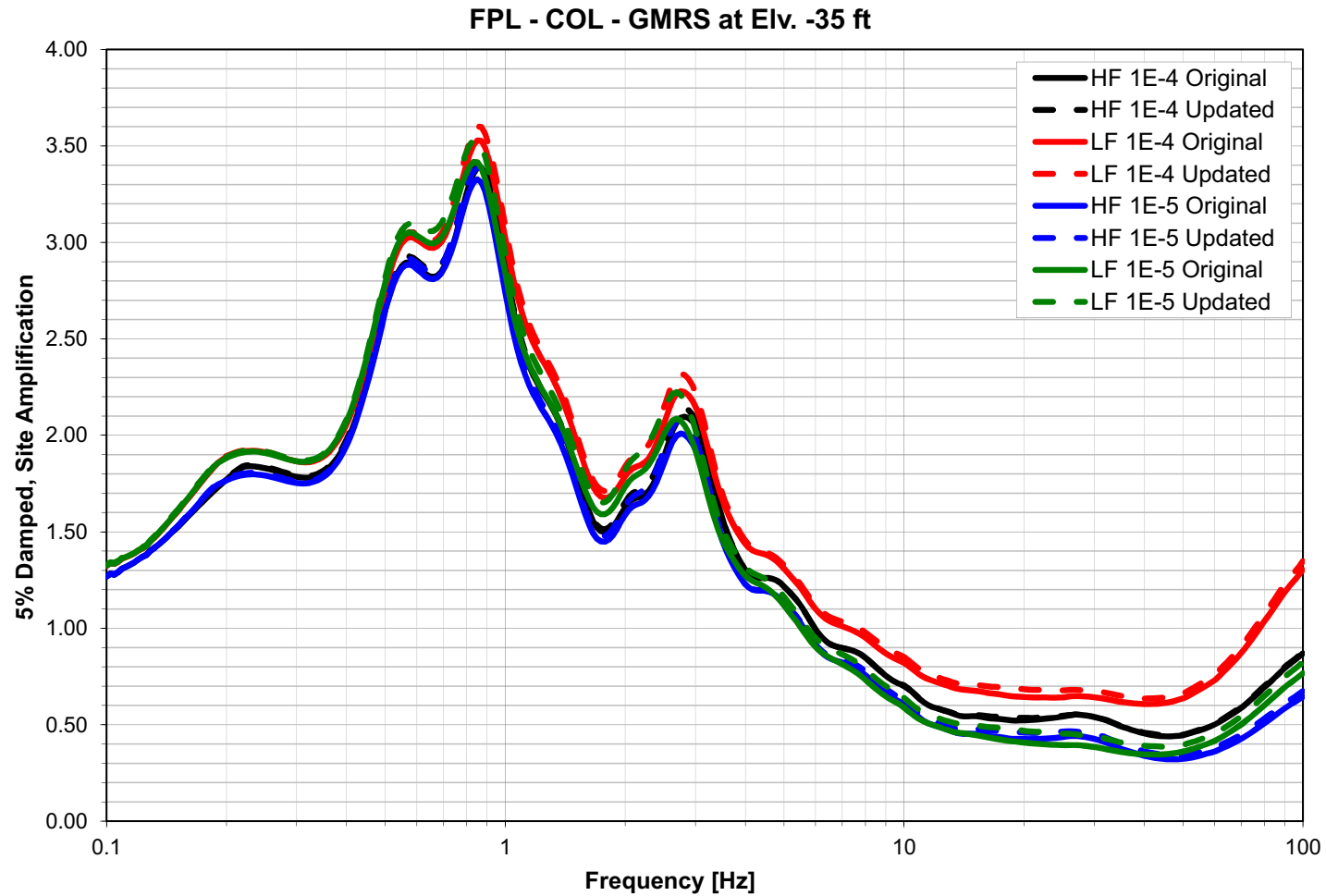


**Figure 3JJ-271 Comparison of the Site Amplification for the GMRS Calculation Between the Sensitivity and the Initial Analysis**



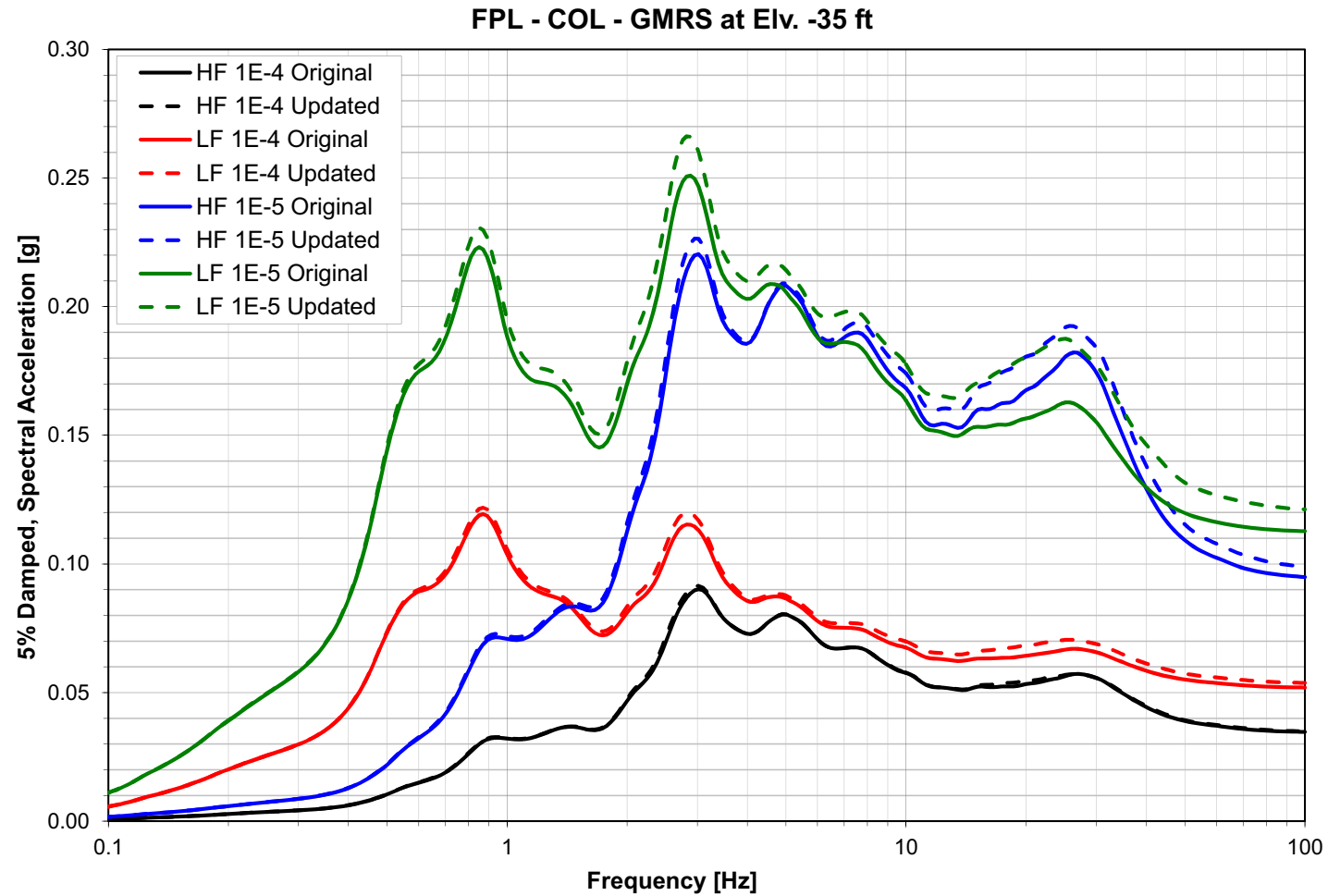


**Figure 3JJ-272 Comparison of the ARS for the GMRS Calculation Between the Sensitivity and the Initial Analysis**

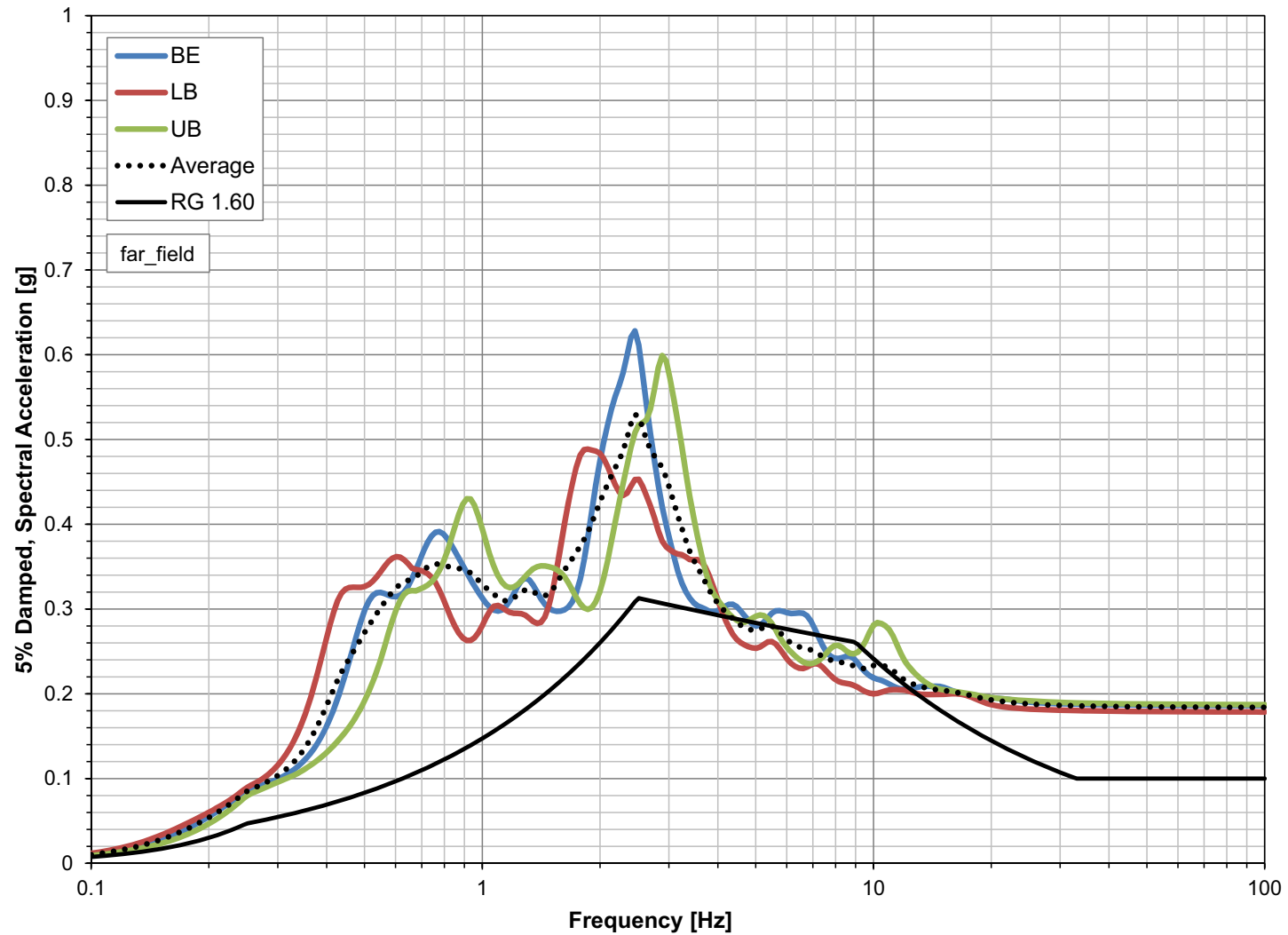


Figure 3JJ-273 First Iteration of the Iterative RG 1.60 Process for the FAR Profile with “Updated” Properties

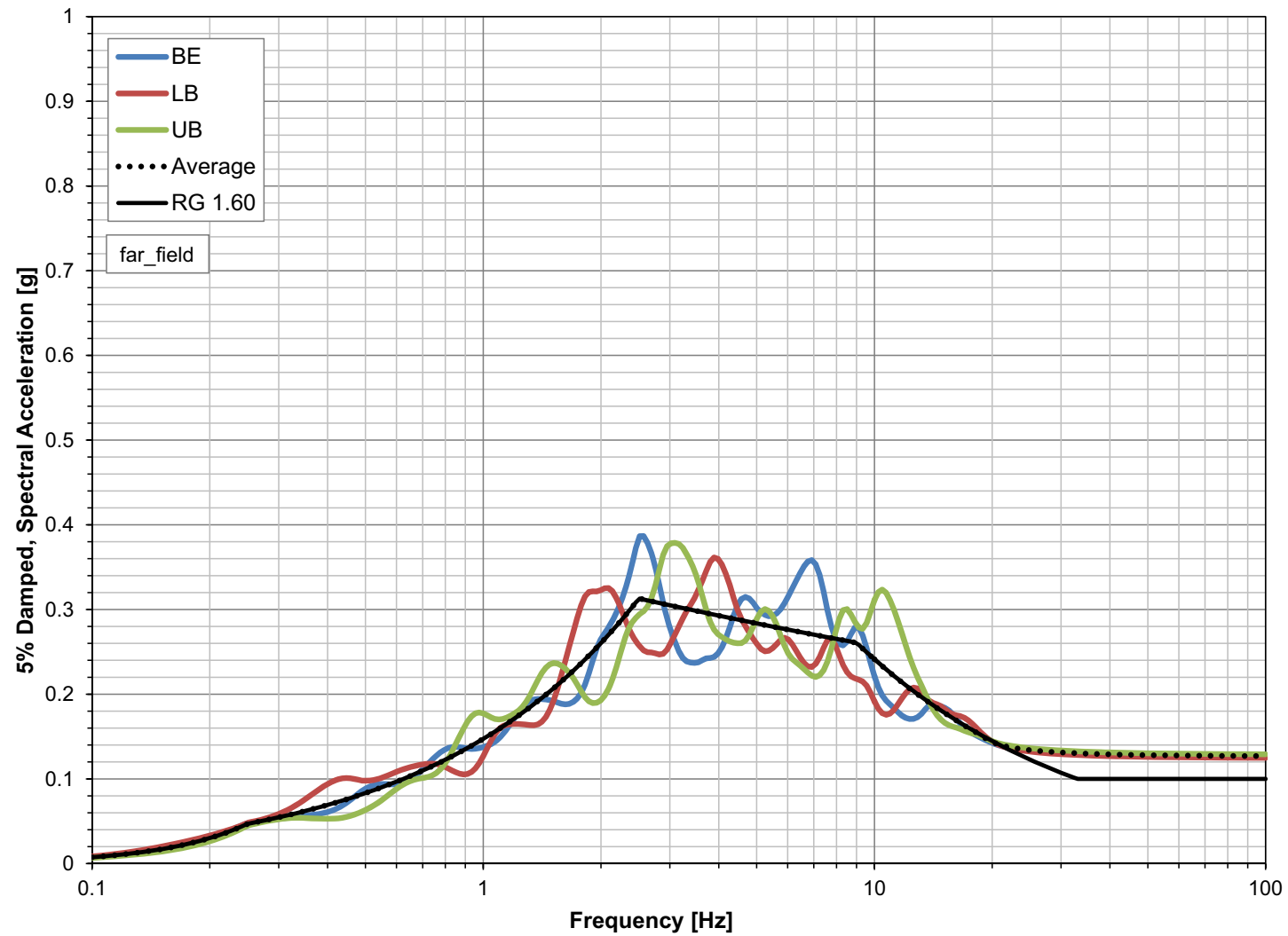
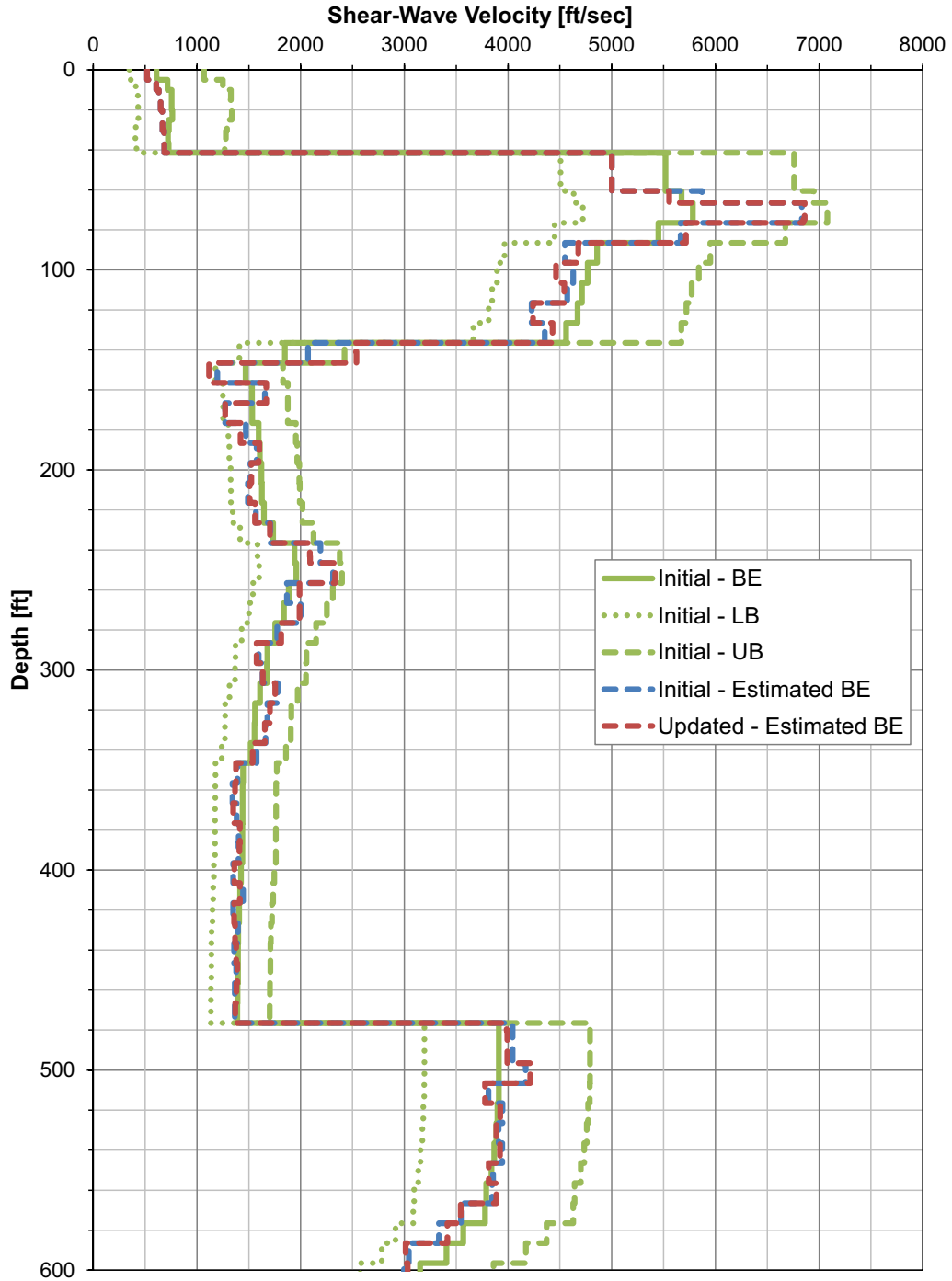
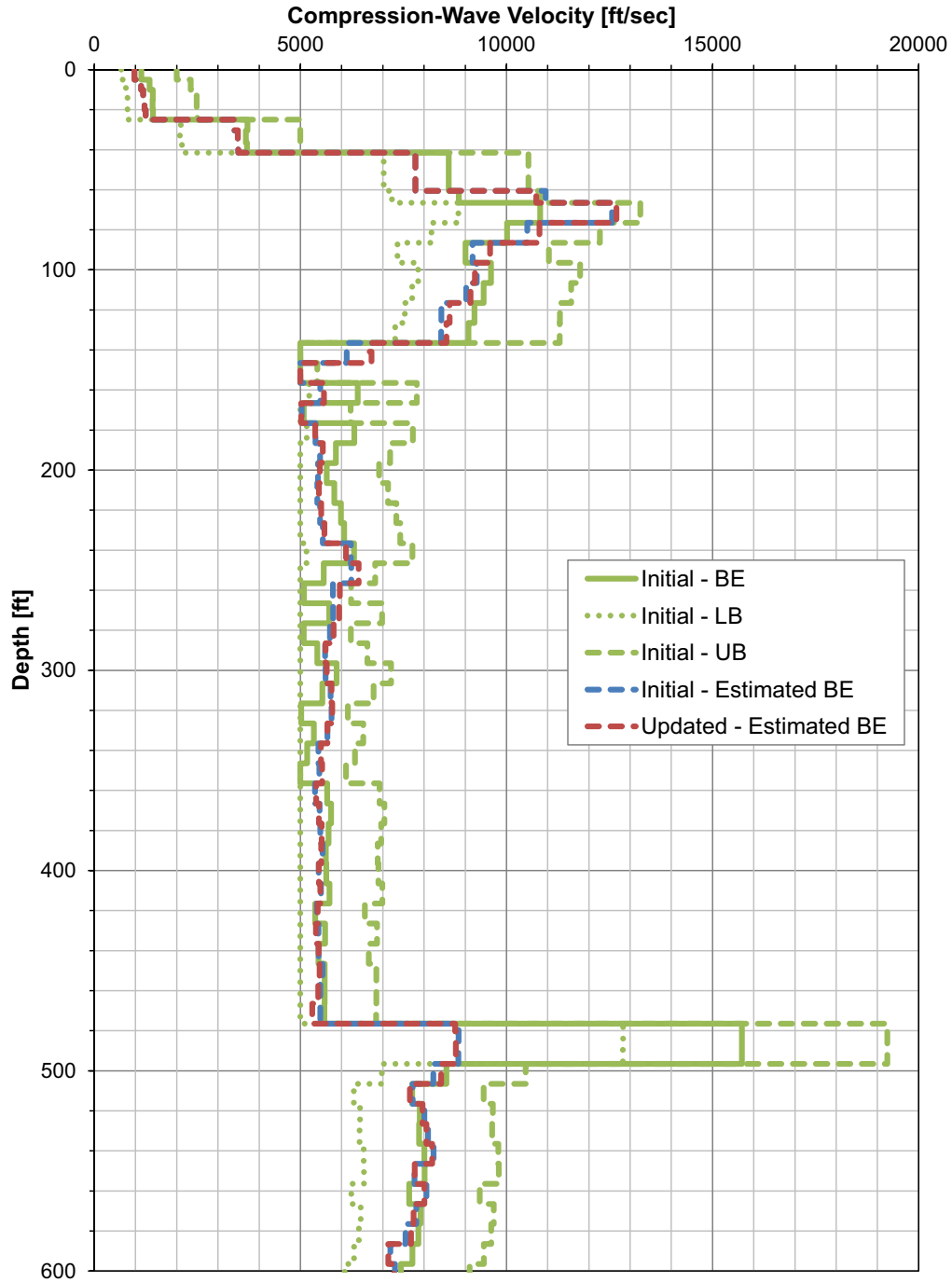


Figure 3JJ-274 Tenth Iteration of the Iterative RG 1.60 Process for the FAR Profile with “Updated” Properties



**Figure 3JJ-275 Estimated Best-Estimate S-Wave Velocity Profile for the NI Profile for the RG 1.60 Motion**



**Figure 3JJ-276 Estimated Best-Estimate P-wave Velocity Profile for the NI Profile for the RG 1.60 Motion**

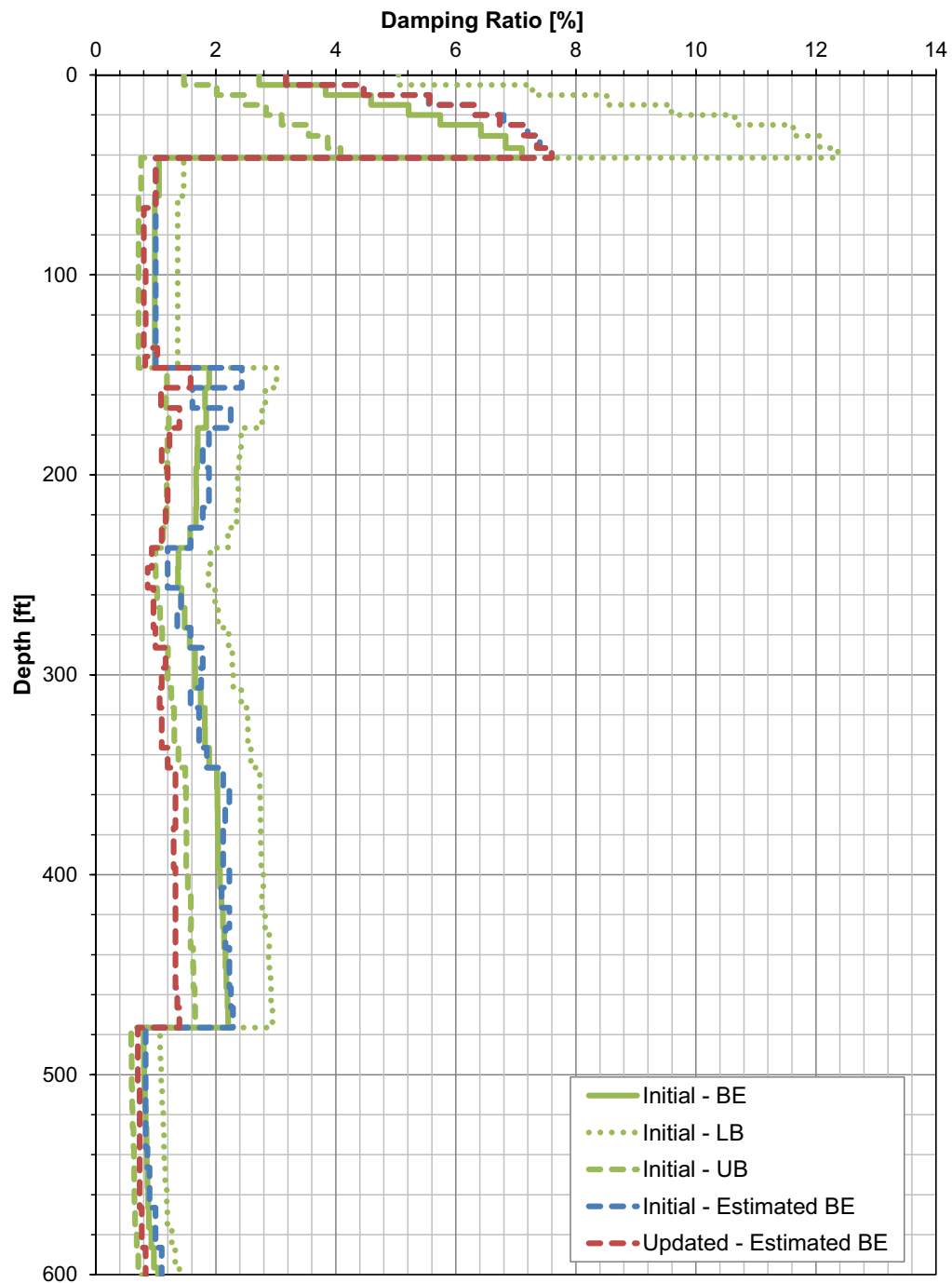


**Figure 3JJ-277 Estimated Best-Estimate Damping Profile  
for the NI Profile for the RG 1.60 Motion**

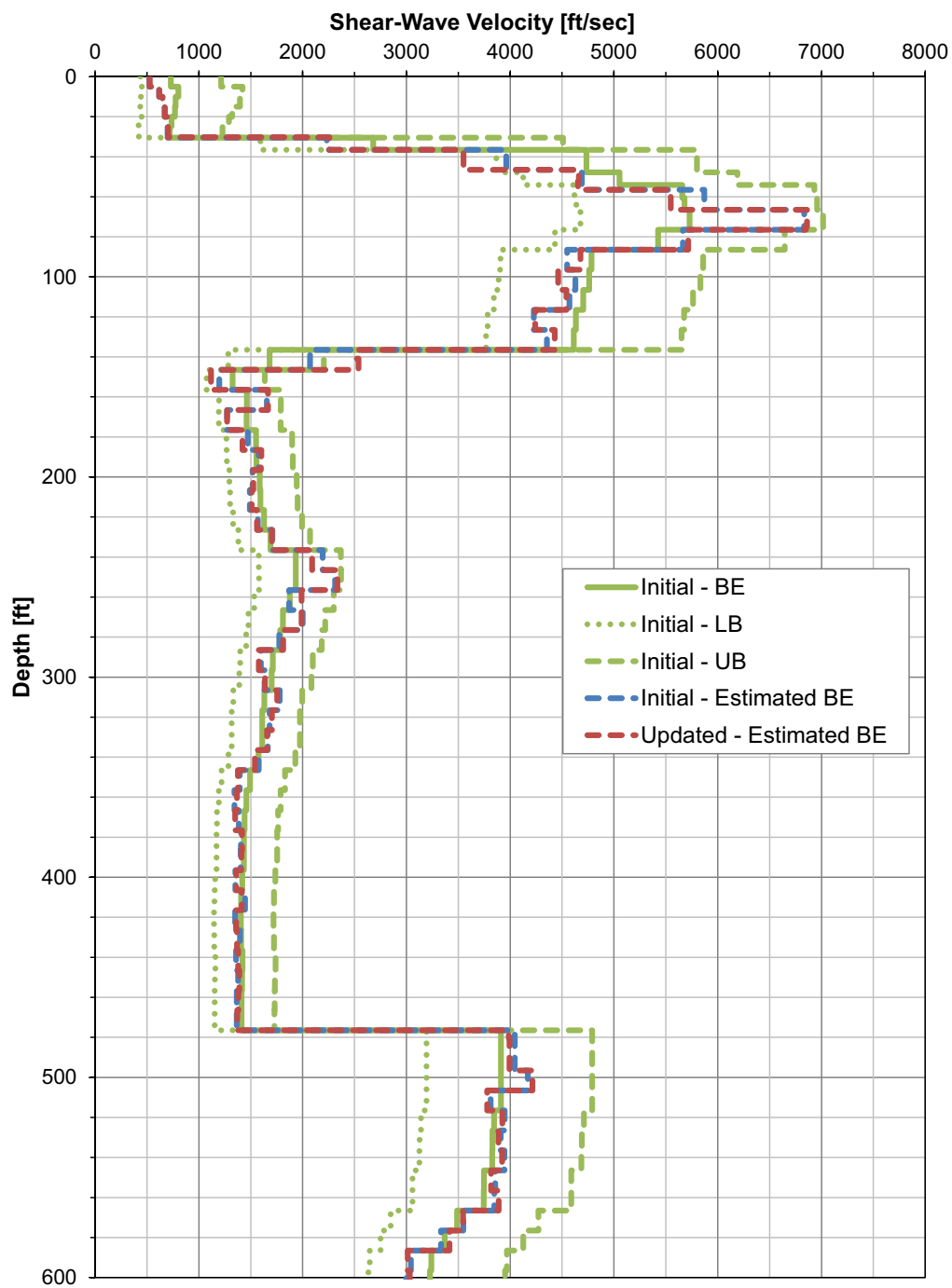


**Figure 3JJ-278 Estimated Best-Estimate S-Wave Velocity Profile for the FAR Profile**

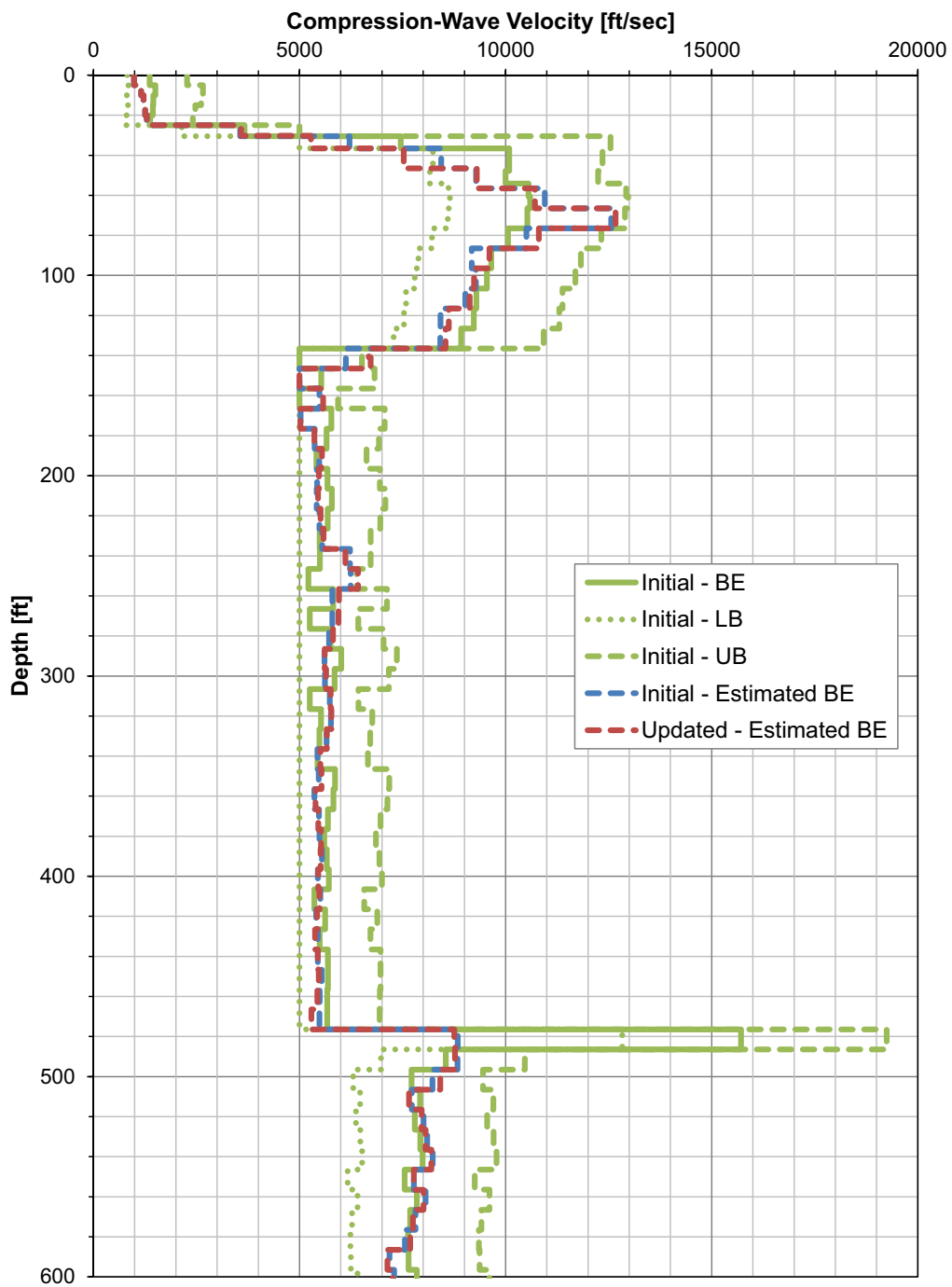


**Figure 3JJ-279 Estimated Best-Estimate P-Wave Velocity Profile for the FAR Profile**



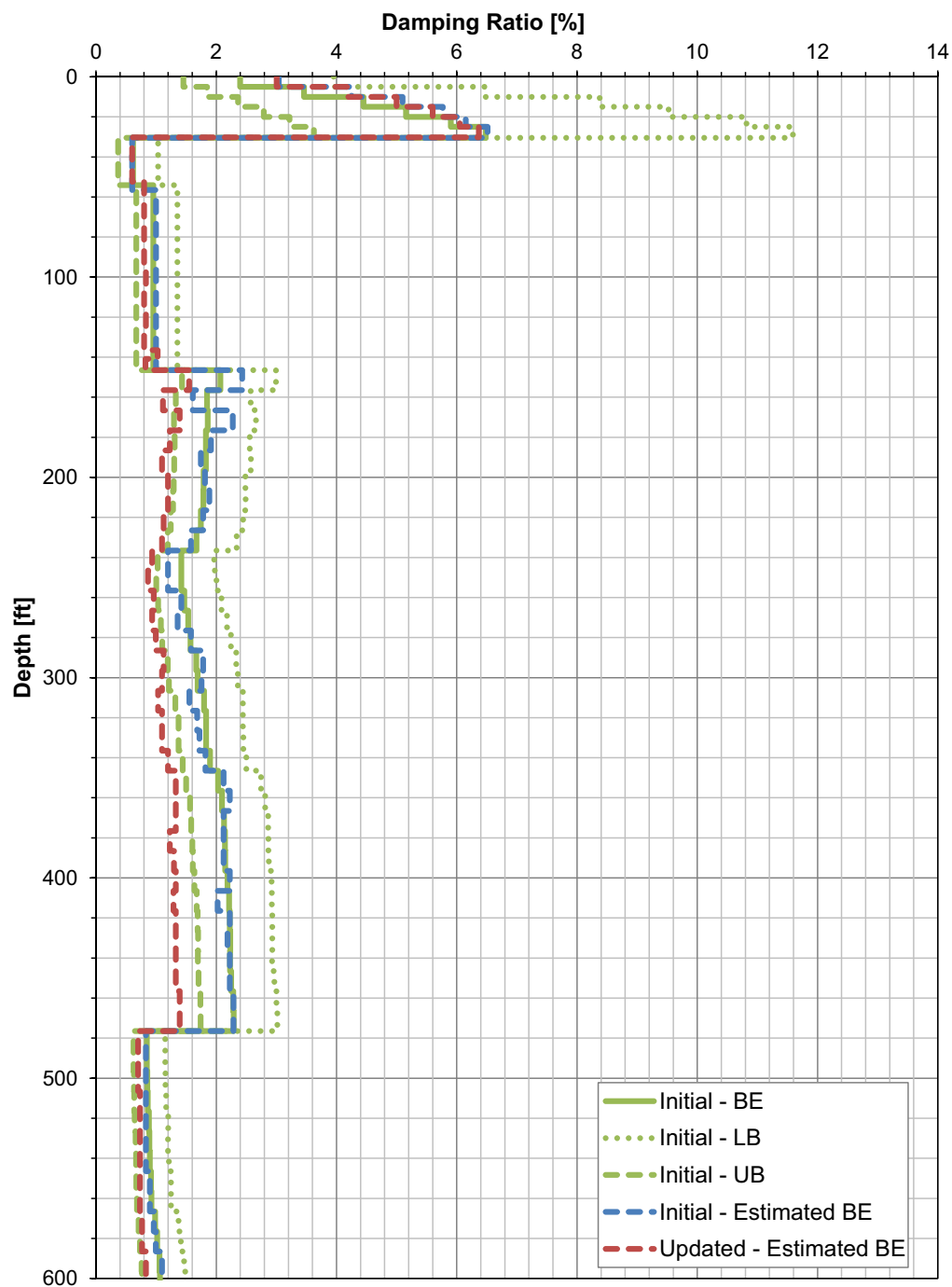
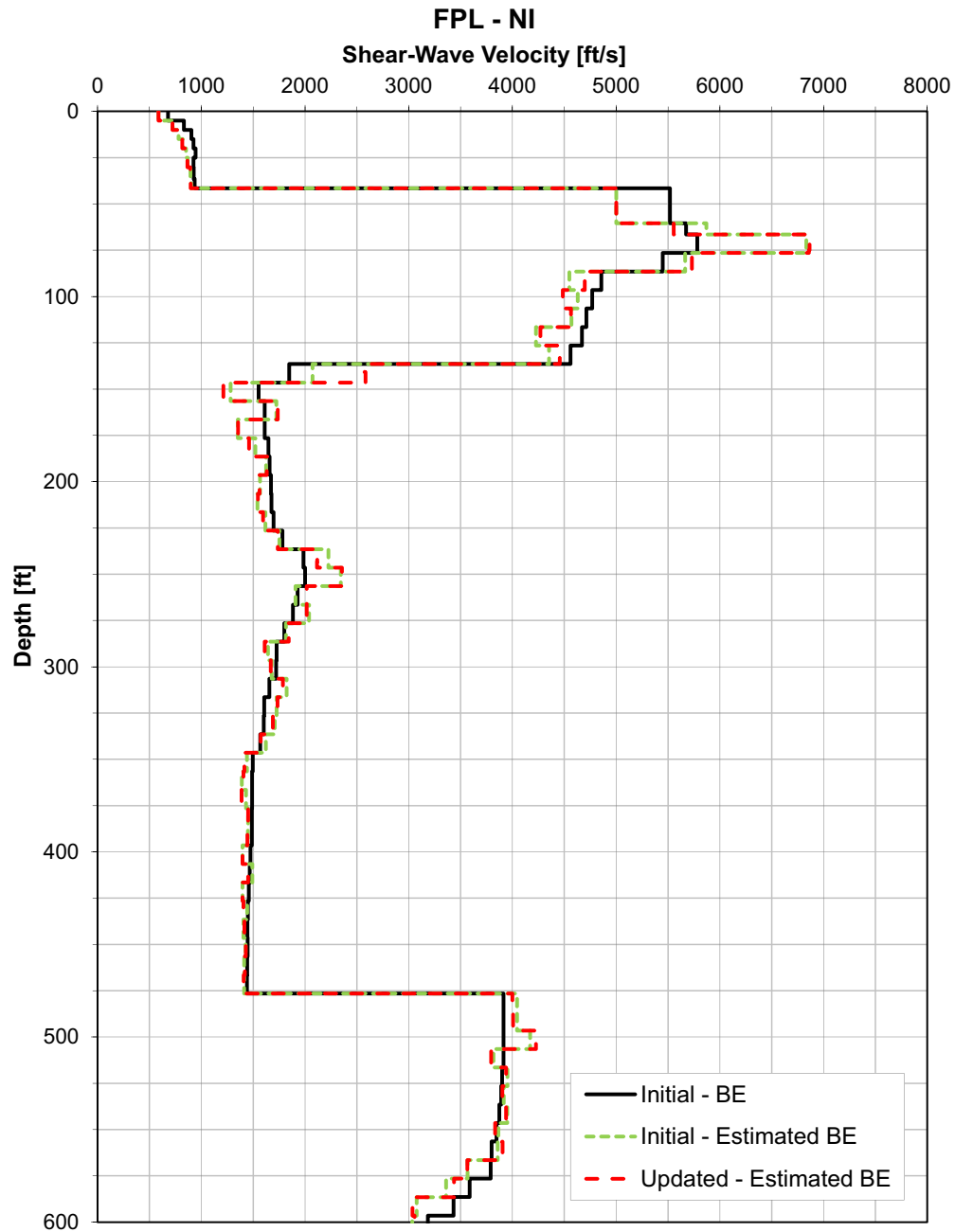
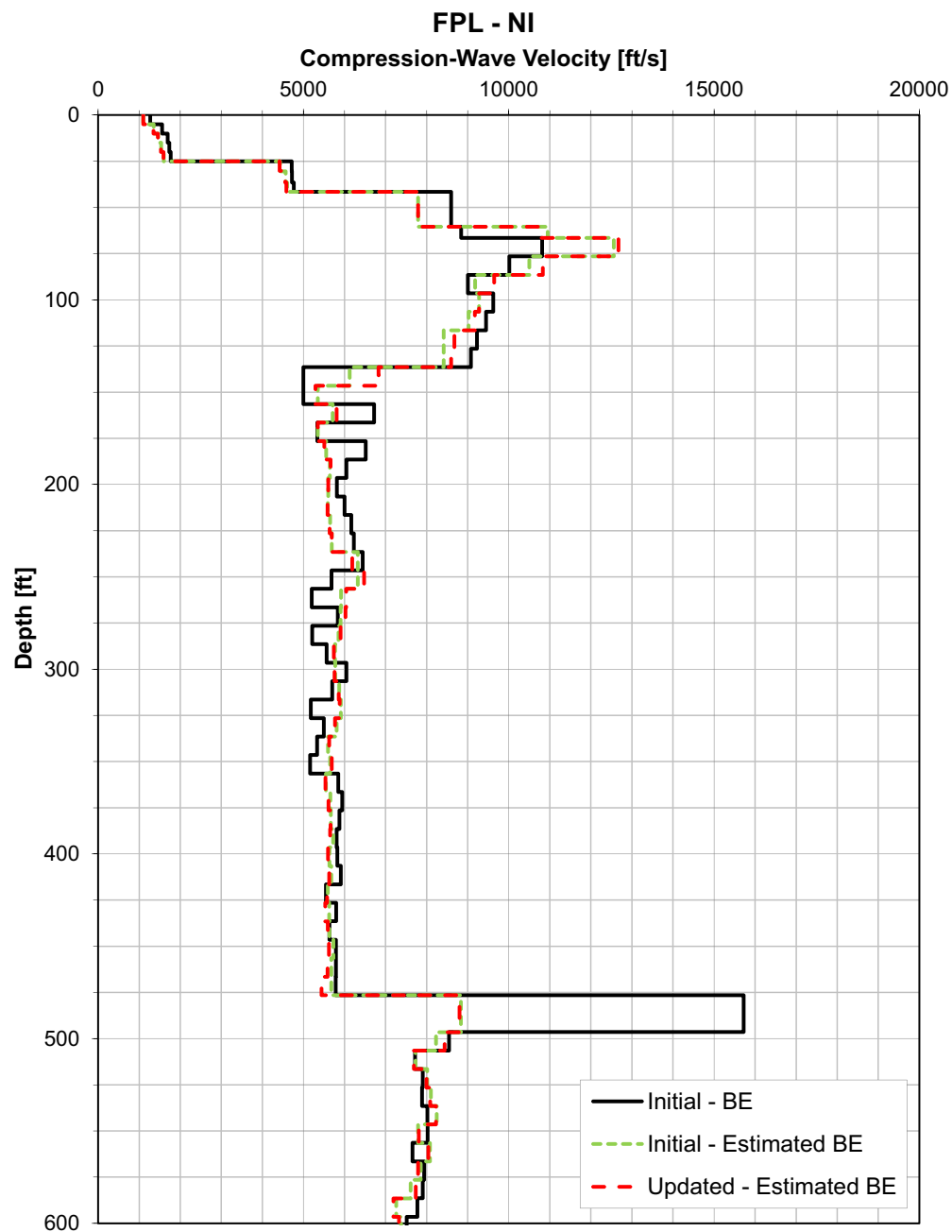


Figure 3JJ-280 Estimated Best-Estimate Damping Profile for the FAR Profile



**Figure 3JJ-281 Estimated Best-Estimate S-Wave Velocity Profile for the NI Site Column for the Site-Specific Motion**



**Figure 3JJ-282 Estimated Best-Estimate P-Wave Velocity Profile  
for the NI Site Column for the Site-Specific Motion**

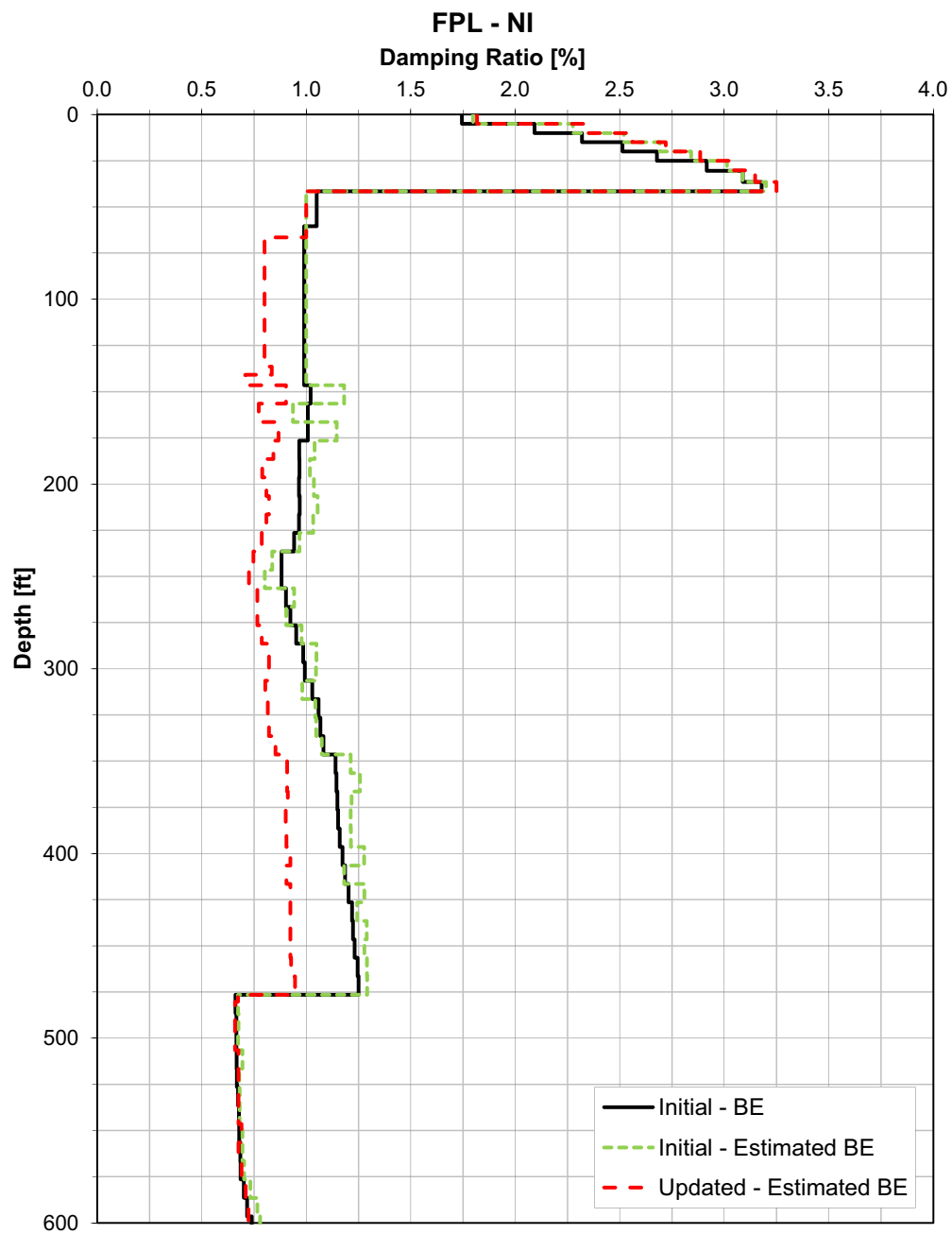


**Figure 3JJ-283 Estimated Best-Estimate Damping Profile  
for the NI Site Column for the Site-Specific Motion**

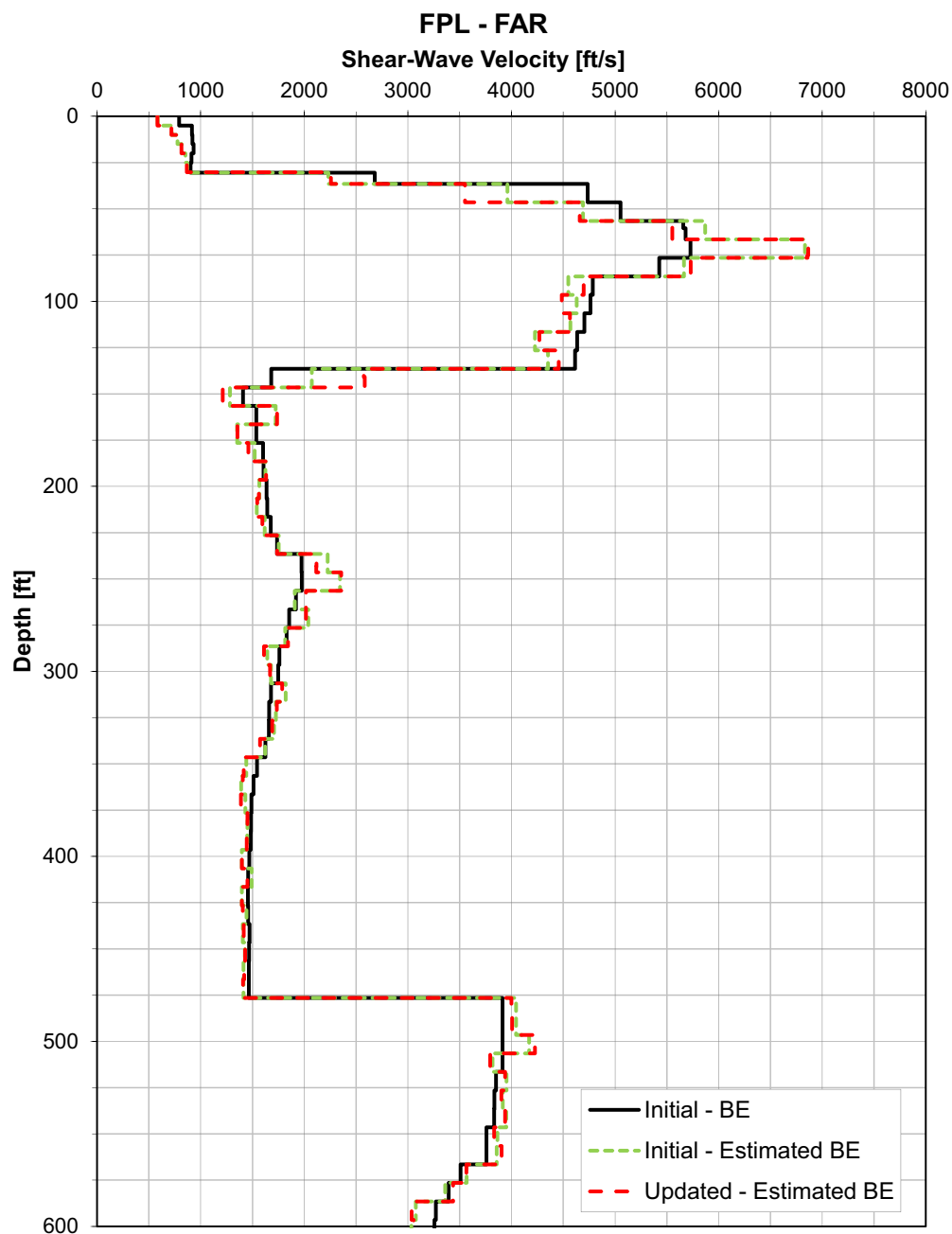


**Figure 3JJ-284 Estimated Best-Estimate S-Wave Velocity Profile for the FAR Site Column for the Site-Specific Motion**

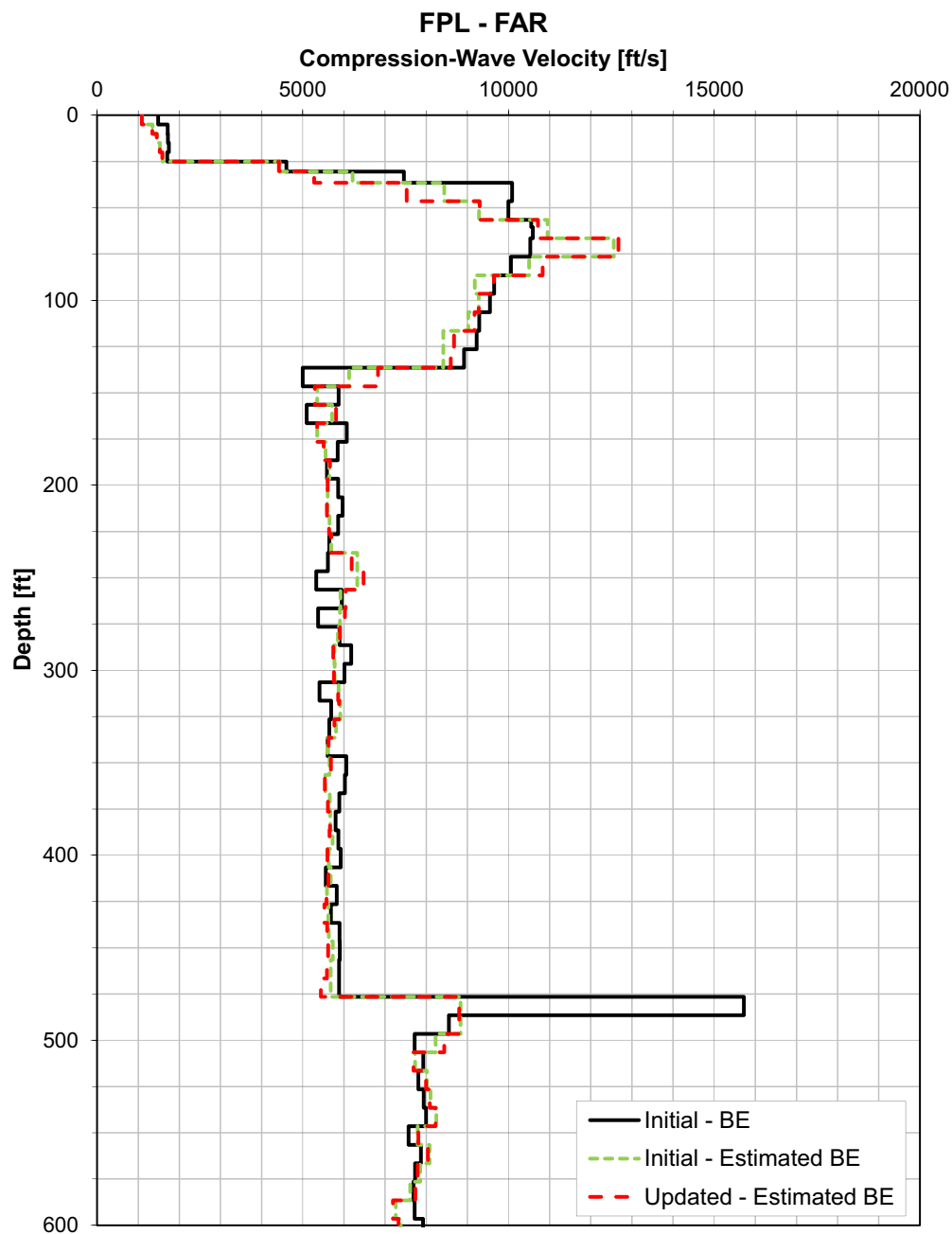


**Figure 3JJ-285 Estimated Best-Estimate P-Wave Velocity Profile  
for the FAR Site Column for the Site-Specific Motion**

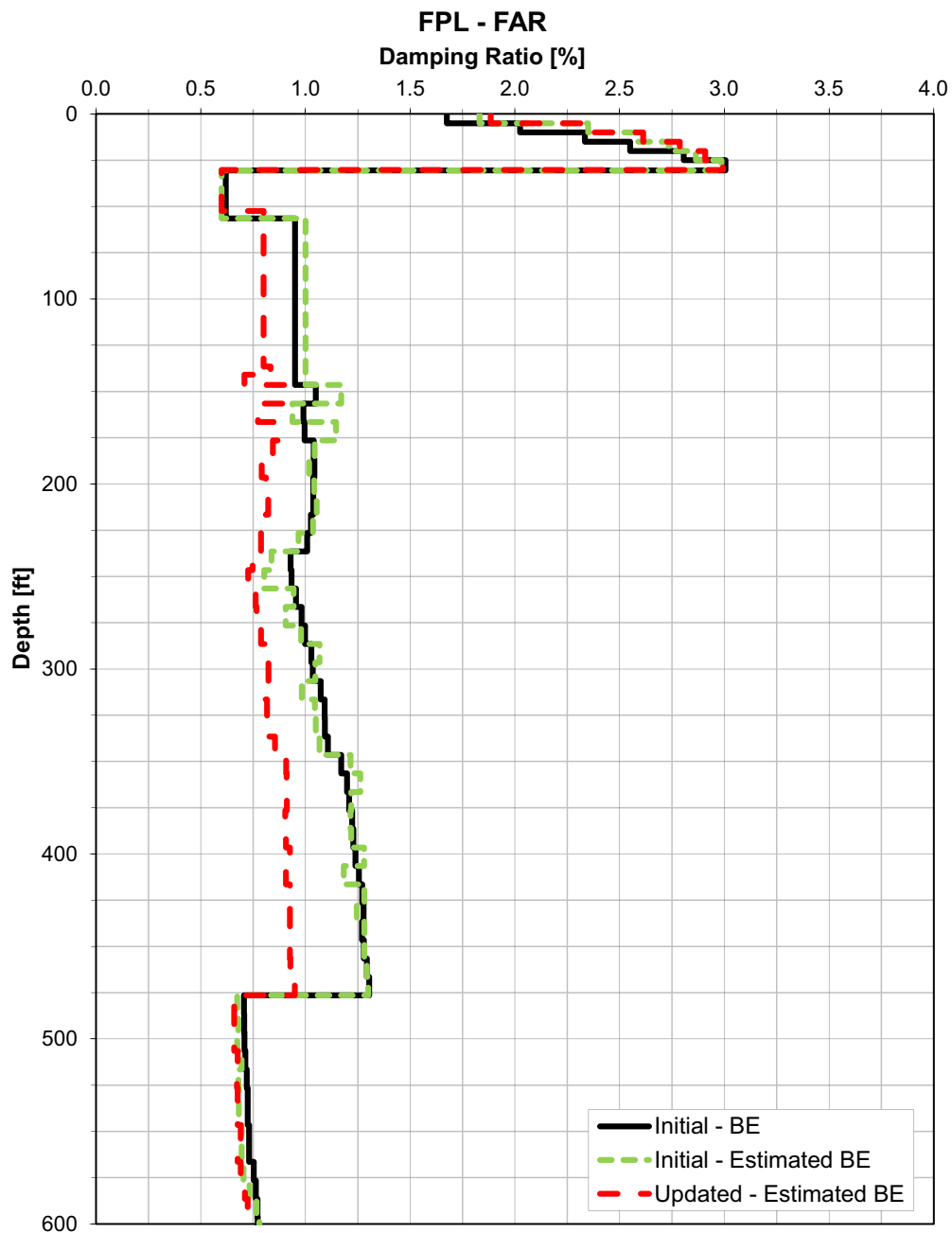


**Figure 3JJ-286 Estimated Best-Estimate Damping Profile  
for the FAR Site Column for the Site-Specific Motion**